INTER-KINGDOM SIGNALING INTERACTIONS IN ENTEROHEMORRHAGIC *ESCHERICHIA COLI* INFECTIONS

A Dissertation

by

TARUN BANSAL

Submitted to the Office of Graduate Studies of
Texas A&M University
in partial fulfillment of the requirements for the degree of

DOCTOR OF PHILOSOPHY

August 2010

Major Subject: Chemical Engineering

INTER-KINGDOM SIGNALING INTERACTIONS IN ENTEROHEMORRHAGIC *ESCHERICHIA COLI* INFECTIONS

A Dissertation

by

TARUN BANSAL

Submitted to the Office of Graduate Studies of
Texas A&M University
in partial fulfillment of the requirements for the degree of

DOCTOR OF PHILOSOPHY

Approved by:

Co-Chairs of Committee,	Arul Jayaraman
	Thomas K. Wood
Committee Members,	Mariah Hahn
	Jeffrey D. Cirillo
Head of Department,	Michael V. Pishko

August 2010

Major Subject: Chemical Engineering

ABSTRACT

Inter-Kingdom Signaling Interactions in Enterohemorrhagic *Escherichia coli* Infections.

(August 2010)

Tarun Bansal, B. Tech., U.D.C.T. (University of Mumbai), India

Co-Chairs of Advisory Committee: Dr. Arul Jayaraman
Dr. Thomas K. Wood

The overall goal of this research was to understand the role of inter-kingdom signaling in enterohemorrhagic *Escherichia coli* (EHEC) infections of the human gastro-intestinal (GI) tract from the perspective of both the invading pathogen and the human intestinal epithelial cells, which they colonize. Differential gene expression of EHEC was studied upon exposure to the human neuroendocrine hormones epinephrine and norepinephrine. We determined that these hormones increase EHEC chemotaxis, motility, biofilm formation, colonization of host cells, and virulence gene expression. We also studied the EHEC response to the GI tract commensal bacterial signaling molecules indole and autoinducer-2 (AI-2). We observed that indole decreases all the EHEC phenotypes that are increased by the human hormones and represses EHEC virulence. However, the effect of AI-2 was similar to that observed with hormones and opposite to that observed with indole, i.e. AI-2 increases EHEC virulence phenotypes.

We studied changes in host cell transcriptome in the presence of the commensal bacterial signal indole. Indole increases expression of genes involved in tight junction and gap junction formation, and production of mucins and actin cytoskeleton genes. Indole also down-regulates genes encoding for pro-inflammatory cytokines, chemokines, and Toll-like receptors. The gene expression results were confirmed with phenotypic assays where we observed an increase in trans-epithelial resistance, increase in the anti-inflammatory cytokine IL-10, decrease

in the pro-inflammatory cytokine IL-8, decrease in the activity of the pro-inflammatory transcription factor NF-κB, and decrease in colonization by EHEC of the indole-pre-treated HCT-8 cells.

We established that factors secreted by epithelial cells are important determinants of EHEC virulence. Gene expression studies showed that 34 out of 41 LEE virulence genes were induced when EHEC was cultured in conditioned medium. In addition, the data showed increased expression of the shiga toxin-2 prophage 933W. These changes in gene expression were corroborated by a 5-fold increase in HCT-8 cell colonization and increased intracellular Stx2 phage titers. We determined that the HCT-8-secreted factor(s) was protein-based and that it was greater than 3 kDa in size.

In conclusion, we have characterized the pathogen response to various eukaryotic and prokaryotic GI tract signals. We have established, for the first time, that the commensal bacterial signal indole is an inter-kingdom signal for the host epithelial cells. Overall, our studies provide a greater understanding of host-pathogen interactions.

DEDICATION

To

my parents, Praphulla and Indra, and my sisters, Barkha and Prachi

ACKNOWLEDGEMENTS

I would like to sincerely thank my co-advisors, Dr. Thomas K. Wood and Dr. Arul Jayaraman, for their guidance over the past five years of my Ph.D. It has been a great pleasure to work in their labs and learn science under their wings. Having co-advisors was a very unique experience and I will always cherish the ups and downs of the entire process.

Special thanks go to Dr. Wood lab members, Dr. Jintae Lee, Dr. Can Attila, Dr. Rodolfo Garcia, Dr. Xuesong Zhang, Dr. Xiaoxue Wang, Dr. Younghoon Kim, Dr. Akihiro Ueda, Dr. Toshinari Maeda, Dr. Sage Hiibel, Dr. Uma Sagaram, Seok Hoon Hong, Viviana Sanchez, Qun Ma, Andrea Garzon, and Justin Pella. I will also gratefully acknowledge Dr. Jayaraman lab members, Dr. Jeongyun Kim, Dr. Derek Englert, Colby Moya, Billy Newton, Fatih Senocak, Sun Ho Kim, and Allison Labile. My very special gratitude is towards Manjunath Hegde, who shares office and lab space with me, and has been an excellent research buddy through the past four years.

Dr. Jeff Cirillo helped me develop EHEC colonization assay protocol, which was extremely useful in understanding EHEC infection process. Dr. Robert Alaniz and his lab members, Jane Miller and Kristina Ryden, provided great help with flow cytometry. Dr. Alaniz also helped me understand immunology, and scientific discussions with him were very rewarding. Dr. Mariah Hahn was an excellent mentor and a wonderful friend in the corridors of the 5th floor of Jack E. Brown building. Dr. Robert Burghardt was instrumental in my understanding of optical and fluorescence microscopy and I believe his teachings will help me immensely in my future work.

I am grateful for the HCT-8 cells provided by Dr. Guan Zhu, the NF-κB reporter lentivirus provided by Dr. Stelios Andreadis, and the assistance with TER measurements

provided by Dr. Sangeeta Khare. It would be difficult to conduct my experiments without their help. Dr. Palmy Jesudhasan and Dr. Suresh Pillai provided AI-2 whenever I required it for my experiments. I thank Prof. R. Jayaraman for critical reading of my manuscripts and interpretation of experimental data.

The acknowledgement section will be incomplete without expressing my deep and sincere appreciation for the efforts of my parents, Praphulla and Indra, and the affection of my sisters, Barkha and Prachi. It is fair to say that they have been the biggest inspiration for me throughout my life and in all my endeavors.

TABLE OF CONTENTS

Page

ABSTRACT iii

DEDICATION v

ACKNOWLEDGEMENTS vi

TABLE OF CONTENTS viii

LIST OF FIGURES x

LIST OF TABLES xi

CHAPTER

I INTRODUCTION 1

1.1 Background 1
1.2 Motivation 2
1.3 Research objectives, importance, and novelty 4

II LITERATURE REVIEW 6

2.1 Human gastro-intestinal tract 6
2.2 Intestinal barrier function 9
2.3 Enterohemorrhagic *Escherichia coli* 10
2.4 Major virulence factors of EHEC 12
2.5 EHEC infection process 15
2.6 Important bacterial signaling molecules in the GI tract 15
2.7 Important host-derived signaling molecules in the GI tract 18

III DIFFERENTIAL EFFECTS OF EPINEPHRINE, NOREPINEPHRINE, AND INDOLE ON EHEC CHEMOTAXIS, COLONIZATION, AND GENE EXPRESSION 22

3.1 Overview 22
3.2 Introduction 23
3.3 Materials and methods 25
3.4 Results 30
3.5 Discussion 47

CHAPTER Page

IV TEMPORAL REGULATION OF ENTEROHEMORRHAGIC *ESCHERICHIA COLI* VIRULENCE MEDIATED BY AUTOINDUCER-2 56

4.1 Overview 56
4.2 Introduction 57
4.3 Materials and methods 59
4.4 Results 72
4.5 Discussion 79

V THE BACTERIAL SIGNAL INDOLE INCREASES EPITHELIAL CELL TIGHT JUNCTION RESISTANCE AND ATTENUATES INDICATORS OF INFLAMMATION 85

5.1 Overview 85
5.2 Introduction 86
5.3 Materials and methods 88
5.4 Results 96
5.5 Discussion 128

VI A SECRETED FACTOR FROM HUMAN INTESTINAL EPITHELIAL CELLS INCREASES ENTEROHEMORRHAGIC *ESCHERICHIA COLI* VIRULENCE …. 133

6.1 Overview 133
6.2 Introduction 134
6.3 Materials and methods 136
6.4 Results 143
6.5 Discussion 152

VII CONCLUSIONS AND RECOMMENDATIONS 157

7.1 Conclusions 157
7.2 Recommendations 158

REFERENCES 163

VITA 183

LIST OF FIGURES

FIGURE		Page
2.1	GI tract schematic	7
2.2	EHEC infection model	14
3.1	Agarose plug chemotaxis	31
3.2	Epi, NE, and indole affect EHEC motility and biofilm formation	33
3.3	Gene expression in EHEC biofilms upon exposure to epi, NE, or indole	43
3.4	Epi, NE, and indole affect EHEC attachment to HeLa cells	48
3.5	Hypothetical model for EHEC colonization in the GI tract	54
4.1	Agarose plug chemotaxis assay	73
4.2	AI-2 effects on VS94 motility and attachment to HeLa cells	74
4.3	AI-2 uptake assay	76
4.4	Changes in VS94 gene expression with AI-2 as a function of time	78
4.5	Overall changes in VS94 gene expression in presence of AI-2	82
5.1	Classification of genes differentially expressed upon indole exposure	97
5.2	Changes in tight junction proteins and trans-epithelial resistance	117
5.3	Changes in Toll-like receptor, IL-8 and IL-10 signaling	119
5.4	Modulation of NF-κB expression by indole	123
5.5	Chemical structure of indole-like compounds used in the study	125
5.6	Changes in HCT-8 cell phenotypes with aromatic bicyclic compounds	126
6.1	Number of genes differentially regulated by conditioned medium	142
6.2	Virulence-related genes regulated by conditioned medium	144
6.3	EHEC virulence assays	150
6.4	EHEC colonization assay	153

LIST OF TABLES

TABLE		Page
2.1	Major virulence factors of EHEC	11
3.1	Primers used for quantitative RT-PCR	29
3.2	Summary of changes in EHEC biofilm gene expression	34
3.3	Changes in the expression of AI-2 uptake genes in EHEC biofilms after 7 h exposure to epi and NE	45
4.1	Summary of changes in VS94 gene expression in presence of AI-2	62
5.1	Sequences of primers used for RT-PCR	95
5.2	Classification of genes differentially regulated by 1 mM indole at 24 h	98
5.3	Partial list of genes differentially regulated by 1 mM indole at 24 h	100
6.1	Sequences of primers used for qRT-PCR	141
6.2	Important genes up-regulated in the presence of conditioned medium	145

CHAPTER I

INTRODUCTION

1.1 BACKGROUND

A majority of bacteria exist in the natural world as surface attached (i.e. in the form of a biofilm) rather than as free planktonic cells (1). While biofilms are deleterious in most scenarios (2), there are instances when bacterial communities are beneficial. For example, the human gastro-intestinal (GI) tract is colonized by approximately 10^{14} bacteria (3) that belong to hundreds of species and exist in a symbiotic relationship with the host (4-5). This symbiosis is disturbed when pathogenic bacteria enter the GI tract, which leads to enteric infection. One of the most potent and dangerous pathogens is from the genus *Escherichia*. This genus has six reported pathogenic strains, of which, enterohemorrhagic *E. coli* (EHEC) is a food-borne pathogen (6) and responsible for causing bloody diarrhea and hemolytic uremic syndrome (HUS) (7), leading to kidney failure and even death in certain cases. The presence of pathogenicity islands (PAI) in its genome makes this pathogen different from other non-pathogenic *E. coli* strains in the GI tract. EHEC produces a histopathological lesion on epithelial cells called an attaching and effacing (A/E) lesion (8), and the formation of this lesion is thought to be the primary cause of pathogenicity. The EHEC genome contains a 43 kb PAI known as the Locus of Enterocyte Effacement (LEE), which contains all of the genes required for formation of A/E lesions on host epithelial cells (8). Five LEE operons (LEE1 through LEE5) make up the entire

---

This dissertation follows the style of *Proceedings of the National Academy of Sciences of the United States of America*.

LEE PAI, and these operons are regulated by the LEE-encoded regulator (Ler) which is considered to be the single most important regulator of virulence genes in EHEC.

EHEC infections have been reported to progress through a three-step mechanism, namely migration of the pathogen toward the epithelial cell surface, colonization of epithelial cells, and infection of cells by releasing toxins (8-9). In this work, we address the role of inter-kingdom (IK) signaling on all three of the critical steps that are involved in EHEC infection.

1.2 MOTIVATION

EHEC has been widely reported to be the prime cause of bloody diarrhea prevalent in many countries (10). Each year, EHEC causes approximately 3,000 infections all over the USA, and 2,100 hospitalizations, with an overall cost of $405 million (11). This is part of the 76 million food-related infections per year in the U.S., which result in 325,000 hospitalizations, 5,000 deaths, and a cost of $152 billion/year (http://www.producesafetyproject.org/admin/assets /files/Health-Related-Foodborne-Illness-Costs-Report.pdf-1.pdf). EHEC infections pose a serious clinical problem as they are often associated with complications and permanent disabilities, including neurological defects, hypertension, and renal insufficiency (12). Notably, the infective dose of EHEC is very low (10-100 colony forming units) (13). Currently EHEC infections are not treated with antibiotics as this has been shown to increase development of HUS in infected children (14), as well as lead to the increased release of shiga-like toxins (10) since the shiga-like toxins are related to prophage in this strain, and the antibiotics cause the phage to become lytic due to an SOS response (15). Given the seriousness of EHEC infections, understanding the mechanisms underlying EHEC infection can lead to the development of approaches for combating human GI tract infections. The overall goal of this work is to

investigate the effects of different eukaryotic and prokaryotic signaling molecules on EHEC infection.

EHEC is exposed to a wide range of signaling molecules in the GI tract. These include bacterial quorum sensing molecules such as autoinducer-2 (AI-2) and autoinducer-3 (AI-3) that are involved in the regulation of phenotypes crucial for virulence and infection (16-17); note the identity of AI-3 has not been confirmed. For example, adhesion of pathogenic *E. coli* to host cells is regulated by AI-2 and AI-3 (16, 18). An EHEC *luxS* mutant that is deficient in the synthesis of the AI-2 demonstrated markedly decreased expression of flagella and motility genes required for adherence to epithelial cells (19), and we have found that direct addition of AI-2 stimulates *E. coli* biofilm formation (20). The concentration of these bacteria-derived soluble signals is expected to be high in the GI tract, as non-pathogenic commensal bacteria that reside in the GI tract (3) produce AI-2 and AI-3. Other bacterial signaling molecules such as the stationary-phase signal indole (21) that are produced by *E. coli* (22), are also expected to be present at high concentrations in the GI tract. Indole decreases motility and biofilm formation of non-pathogenic *E. coli* (22), and could be important in EHEC infections since it has been shown to regulate virulence genes in enteropathogenic *E. coli* (23).

Apart from these prokaryotic signals, the GI tract contains high concentrations of eukaryotic signaling molecules, like hormones. The GI tract is richly enervated with sympathetic nerve fibers with approximately one million such nerves fibers present in various layers, including the mucosal layer to which EHEC adheres during infection (24). These nerves lead to the production of different human neuroendocrine hormones like dopamine and norepinephrine (NE), which can spill over into the lumen through diffusion. Two such hormones that seem to influence the behavior of EHEC are epinephrine (epi) and NE, which act as neurotransmitters inside the human body. It has been reported that NE increases the growth rate of commensal

bacteria as well as EHEC (4), and that both epi and NE influence the production of virulence factors in EHEC (16). Though these reports strengthen the possibilities of bacteria – host cell interactions, the complete mechanism behind these interactions is not yet understood.

1.3 RESEARCH OBJECTIVES, IMPORTANCE, AND NOVELTY

We studied the effects of individual signaling molecules, prokaryotic as well as eukaryotic, on EHEC phenotypes relevant to infection (chemotaxis, colonization of epithelial cells, and release of toxins) and EHEC gene expression. We also investigated the changes in gene expression of human intestinal epithelial cells when they are exposed to bacterial signals. These experiments will lead to a better understanding of the EHEC infection process and identification of variables that influence it.

This is the first study of EHEC virulence phenotypes and gene expression in presence of both eukaryotic hormones (epi and NE) and prokaryotic signaling molecules (indole and AI-2), which are present in the GI tract (25-26) and are encountered by EHEC during infection. Human epithelial cell gene expression has not been studied in the presence of these signaling molecules and our objectives were to investigate this in detail, to develop a fundamental understanding of the response of human cells to commensal and pathogenic bacteria.

The specific objectives were to:

- Determine the changes in gene expression and virulence phenotypes (such as chemotaxis, motility, biofilm formation, and colonization of epithelial cells) of EHEC on exposure to the eukaryotic hormones epi and NE
- Study the changes in gene expression and virulence phenotype of EHEC on exposure to the bacterial signals indole and AI-2

- Study the changes in human intestinal epithelial cell gene expression, trans-epithelial resistance, inflammatory cytokine and transcription factor production, anti-inflammatory cytokine production, and resistance to pathogen colonization on exposure to the commensal bacterial signal indole
- Investigate the effects of host cell-secreted factors on EHEC gene expression, colonization and release of toxins

CHAPTER II

LITERATURE REVIEW

2.1 HUMAN GASTRO-INTESTINAL TRACT

The human GI tract acts as an interface between the outside and internal human environment, and at nine meters long and 400 m^2 in surface area, is as large as a tennis court (27). The GI tract contains roughly the same number of neurons as the spinal cord. These neurons produce hormones that are secreted into the lumen of the intestine (Fig. 2.1A). The GI tract also houses a large variety of microorganisms, belonging to more than 500 diverse species and at 10^{14} cells, outnumbering the human cells by a factor of 10 (28). Intestinal epithelial cells act as a barrier for intestinal microbial pathogens and absorb water and nutrition. Colonization of the gut begins immediately once an infant is born, is affected by external environment and nutrition (27), and stabilizes about a week after birth.

Due to the presence of acid and other secretions (bile, pancreatic juice) in the stomach and duodenum, very few bacteria colonize these organs, and thus, the upper GI tract contains less than 10^3 bacteria per gram of luminal content (27). The number of resident bacteria increases progressively in the lower GI tract, with the jejunum and the ileum containing 10^4 and 10^8 cells per gram, respectively (27). The lower GI tract (i.e. the colon) contains the most complex microbial ecosystem, containing roughly 10^{12} cells per gram of luminal content (27). A majority of the 500 species that are estimated to colonize the GI tract have never been cultivated in the lab. Also, about 30-40 species account for more than 90% of the total bacterial population, and anaerobic bacteria outnumber aerobic bacteria by a factor of 1000 (27). The important genera of microbes include *Bacteroides, Bifidobacterium, Eubacterium, Clostridium, Lactobacillus*, and *Enterococcus* (27).

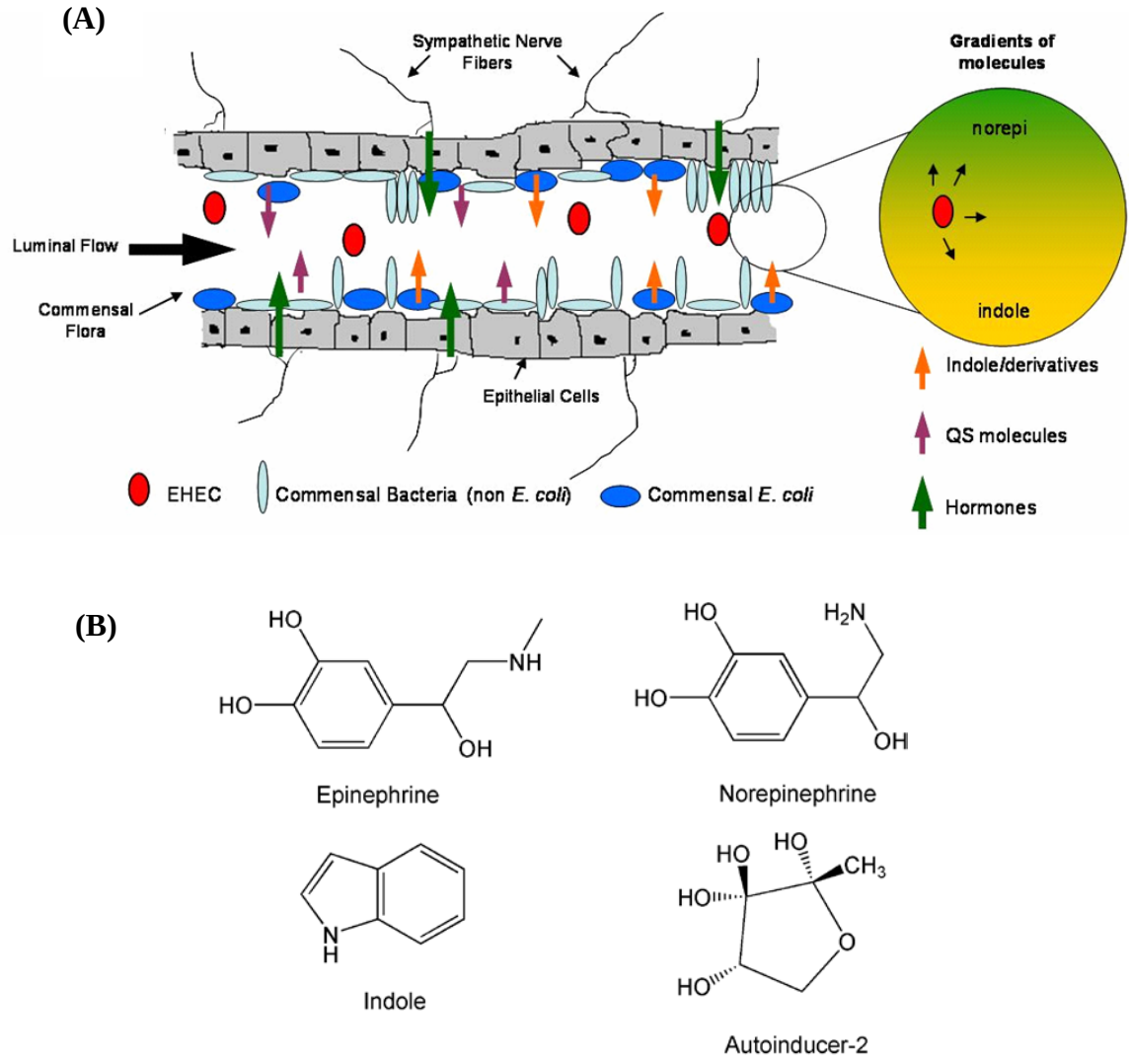

Fig. 2.1. GI tract schematic. (A) Intestinal epithelial cells are enervated by sympathetic nerves that release hormones into the lumen and are colonized by commensal bacteria that release bacterial signals. EHEC encounters all of these signals on entering GI tract. (B) Chemical structures of important GI tract signals.

A symbiotic relationship exists between commensal bacteria and host cells. The host GI tract provides a nutrient-rich environment for the microbes while they play an important role in development of the host immune system. Microbes also control the proliferation of epithelial cells by accelerating their differentiation cycle during morphogenesis (29). In addition, microbes ferment non-digestible dietary residues and provide biochemical pathways that are not available in the hosts. Importantly, commensal bacteria provide a barrier against pathogen colonization through the production of bacteriocins, (Fig. 2.1A), alterations in pH, and by competing for nutrients required by pathogens for growth (27).

However, any alteration in the homeostasis between the host cells and bacteria leads to serious consequences. Inappropriate immune and inflammatory responses toward commensal bacteria lead to inflammatory bowel disease (IBD), pathologies such as Crohn's disease and ulcerative colitis (30). IBD is known to affect 1.4 million Americans, with most patients in the age range of 15 to 30 years. Crohn's disease affects mostly the ileum and colon, while ulcerative colitis involves the rectum (30). In IBD, infiltration of lamina propia with innate (neutrophils, macrophages etc.) and adaptive (B and T cells) immune cells results in pronounced inflammation. In addition, expression of pro-inflammatory cytokines, like TNF-α and IL-23, leads to activation of pro-inflammatory pathways. Treatment options for these diseases are limited, although recent studies involve administering anti-TNF-α antibody, and IL-10-producing T cells and bacteria, both of which reduce inflammation (30). Thus, it is extremely important to maintain homeostasis.

2.2 INTESTINAL BARRIER FUNCTION

Intestinal goblet cells secrete a gel-like substance called mucin, which forms a barrier between the luminal contents and the intestinal epithelial cell layer (31). Mucins are also responsible for absorption of nutrients and help in waste removal. It has been reported that deficiencies in the mucosal layer can lead to several inflammatory diseases. The GI tract has the largest mucosal surface in the body, and is especially critical, since the GI tract is continuously in close contact with the commensal, and sometimes pathogenic, microorganisms. Mucosa-associated lymphoid tissue consists of T cells, B cells, and macrophages, and is responsible for innate and adaptive immune responses in the host.

Intestinal cells present a selectively permeable barrier to allow certain nutrients to pass through. This paracellular system consists of tight junction proteins, adherens junction proteins and desmosomes (31). The tight junction system is comprised of occludins, claudins, myosins, and zona occludens. Occludin was the first tight junction protein identified; and claudins are important transmembrane proteins that regulate permeability of the epithelial layer. Zona occludens, like ZO-1 and ZO-2, are required for tight junction assembly. Adherens junctions are made up of E-cadherin, catenins and F-actin. Adherens junctions are also required for the assembly of tight junctions, which then seal the paracellular space. Loss of adherns junction proteins leads to a defective cell-matrix, defective differentiation and cell apoptosis.

Tight junction properties are regulated by the intestinal immune response, particularly by pro-inflammatory cytokines TNF-α and IFN-γ. Increased TNF-α secretion leads to high cellular permeability and, thus, leads to colitis. In order to enhance cellular barrier properties and to prevent diseases such as Crohn’s, it has been suggested that an increase in claudin expression should be targeted. Tight junctions are responsible for maintaining homeostasis by allowing only

select molecules to pass through and, thus, maintenance of this barrier is very important in healthy tissue.

2.3 ENTEROHEMORRHAGIC *ESCHERICHIA COLI*

E. coli is a facultative Gram-negative anaerobe present in the human GI tract as a commensal bacterium. However, certain strains of *E. coli* possess virulence factors that make them pathogenic for host cells. EHEC is a foodborne pathogen responsible for severe disease outbreaks in humans worldwide. EHEC survives well in the environment and also within healthy cattle, which are usually asymptomatic when carrying this pathogen. Among the serotypes of EHEC, such as O26:H11, O91:H21, O111:H8, O157:H7 and O157:NM that are frequently associated with disease, O157:H7 is the most common and widely prevalent in the USA, the UK and Japan. EHEC serotype O157:H7 was first identified in 1982 as a human pathogen causing bloody diarrhea (32), and later as a cause of HUS, a disease characterized by acute renal failure, mostly affecting children. EHEC are defined as pathogenic *E. coli* strains that produce shiga-like toxins (Stx) and cause hemorrhagic colitis and HUS (33). The Centers for Disease Control and Prevention have estimated that EHEC O157:H7 cause 73,000 infections, 2,200 hospitalizations and 60 deaths annually in the USA (34), and the annual cost associated with these infections is $405 million (11). Currently, there is no specific treatment for EHEC infections, and the use of antibiotics is avoided. Thus, fluids and electrolytes are administered to limit the extent of symptoms and prevent complications. This makes it imperative to prevent and control EHEC infections.

Table 2.1. Major virulence factors of EHEC (33)

Factor	Location	Components	Function
LEE Pathogenicity Island	Chromosome	LEE1 LEE2 LEE3 LEE4 LEE5	- Type III secretion system - Attaching and effacing lesion
Shiga toxins	Phage DNA inserted in chromosome Stx1 – phage CP-933V Stx2 – phage BP-933W		- Host cell damage - release of cytotoxins
Plasmid O157	F-like plasmid	*ehxA* *katP* *etp* *espP* *toxB*	- Hemolysin - Peroxidase - Type II secretion - Serine protease - Adhesion/colonization factor
RpoS	Chromosome		- Acid, heat and salt resistance
Iha	Chromosome		- Adherence conferring molecule

2.4 MAJOR VIRULENCE FACTORS OF EHEC

Several virulence factors are associated with EHEC pathogenesis. Stx are major but not the only virulence factors and others include LEE, plasmid O157 (pO157), enterotoxin, and acid, heat and salt resistance (Table 2.1).

2.4.1 Shiga Toxins

Stx is a very potent cytotoxin and causes damage to a variety of cell types (35). There are two types of EHEC Stx, Stx1 and Stx2. EHEC can express Stx1, Stx2, or both. Expression of Stx2 alone is associated with more toxicity than expression of Stx1 alone or expression of both Stx1 and Stx2. Thus, strains producing Stx2 are more virulent and associated with HUS (33). Stx has a conserved structure consisting of one active A subunit and five receptor binding B subunits, making an AB_5 complex (33). The B_5 subunit binds to host receptor globotriaosylceramide (Gb3) or globotetraosylceramide (Gb4) and after binding, the A subunit is internalized, which then inhibits protein synthesis inside the host cell.

2.4.2 Locus of Enterocyte Effacement

During colonization of the intestinal mucosa, EHEC induce the A/E histopathological lesion on the intestinal epithelial cells (8). Once attached, bacteria stimulate host cell actin polymerization, and express components of the type III secretion system (T3SS), which releases several toxins into the host cells (8). First, an adhesin called intimin is secreted along with its receptor Tir, and later EHEC secreted proteins (Esp), like EspA and EspB, are injected into the host cell, which modify host cell signal transduction leading to cell death. The genes responsible for A/E lesions are located in LEE Pathogenicity Island (36). This pathogenicity island is 43 kb in size and consists of 41 open reading frames (ORFs) distributed in five operons (LEE1 through

LEE5), and three major regions. The middle region of LEE contains *eae* and *tir*, and T3SS encoding-genes are present upstream. The region downstream of *eae* consists of T3SS-secreted proteins like EspA, EspB, EspD and EspF. The LEE genes are regulated *in trans* by Ler. Additionally, non-LEE encoded virulence effectors, e.g. NleH1 and NleH2, have recently been discovered (37).

2.4.3 Plasmid O157

A plasmid is circular extrachromosomal DNA that is capable of replicating independently of the chromosome. Plasmids are responsible for providing antibiotic resistance, producing virulence factors, and toxin-anti-toxin pairs (33). EHEC contains a plasmid O157 (pO157) that is highly conserved between the different pathogenic *E. coli* strains and confers additional virulence traits to this pathogen (33). Its size ranges from 92 to 104 kb and has been sequenced. This plasmid is comprised of sequences for transposons and prophages. Some of the virulence genes encoded in pO157 (Table 2.1) are hemolysin (*ehxA*), type II secretion (*etp*), serine protease (*espP*), *eae* fragment (*ecf*), and *toxB* adhesin (38-39). Hemolysin was the first virulence factor identified in pO157 and consists of 3.4 kb fragment. Thirteen genes encode for type II secretion (T2SS) in pO157 and are similar to T2SS of Gram-negative bacteria (39). EspP cleaves pepsin A and human coagulation factor V, affects colonization and adherence of EHEC, and may be responsible for mucosal hemorrhage. ToxB also induces adherence of EHEC to host cells through the increased secretion of T3SS (40) and may inhibit host lymphocytes. Several published studies have produced conflicting evidence on the role of pO157 in EHEC pathogenesis, and thus, the precise function of pO157 has yet to be elucidated.

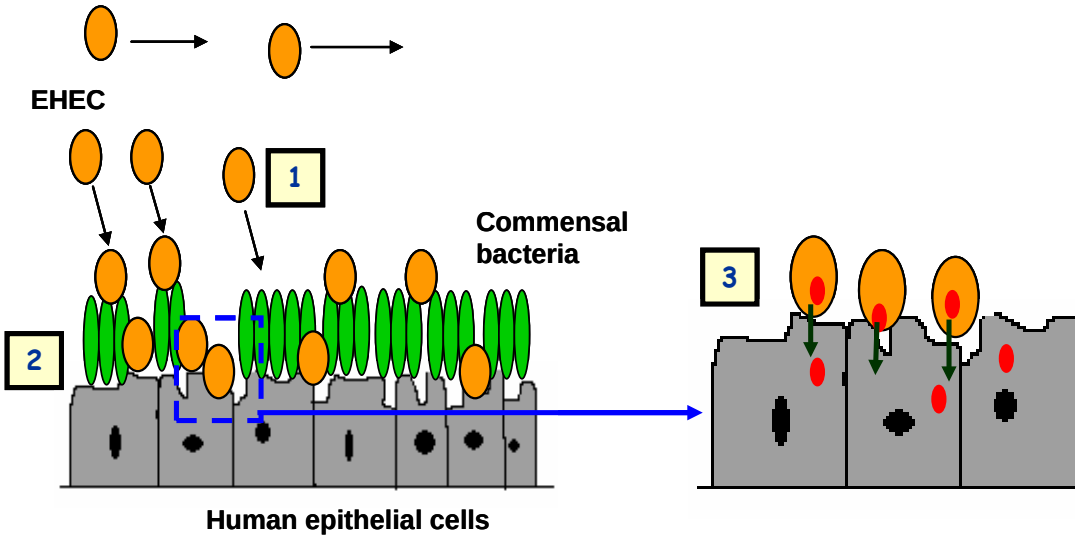

Fig. 2.2. EHEC infection model. The figure details steps during EHEC infection of the GI tract. Migration towards epithelial cell surface (1), colonization of epithelial cells (2), and release of toxins (3).

2.5 EHEC INFECTION PROCESS

The EHEC infection process follows three distinct steps *in vivo* and it is necessary for the pathogen to colonize the GI tract to initiate infection (6). EHEC specifically colonizes the large intestine in humans. The first step in the infection process is migration of the pathogen from the intestinal lumen towards the host cell surface. The second important step is adherence to the host cell surface and formation of A/E lesions through the T3SS. Tir is then translocated into the host cell cytoplasm. The third step involves secretion of virulence factors such as EspA and EspB into the host cell, leading to host cell lysis (Fig. 2.2).

2.6 IMPORTANT BACTERIAL SIGNALING MOLECULES IN THE GI TRACT

2.6.1 Indole

Indole (Fig. 2.1B) is a stationary phase bacterial signaling molecule (41) that is produced in large amounts by approximately 85 species of Gram-positive and Gram-negative bacteria (42). It was first discovered in 1897 that *E. coli* and *Vibrio cholerae* produce indole in stationary phase (43). Commensal *E. coli* produce as much as 600 μM of indole in suspension cultures (22) and indole has been detected in human feces at comparable concentrations (~ 250 - 1100 μM) (44-45).

Indole is produced in *E. coli* from *L*-tryptophan via tryptophan indole-lyase or tryptophanase (encoded by *tnaA*) (41). Initially, indole was dismissed as a mere metabolite and not a signaling molecule due to limited research (46). However, work from our laboratory has shown that indole is an extracellular signal (41), represses *E. coli* K-12 biofilm formation through the sensor for quorum sensing signals, SdiA (41), and is more effective in repressing *E. coli* K-12 biofilm at low temperatures, i.e., 25^{o}C and 30^{o}C (47). Indole also affects drug

resistance and plasmid stability in *E. coli* (48-49). Additionally, in non-indole-producing bacteria, like *Pseudomonas aeruginosa,* and eukaryotes, like fungi, indole reduces virulence and cell growth, respectively (50-51). Thus, indole is a very important interspecies signal.

2.6.2 Autoinducer-2

Previously, it was assumed that bacteria lived unicellularly, and respond to external stimuli singularly and not as a community. However, recent reports have revealed that this assumption is simplistic and somewhat incorrect (52). In fact, bacteria communicate with each other through 'signaling molecules' (52). Through these chemicals, bacteria can monitor their population density, and accordingly regulate gene expression and other phenotypes like motility and biofilm formation (53). This communication is important for bacterial communities to either survive or prosper in the environment that they are within (53). This cell density-dependent, cell-to-cell signaling mechanism is called quorum sensing (QS) and the signal is called an autoinducer (52). Autoinducers are small, hormone-like organic molecules, that on exceeding a critical threshold, cause the bacteria to alter their gene expression (52). Several QS circuits (52) have been identified for both Gram-positive and Gram-negative bacteria that use peptides and acyl-homoserine lactones (AHL) as signals, respectively. In addition, there exists an inter-species signaling system based on the *luxS* – autoinducer-2 (AI-2) signaling.

AI-2 is a stationary phase signaling molecule that unlike other autoinducers, is produced by a large number of bacterial species, including those of *Escherichia, Vibrio, Pseudomonas, Agrobacterium, Erwinia* (54), and thus, is considered to be a common bacterial signal (55). AI-2 is synthesized in bacteria through the conversion of *S*-adenosylhomocysteine to *S*-ribosylhomocysteine, and then *S*-ribosylhomocysteine to (*S*)-4,5-dihydroxypentane-2,3-dione

(DPD) by the enzymes Pfs and LuxS, respectively (55). DPD spontaneously cyclizes to form a number of molecules, and AI-2 (Fig. 2.1B) is one of them.

AI-2 was first identified in *Vibrio harveyi* and it is involved in cell density-dependent light production in these bacteria (55). Bacteria like *E. coli*, in different phases of growth, both produce and consume AI-2 (56). AI-2 is produced and released extracellularly in the exponential phase of bacterial growth, while it is imported back inside the cell during the stationary phase of growth (56). The *lsr* operon is responsible for uptake of AI- 2 and LsrR represses this operon (56). LsrB is the periplasmic AI-2 binding protein. Upon binding to LsrB, AI-2 is internalized via the LsrCD transport system (52). Once internalized, AI-2 is phosphorylated by LsrK and this phosphorylated AI-2 inhibits LsrR, which in turn de-represses the *lsr* operon. Finally, rapid internalization of all the remaining extracellular AI-2 occurs.

Several organisms use AI-2 to control diverse functions, including but not limited to, regulation of virulence gene expression in *Actinobacillus actinomycetemcomitans* (57), EHEC (58), *P. gingivalis* (59), and *V. cholerae* (60), motility, cell division, and biofilm formation in *E. coli* (18, 20, 61), and biofilm formation and carbohydrate metabolism in *Streptococcus gordonii* (62).

Recently, QS systems have been linked with inter-kingdom signaling. In one such example, the AHL-based QS system of the plant pathogen *Serratia liquifaciens* is inhibited by furanone produced by the marine algae *Delisea pulchra* (63). Additionally when AHLs are administered to the legume *Medicago truncatula*, it differentially expresses several proteins (64). Bacterial AHLs also modulate mammalian host cell gene expression; for example, the *P. aeruginosa* signal 3OC12-HSL regulates production of NF-κB in host cells (65) and helps the pathogen to maintain persistent infections. Thus, bacteria communicate not only amongst themselves, they also interact with host cells through these intricate signaling systems.

2.7 IMPORTANT HOST-DERIVED SIGNALING MOLECULES IN THE GI TRACT

2.7.1 Norepinephrine

The human GI tract is enervated with millions of sympathetic nerve fibers (66) that run along the arteries and terminate in the mucosa (67). The sympathetic nervous system (SNS) produces human the hormone NE (Fig. 2.1B) along with several other molecules in small and large vesicles (66). It is important to realize that, in addition to being produced in the adrenal medulla, NE is also produced locally in the GI tract and, thus, local concentrations of this neuroendocrine hormone can be very high (67). NE is directly involved with several immune responses; e.g., NE enhances the migration of monocytes, and increases the pro-inflammatory cytokine IL-8 secretion (67). High concentrations of NE stimulate apoptosis in certain cell types (68). NE also inhibits phagocytosis and natural killer (NK) cell activity at high concentrations (10^{-7} to 10^{-5} M) and reduces secretion of TNF-α, IL-12 and IFN-γ. During Crohn's disease, tissue levels of NE are lower in patients than control subjects (69). Thus, SNS represses the inflammatory reaction via β-adrenergic receptors.

NE has also been studied for a possible role in inter-kingdom signaling. NE has been shown to increase the growth rate of commensal *E. coli*.NE also enhances growth of the pathogen EHEC (70-71) and increases virulence factor production. For example, the K99 pilus adhesion virulence-related factor of EHEC increases in NE-supplemented culture over a 9-15 h incubation period (72), and NE also upregulates iron uptake through enterobactin. Additionally, production of Shiga toxins by EHEC is enhanced (Stx1 by over 100-fold) in the presence of NE (24). Thus, NE could play an important role as an inter-kingdom signal.

2.7.2 Cytokines

Interleukin-8 (IL-8) was first described as an important neutrophil chemotactic factor in 1987 (73). IL-8 is involved in transmigration of leukocytes into tissues, and promotes neutrophil adhesion to a variety of surfaces including, but not limited to, plastic, extracellular matrix proteins, endothelial and epithelial cells. IL-8 is often secreted in response to bacterial infections, as seen *in vitro* with several cell lines (74). IL-8 recruits neutrophils to the site of the infection to clear microbes such as *Candida albicans* (75). Increased IL-8 expression is also observed in diseases such as idiopathic pulmonary fibrosis (76). However, increased IL-8 expression in cystic fibrosis patients reduces the capacity to kill *P. aeruginosa,* thus, resulting in enhanced damage to lungs and increased susceptibility to infection (77). Also, it has been argued that IL-8 induced macrophages may enhance growth of tumor cells by providing growth factors and, thus, IL-8 can promote tumor formation (78).

Interleukin-10 (IL-10) plays an important role in regulation of the immune system through its involvement in several pathophysiological processes. It was first discovered that IL-10 inhibited production of IL-2, tumor necrosis factor α (TNF-α), and interferon γ (IFN-γ) (79) and plays a key role in host immune system suppression. IL-10 blocks inflammatory cytokine production (80) and chemokine secretion (81). Mice lacking IL-10 show symptoms similar to Crohn's disease (82). IL-10 also enhances survival of B cells, T cells, tumor cells, and NK cells. Recently, a report suggested that increased production of IL-10 in the presence of commensal bacteria could be one of the mechanisms of host immune tolerance of the commensal microbial population (83).

Interleukin-12 (IL-12) is a 70kDa heterodimeric protein in its active form, and is a type 1 immune activation cytokine that is released during the early immune response of cells. Dendritic cells and macrophages, which are involved in early cell response to infections, are the primary

producers of IL-12 (84). Thus, IL-12 is secreted in response to tumors, and pathogens such as bacteria, fungi and parasites. Also, release of IL-12 is enhanced in presence of other pro-inflammatory signaling molecules like IFN-γ, IL-4, IL-6 and TNF-α (85-86). It is also important to note that IL-12 is continually secreted until the invading pathogen is cleared from the system.

2.7.3 Nuclear Factor-κB

The NF-κB signaling pathway is an important regulator of the host immune response and plays key role in pathogenesis (87). Pro-inflammatory functions of this pathway are well established. The NF-κB family consists of p50, p52, p65, c-REL, and RELB, which form homo- or hetero-dimers (87). Inhibitor of NF-κB, called IκB, usually keeps this family inactive, and the activation of NF-κB is thus controlled by the IκB kinase (IKK) complex. Once activated, IKK phophorylates IκB, causing subsequent IκB degradation, which allows NF-κB dimerization and active gene transcription.

NF-κB is rapidly activated in response to stress, allowing the host cells to detect potential threats in their environment. NF-κB activates the transcription of genes encoding cytokines, chemokines and antimicrobial molecules (88). However, it also induces the anti-apoptotic genes (89), preventing cellular apoptosis, and reduces necrosis through inhibition of reactive oxygen species (90). Thus, NF-κB protects host cells against infection and helps the cell survive.

2.7.4 Toll-like Receptors

The epithelial innate immune response consists of surface-associated, pattern recognizing receptors called TLRs, which play a critical role in host cell defense against bacterial pathogens (91). There are eleven different types of TLRs and each has its own ligand

that it recognizes and binds to (91); however, they activate similar sets of genes. TLRs recognize pathogen-associated molecular patterns or PAMPs, and activate host cell defense machinery; e.g., the NF-κB signaling pathway, that are important for the immune response.

For example, TLR2 specifically responds to the presence of Gram-positive bacteria through lipoteichoic acid or muramyl dipeptide (92). Similarly, TLR3 detects the presence of double-stranded virus DNA, and activates IRF3, STAT1 and NF-κB. TLR4 is a very important receptor that is responsible for detecting several components of Gram-negative bacteria, primarily lipopolysaccharide (LPS), which is a component of the bacterial cell wall. TLR4-deficient mice are unable to respond to infection with either *Mycobacterium tuberculosis* or LPS (93). Other proteins that TLR4 responds to are pneumolysin, a streptococcal protein, taxol, fibrinogen and fibronectin (91-92). TLR5 has flagellin as its ligand, while TLRs 7-9 recognize foreign RNA and DNA strands. Unlike all of the other TLRs, which are present on cell surface, TLR3, and TLRs 7-9 are present on the endosome. TLR-2, TLR-3, and TLR-9 have been reported to modulate intestinal inflammation and maintain homeostasis (91), unlike other TLRs that are pro-inflammatory in nature. Since TLRs play a crucial role in development of mucosal inflammation, researchers are interested in blocking their activity to reduce inflammation during diseases such as IBD and Crohn's disease. By understanding the mechanism of TLR signaling, anti-inflammatory strategies can be developed for treatment.

CHAPTER III

DIFFERENTIAL EFFECTS OF EPINEPHRINE, NOREPINEPHRINE, AND INDOLE ON EHEC CHEMOTAXIS, COLONIZATION, AND GENE EXPRESSION*

3.1 OVERVIEW

During infection in the GI tract, EHEC is exposed to a wide range of signaling molecules, including the eukaryotic hormones epi and NE, and bacterial signal molecules such as indole. Since these signaling molecules have been shown to be involved in the regulation of phenotypes such as motility and virulence that are crucial for EHEC infections, we hypothesized that these molecules also govern the initial recognition of the large intestine environment and attachment to the host cell surface. Here, we report that epi and NE exert divergent effects on EHEC chemotaxis, motility, biofilm formation, gene expression, and colonization of HeLa cells, as compared to indole. Using a novel two flourophore chemotactic assay, it was found that EHEC is attracted towards epi and NE while it is repelled by indole. In addition, epi and NE also increased EHEC motility and biofilm formation while indole attenuated these phenotypes. DNA microarray analysis of surface-associated EHEC indicated that epi/NE up-regulated the expression of genes involved in surface colonization and virulence while exposure to indole decreased their expression. The gene expression data also suggested that AI-2 uptake was

---

repressed upon exposure to epi/NE but not indole. *In vitro* adherence experiments confirmed that epi and NE increase attachment to epithelial cells while indole decreased adherence. Taken together, these results suggest that epi and NE increase EHEC infection while indole attenuates the process.

3.2 INTRODUCTION

The GI tract is colonized by approximately 10^{14} commensal bacteria consisting of hundreds of bacterial species, including the genus *Escherichia* (3-5). The introduction of pathogenic bacteria such as EHEC into the human gastrointestinal GI tract results in colonization of host cells and leads to the onset of bloody diarrhea and HUS (7, 13). EHEC infections progress through a three-step mechanism, the first of which involves adhesion of bacteria to host cells and the formation of microcolonies (8-9). EHEC infections pose a serious clinical problem as they are often associated with complications and permanent disabilities, including neurological defects, hypertension, and renal insufficiency (12). Understanding the mechanisms underlying EHEC pathogenicity could lead to better approaches for attenuating the deleterious consequences associated with GI tract infections (14). EHEC is exposed to a wide range of signaling molecules in the GI tract. These include bacterial quorum sensing molecules such as AI-2 and AI-3 that are involved in the regulation of phenotypes crucial for virulence and infection (16-17). For example, Sperandio et al. (16, 18) have shown that the adhesion of pathogenic *E. coli* to host cells, which is an important initial step in the infection process, is regulated by these soluble signals. An EHEC *luxS* mutant that is deficient in the synthesis of the AI-2 and AI-3 demonstrated markedly decreased expression of flagella and motility genes required for adherence to epithelial cells (19) and we have found direct addition of AI-2 stimulates *E. coli* biofilm formation (20). The concentration of these bacteria-derived soluble

signals is expected to be high in the GI tract, as both pathogenic as well as non-pathogenic commensal bacteria that reside in the GI tract (3) produce AI-2 and AI-3. Other bacterial signaling molecules such as the stationary-phase signal indole (21) that are produced by commensal *E. coli* (22), are also expected to be present at high concentrations in the GI tract. Indole decreases motility and biofilm formation of non-pathogenic *E. coli* (22), and could be especially important in EHEC infections since it has been shown to regulate virulence genes in enteropathogenic *E. coli* (23).

Recent studies have also shown that eukaryotic signals in the GI tract also play an important role in EHEC adhesion and infections. Catecholamines such as epi and NE have been shown to enhance the growth of pathogenic bacteria (70, 94-95) and production of virulence factors (72, 96). NE has also been shown to increase adhesion of EHEC to cecal mucosa (97), colonic mucosa (4), and ileum (98). Sperandio et al. (16) initially demonstrated that the epi and NE function similarly to AI-3 by activating the virulence genes (e.g., LEE genes) in EHEC (16). Recent studies by Clarke et al. (99) and Walters and Sperandio (17) have also shown that AI-3 and epi utilize the same receptor (QseC) and suggest a synergistic relationship between these two molecules in the expression of virulence genes.

The goal of this work was to investigate the effect of eukaryotic and prokaryotic extracellular molecules on phenotypes important in EHEC infections. We hypothesized that EHEC infection is influenced to different degrees by the different eukaryotic and prokaryotic molecules present in the GI tract. Therefore, we investigated the effect of three molecules – the eukaryotic hormones epi and NE, and the *E. coli* stationary-phase signal indole - on EHEC chemotaxis, biofilm formation, and adherence to epithelial cells. The molecular basis of the alterations in EHEC physiology upon exposure to epi, NE, and indole was also investigated using DNA microarrays. Our results suggest molecular-level interactions between prokaryotic

and eukaryotic signaling molecules in EHEC colonization. To our knowledge, this is the first report of EHEC chemotaxis, motility, and biofilm formation in response to eukaryotic signaling molecules.

3.3 MATERIALS AND METHODS

3.3.1 Bacterial strains, materials and growth

EHEC and *E. coli* TG1 were obtained from ATCC (Manassas, VA) and Stratagene (La Jolla, CA), respectively. Plasmids pCM18 (100) and pDS-RedExpress (Clontech, CA) were used to constitutively express the green fluorescent protein and the red fluorescent protein, respectively. Luria-Bertani medium (LB) was used for overnight cultures of EHEC (ATCC, Manassas, VA). LB supplemented with 0.2% (w/v) glucose (LB glu) was used in all biofilm experiments. Epi and NE were purchased from MP Biomedicals (Irvine, CA). Indole was purchased from Sigma Chemical Co. (St. Louis, MO).

3.3.2 Agarose plug chemotaxis assay

Chemotaxis experiments in agarose plugs were performed by adapting the procedure of Yu and Alam (101) to include live cells tagged with the green fluorescent protein (GFP) and dead cells tagged with the red fluorescent protein (RFP). Briefly, an overnight culture of EHEC/pCM18 was used to inoculate 10 mL of growth medium (10 g/L typtone, 5 g/L yeast extract, 2 mM $MgSO_4$, 2 mM $CaCl_2$) to a turbidity of ~ 0.05 at 600 nm, and grown to mid-exponential phase (turbidity at 600 nm of ~ 0.7). The chemotaxis compound was also added to the medium during growth. Cells were harvested, washed twice, and resuspended in 1 mL of chemotaxis buffer (CB, 1X phosphate buffered saline pH 7.4, 0.1 mM EDTA, 10 mM sodium

succinate). In addition, kanamycin-killed *E. coli* TG1 (pDsRedExpress) was also added to the cell suspension such that the live cell to dead cell ratio was 2:1. In parallel, the chemotaxis compound was mixed with a 2% low melting agarose in CB containing trace amounts of bromophenol blue (to help visualization of the plug) at 55^{o}C. A 10 µl aliquot of the agarose solution containing the chemotaxis compound was added between a glass slide and a raised glass coverslip. Two hundred µl of the cell suspension was immediately added to the slide and the migration of bacteria toward or away from the agarose plug imaged on a Zeiss Axiovert 200 fluorescence microscope (Thornwood, NY). Green and red fluorescence images were obtained every 5 min for 30 min. Images were processed and analyzed using the Zeiss Axiovision 4.5 software.

3.3.3 Motility and biofilm assays

Motility assays were performed as described by Sperandio et al. (102). Briefly, overnight cultures of EHEC were subcultured 1:100 in LB medium and grown to a turbidity of ~ 1.0 at 37^{o}C. Epi (50 µM), NE (50 µM) or indole (500 µM) were added to the motility agar plates (1% tryptone, 0.25% NaCl, and 0.3% agar), and the size of the motility halos were measured after 8 h. Six motility plates were used for each molecule, and the experiment was repeated with three independent cultures (total of 18 motility plates per molecule).

Biofilms assays were performed in 96 well polystyrene plates according to the protocol described by Pratt and Kolter (103). Cells were grown for 24 h without shaking in the presence of epi (50 µM), NE (50 µM), or indole (500 µM). Each data point was averaged from 18 replicate wells (six wells from three independent cultures).

Biofilms for microarray experiments were formed on glass wool for RNA extraction and DNA microarray analysis (104). Briefly, an overnight culture of EHEC was used to inoculate 10

g of glass wool in 250 mL of LB glu medium to a starting turbidity of ~ 0.03. Biofilms were developed at 37^{o}C for 7 h with shaking in the presence of epi (50 µM), NE (50 µM), or indole (500 µM). Based on our unpublished data showing that extracellular indole levels increase after 4 h of culture (due to depletion of glucose) and indole biosynthesis is subject to catabolite repression (105), the glucose in the medium was replenished after 3.5 h so as to minimize the effects of intracellularly produced indole on the observed gene expression patterns. The glass wool was removed from the culture quickly and gently washed two times in 100 mL 0.85% NaCl buffer at 4^{o}C (less than 30 seconds). Biofilm cells were removed from glass wool by sonication for 2 minutes in 200 mL of 0.85% NaCl buffer at 4^{o}C, cell pellets was stored at -80^{o}C, and RNA was isolated as described previously (104).

3.3.4 RNA isolation and DNA microarrays

Total RNA was isolated from EHEC biofilms and RNA quality assessed using gel electrophoresis (106). *E. coli* Genome 2.0 arrays (Affymetrix, CA) containing approximately 10,000 probe sets for all 20,366 genes present in four strains of *E. coli*, including EHEC, were used to profile changes gene expression in EHEC biofilms upon epi, NE, and indole addition. Hybridization was performed for 16 h, and the total cell intensity was scaled automatically in the software to an average value of 500. The data were inspected for quality and analyzed according to the procedures described in Data Analysis Fundamentals which includes using premixed polyadenylated transcripts of the *B. subtilis* genes (*lys*, *phe*, *thr*, and *dap*) at different concentrations. Genes were identified as differentially expressed if the expression ratio (between biofilms treated with epi/NE/indole and untreated control biofilm cells) was greater than 2.0 (based on the standard deviation of fold-change values) (107) and the change p-value is less than 0.05. The differentially expressed genes were annotated using gene ontology definitions

available in the Affymetrix NetAffx™ Analysis Center (http://www.affymetrix.com/analysis /index.affx). The expression data have been deposited in the NCBI Gene Expression Omnibus (GEO, http://www.ncbi.nlm.nih.gov/geo/) and are accessible through GEO Series accession number GSE5552.

3.3.5 Quantitative reverse-transcription PCR

Quantitative RT-PCR was performed using a Bio-Rad iCycler (Bio-Rad, CA) real-time PCR unit (41). Approximately 50 ng of total RNA (from the same sample used for microarray analysis) from control or epi-treated EHEC was used for reverse transcription. Gene sequences were downloaded from the A Systematic Annotation Package for Community Analysis of Genomes, ASAP) website (https://asap.ahabs.wisc.edu/asap/home.php?formSubmitReturn=1) and gene-specific primers were used for *lsrA, lsrB, lsrC,* and *rpoA* (housekeeping control) (Table 3.1). Threshold cycle numbers were calculated using the MyiQ software (Bio-Rad), and PCR products were verified using agarose electrophoresis.

3.3.6 *In vitro* adhesion assays

Adhesion of EHEC to HeLa S3 cells was performed using a previously described protocol (9). HeLa S3 cells (ATCC, Manassas, VA) were routinely cultured and propagated in DMEM medium with 10% heat-inactivated fetal bovine serum (FBS) according to standard protocols (ATCC). Low passage HeLa cells were cultured in to standard 24-well tissue culture plates and grown at 37^{o}C in a 5% CO_2 humidified environment until ~ 80% confluency. HeLa cell monolayers were washed thrice with sterile PBS to remove unattached cells, and the growth

Table 3.1. Primers used for quantitative RT-PCR

Gene	Forward Primer (5'-3')	Reverse Primer (5'-3')
lsrA	AACATCCTGTTTGGGCTGGCAA	AAACAAGCGTTCGGTTTCCGCA
lsrB	AGCATCCTGGCTGGGAAATTGT	AAATTCTTTCACCGTGCCGCGT
lsrC	ACAGCGTTTGGACGCAGTTT	ACGCAGGCTGCAATTGCTTT
rpoA	CGCGGTCGTGGTTATGTG	GCGCTCATCTTCTTCCGAAT

medium was replaced with antibiotic-free DMEM medium with 10% FBS. Approximately 5 x 10^6 of a freshly grown EHEC culture (turbidity of ~ 1.0) was added to each well and incubated for 3 h at 37^{o}C in a 5% CO_2 environment. Loosely attached cells were removed by washing the wells thrice with sterile PBS, and the HeLa cells were lysed in the wells using 0.1% Triton X-100 in PBS. The cell suspension in each well was vigorously vortexed, and serial dilutions of the bacteria were plated on LB plates. Colonies were counted after 24 h incubation at 37^{o}C.

3.4 RESULTS

3.4.1 Effect of epi, NE, and indole on EHEC chemotaxis, motility, and biofilm formation

A standard agarose plug assay (101) was modified to include a live and dead strain, each tagged with a different fluorophore, to create a new assay for studying chemoattraction or repulsion exhibited by EHEC towards epi, NE, and indole. EHEC expressing GFP and kanamycin-killed *E. coli* TG1 with RFP were mixed together and introduced into the vicinity of an agarose plug containing the chemotaxis molecule. Diffusion of epi and NE from the agarose plug resulted in attraction of EHEC (green) and accumulation near the agarose plug while the dead cells (red) were evenly distributed (Figs. 3.1A & 3.1B). The concentration at the edge of the plug was not inhibitory to EHEC as cells were observed attached to the agarose plug after 30 min of exposure. A distinct clearance zone was also detected between the attracted cells and cells in the bulk fluid (i.e., away from the agarose plug), which also suggested a concentration-dependent migration of cells towards epi and NE. This chemoattractive response was similar to that observed with the positive control casamino acids (Fig. 3.1C).

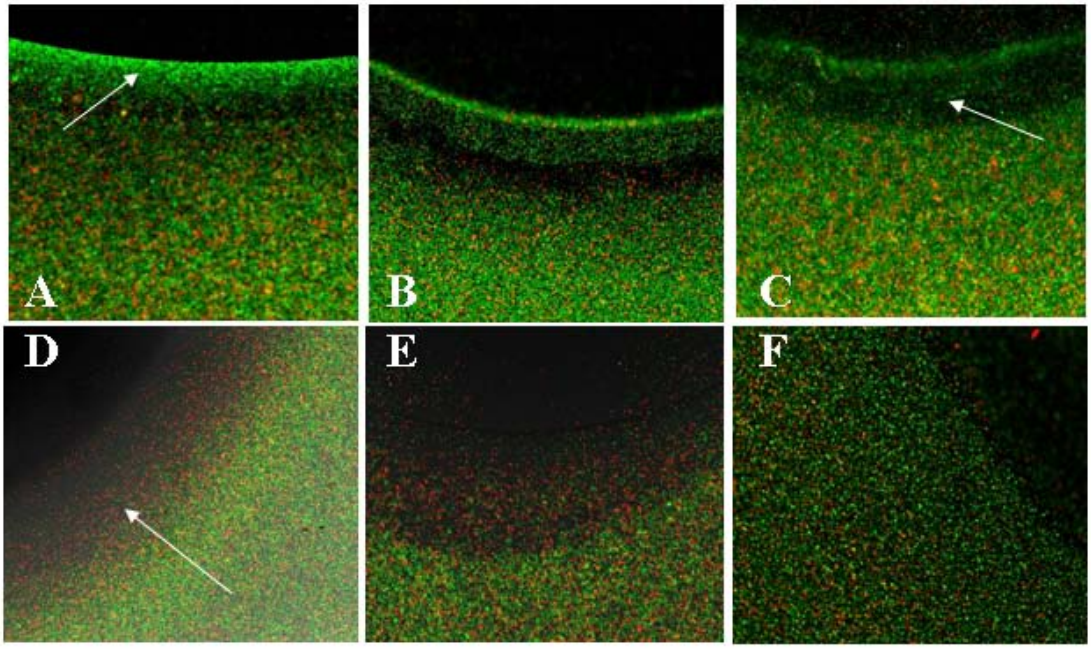

Fig. 3.1. Agarose plug chemotaxis. Attraction or repulsion of EHEC to different chemoeffectants was determined using a modified agarose plug assay. Fluorescence images from bacteria exposed to (A) 500 µM epi, (B) 500 µM NE, (C) 2% casamino acids, (D) 5000 µM Indole, (E) 1 x 10^{-4} M glycerol, (F) 1X M9 salts solution are shown. Green cells are EHEC expressing green fluorescence protein and red cells are kanamycin-killed *E. coli* TG1 expressing red fluorescence protein. Fluorescence images were obtained on a Zeiss Axiovert 200 microscope after 30 min using a 10X objective. Data shown are a representative image from three independent experiments. Arrows indicate chemoattractant ring (Panel A), clearance zone (Panel C), and chemorepellant band (Panel D).

In contrast, exposure to indole resulted in migration of EHEC away from the agarose plug, and a clearance zone was formed closer to the agarose plug (Fig. 3.1D); this repulsion was similar to that observed with the negative control glycerol (Fig. 3.1E). Exposure to a neutral chemoeffectant (M9 salts) did not result in any attraction or repulsion (Fig. 3.1F). These results clearly show that EHEC demonstrates chemotactic attraction towards epi and NE but migrates away from indole.

Based on the significant changes in chemotaxis and its relation to cell motility (20), the effect of epi, NE, and indole on EHEC motility was also investigated. Epi and NE were used at a concentration of 50 μM based on published reports (16), while indole was used at a higher concentration (500 μM) based on the ~ 400 μM extra-cellular concentration of indole in stationary phase cultures of EHEC (25). At these concentrations, no significant alteration in the growth rate of EHEC was observed (1.35 ± 0.02, 1.35 ± 0.02, and 1.33 ± 0.07 for EHEC, EHEC + 50 μM epi and EHEC + 50 μM NE, respectively), indicating that the observed results are not due to changes in growth rate. Addition of epi and NE increased motility by 1.4-fold, as compared to untreated controls, while indole decreased EHEC motility by 2.8-fold (Fig. 3.2).

In addition, the effect of these molecules on EHEC biofilm formation was also determined. Fig. 3.2 also shows that epi and NE resulted in a 1.7- and 1.5-fold increase (statistically significant at $p < 0.01$ using the Student t-test) in EHEC biofilm formation on polystyrene, respectively, after 24 h. On the other hand, addition of indole decreased biofilm formation by 2.4-fold after 24 h. Together, our data indicate that epi, NE, and indole affect EHEC motility and biofilm formation in a manner consistent with their effect on chemotaxis.

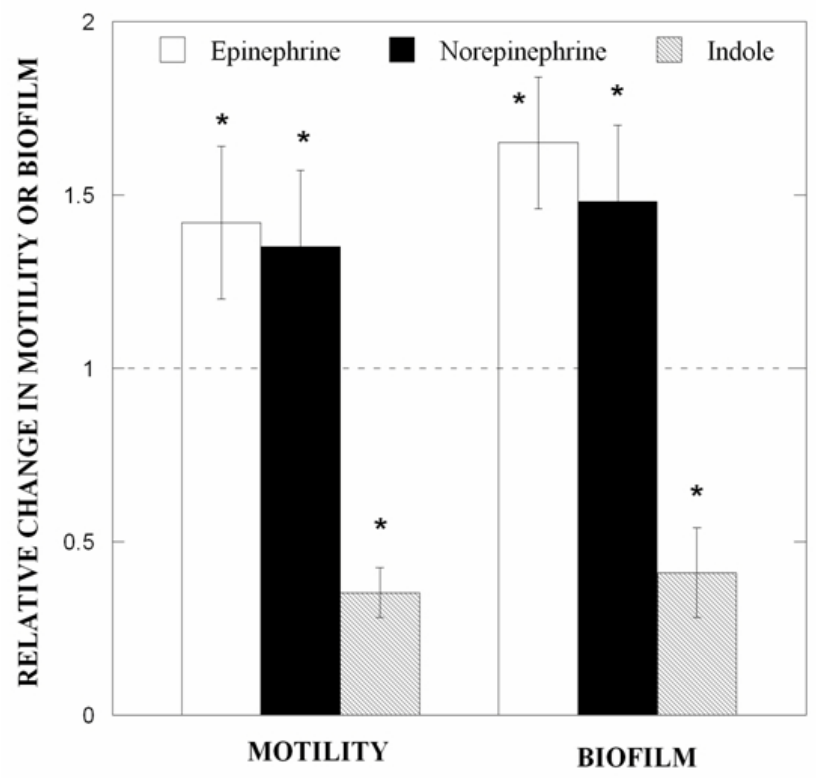

Fig. 3.2. Epi, NE, and indole affect EHEC motility and biofilm formation. The relative change in EHEC motility and biofilm upon exposure to epi (50 µM), NE (50 µM), and indole (500 µM) was determined. Motility data are shown as mean ± one standard deviation from 18 motility agar plates from three independent experiments. Biofilm data are mean ± one standard deviation from 36 wells and three independent experiments. '*' indicates statistical significance determined using the Student t-test ($p < 0.01$).

Table 3.2. Summary of changes in EHEC biofilm gene expression. Significant changes are in bold. Epi = epinephrine; NE = norepinephrine; Ind = indole

Gene Symbol	Fold change Epi	Fold Change NE	Fold Change IND	Gene Title
AI-2 Genes				
c1993	1.4	1.4	1.6	Putative integral membrane transport protein
lsrA	**-9.8**	**-5.3**	1.0	Fused AI2 transporter subunits of ABC superfamily: ATP-binding components
lsrB	**-7.0**	**-5.3**	-1.4	Putative LACI-type transcriptional regulator
lsrC	**-4.3**	**-2.3**	1.2	AI2 transporter
lsrD	**-3.2**	-1.4	1.5	AI2 transporter
lsrG	**-3.2**	**-3.0**	-1.1	Autoinducer-2 (AI-2) modifying protein LsrG
lsrK	**-2.8**	**-2.3**	1.2	AI-2 kinase
lsrR	**-3.7**	**-3.7**	1.1	*lsr* operon transcriptional repressor
Phosphate related Genes				
phnD	**-2.1**	1.2	**2.1**	Phosphonates-binding periplasmic protein precursor
phnG	-1.1	1.5	**2.3**	PhnG protein
phnP	-1.2	1.3	**2.1**	PhnP protein
phoB	**2.1**	**3.0**	**-2.6**	Phosphate regulon transcriptional Regulatory protein *phoB*
phoH	**-4.9**	**-4.6**	-1.9	PhoH protein
phoR	**2.6**	**3.5**	-1.6	Phosphate regulon sensor protein *phoR*
phoU	1.9	**2.1**	**-3.7**	Phosphate transport system protein *phoU*
pstA	**2.5**	**2.6**	**-3.2**	Phosphate transport system permease protein *pstA*
pstB	1.3	1.5	**-3.7**	Phosphate transport ATP-binding protein *pstB*

Table 3.2. Contd.

Gene Symbol	Fold change Epi	Fold Change NE	Fold Change IND	Gene Title
pstC	**2.6**	**3.0**	**-2.3**	Phosphate transport system permease protein *pstC*
pstS	1.1	1.1	**-4.6**	Phosphate-binding periplasmic protein precursor
purE	**3.0**	**3.7**	1.4	Phosphoribosylaminoimidazole carboxylase catalytic subunit
purK	1.2	**2.6**	1.6	Phosphoribosylaminoimidazole carboxylase ATPase subunit
purT	-1.4	**2.5**	**2.1**	Phosphoribosylglycinamide formyltransferase 2
Hydrogenase Genes				
hyaA	**-3.0**	**-3.2**	1.1	Hydrogenase-1 large chain
hyaB	**-4.0**	**-3.5**	1.2	Hydrogenase-1 operon protein *hyaE*
hyaC	**-3.7**	**-3.0**	1.1	Hydrogenase-1 operon protein *hyaF*
hyaD	**-3.2**	**-2.8**	1.2	Hydrogenase-1 small chain precursor
hyaE	**-3.5**	**-2.5**	1.3	Hydrogenase-1 large chain
hyaF	**-3.0**	**-2.6**	1.1	Hydrogenase-1 operon protein *hyaE*
PTS Genes				
mtlA	**-13.9**	**-11.3**	1.0	PTS system, mannitol-specific IIABC component
manX	**-4.6**	**-3.5**	1.1	PTS system, mannose-specific IIAB component
manY	**-2.8**	**-2.3**	1.1	PTS system, mannose-specific IIC component
manZ	**-2.8**	**-2.1**	1.2	PTS system, mannose-specific IID component
fruB	-1.7	**-2.1**	1.2	PTS system, fructose-specific IIA/FPr component

Table 3.2. Contd.

Gene Symbol	Fold change Epi	Fold Change NE	Fold Change IND	Gene Title
Glycerol related Genes				
glgC	**-2.5**	**-3.0**	-1.3	Glucose-1-phosphate adenylyltransferase
glpA	**-4.9**	-1.7	1.7	Anaerobic glycerol-3-phosphate dehydrogenase subunit A
glpD	**-9.2**	**-18.4**	1.3	sn-glycerol-3-phosphate dehydrogenase (aerobic)
glpF	**-5.7**	**-5.7**	1.3	Glycerol uptake facilitator protein
glpK	**-7.5**	**-6.1**	1.1	Glycerol kinase
glpQ	**-2.1**	**-2.5**	-1.1	Glycerophosphoryl diester phosphodiesterase, periplasmic precursor
glpR	-1.6	-2.1	-1.1	Glycerol-3-phosphate regulon repressor
ugpB	**-7.0**	**-6.1**	-1.4	Glycerol-3-phosphate-binding periplasmic protein precursor
Histidine Biosynthesis Genes				
hisA	**-2.1**	**-2.8**	-1.6	1-(5-phosphoribosyl)-5-[(5-phosphoribosylamino)methylideneamino] imidazole-4-carboxamide isomerase
hisB	**-2.3**	**-2.6**	**-2.1**	Bifunctional: histidinol-phosphatase (N-terminal); imidazoleglycerol-phosphate dehydratase (C-terminal)
hisC	**-4.0**	**-4.6**	**-2.8**	Histidinol-phosphate aminotransferase
hisD	**-4.3**	**-4.3**	**-2.6**	Histidine biosynthesis
hisF	**-3.0**	**-3.0**	**-2.0**	Imidazole glycerol phosphate synthase subunit *hisF*
hisG	1.1	-1.3	**-2.8**	ATP phosphoribosyltransferase
hisH	-1.6	**-2.1**	**-2.0**	Imidazole glycerol phosphate synthase subunit *hisH*

Table 3.2. Contd.

Gene Symbol	Fold change Epi	Fold Change NE	Fold Change IND	Gene Title
hisI	**-2.1**	**-2.0**	-1.9	Histidine biosynthesis
hisL	**3.0**	1.1	**-3.7**	His operon leader peptide
hisL	1.7	-1.2	**-3.5**	Histidine biosynthesis
hisP	**-2.5**	-1.4	-1.1	Nucleotide binding
Two Component Signal Transduction Genes				
dos	1.3	**2.1**	1.4	Putative phosphodiesterase, oxygen-sensing protein
evgS	**-3.2**	-1.5	-1.2	Two-component signal transduction system (phosphorelay)
fimZ	1.1	**2.1**	**3.0**	Fimbiral protein Z, putative transcriptional regulator of fimbrial expression (LuxR/UhpA family)
glnL	**3.2**	**2.5**	-1.9	Two-component signal transduction system (phosphorelay)
narL	**-2.6**	**-2.0**	-1.4	Nitrate/nitrite response regulator protein narL
prpR	**-3.5**	**-3.7**	1.1	Regulator for *prp* operon
rstA	**2.5**	1.9	-1.3	Transcriptional Regulatory protein *rstA*
yedV	1.4	**2.6**	**2.0**	Putative 2-component sensor protein
ygeV	**-2.1**	-1.4	-1.5	Two-component signal transduction system (phosphorelay)
Sulfate Genes				
cysD	**-3.0**	**-3.0**	-1.6	Sulfate adenylyltransferase (ATP) activity
cysI	**-3.5**	**-3.0**	-1.2	Sulfite reductase [NADPH] hemoprotein beta-component
cysJ	**-4.3**	**-2.8**	1.0	Sulfite reductase [NADPH] flavoprotein alpha-component
sseA	**-2.1**	-1.9	1.4	3-mercaptopyruvate sulfurtransferase

Table 3.2. Contd.

Gene Symbol	Fold change Epi	Fold Change NE	Fold Change IND	Gene Title
Motility/Chemotaxis genes				
acs	**-8.0**	**-4.3**	1.1	Acetyl-coenzyme A synthetase
c2129	**3.0**	**2.5**	1.5	Cell division activator cedA
c4004	1.3	2.1	1.1	Hypothetical protein
csgA	**-4.3**	**-2.8**	1.5	Cell adhesion
csgB	**-5.7**	**-4.6**	-1.1	Minor curlin subunit precursor
csgF	**-3.7**	**-2.5**	-1.4	Curli production assembly/transport component *csgF* precursor
fimZ	1.1	2.1	**3.0**	Fimbiral protein Z, putative transcriptional regulator of fimbrial expression (LuxR/UhpA family)
fliD	**2.0**	**2.1**	1.4	Cell motility
fliR	-1.1	1.9	**2.3**	Flagellar biosynthetic protein *fliR*
gidB	1.4	**2.1**	1.5	Methyltransferase *gidB*
motB	**-2.3**	-1.2	1.3	Chemotaxis *motB* protein
mreC	1.5	**2.1**	1.2	Rod shape-determining protein *mreC*
sfmA	-1.2	1.5	**2.1**	Putative fimbrial-like protein
sfmF	1.0	1.5	**2.3**	Putative fimbrial-like protein
sfmH	**-2.0**	1.0	**2.5**	Fimbrial assembly protein
yhhP	1.7	**2.5**	1.5	SirA protein
Z0020	1.5	**2.5**	**2.1**	Cell adhesion
Z4971	-1.9	**3.7**	1.9	Cell adhesion
Cytochrome Genes				
appB	**-3.0**	**-2.3**	1.2	Cytochrome BD-II oxidase subunit II

Table 3.2. Contd.

Gene Symbol	Fold change Epi	Fold Change NE	Fold Change IND	Gene Title
appC	**-2.5**	**-2.1**	1.1	Cytochrome BD-II oxidase subunit I
cyoC	**-2.1**	**-3.0**	1.0	Cytochrome O ubiquinol oxidase subunit III
nrfA	**-3.2**	-1.5	1.5	Cytochrome c552 precursor
nrfB	**-2.8**	1.0	1.5	Cytochrome c-type protein nrfB precursor
Cold-shock Protein Genes				
cspA	1.5	1.5	**-3.2**	Cold shock protein *cspA*
cspE	**2.3**	**2.5**	-1.1	Cold shock-like protein *cspE*
cspG	**8.0**	**6.1**	**-4.0**	Cold shock-like protein *cspG*
cspH	**22.6**	**21.1**	**-2.5**	Cold shock-like protein *cspH*
deaD	**2.1**	**2.6**	-1.2	Cold-shock DEAD-box protein A
Anti-sense RNA Genes				
dsrA	**3.5**	**4.9**	1.3	Anti-sense RNA, silencer of *rcsA* gene, interacts with *rpoS* translation
rdlD	**4.0**	**4.0**	**-2.5**	Antisense RNA, trans-acting regulator of *ldrD* translation
sokB	**9.2**	**7.0**	-1.1	Antisense RNA blocking *mokB* and *hokB* translation
sokC	**2.0**	**2.6**	-1.6	Antisense RNA blocking *mokC* (orf69) and *hokC* (gef) translation
Glutamine/Glutamate Genes				
c0018	**24.3**	**24.3**	**5.7**	Putative glutamate dehydrogenase
glnA	1.6	1.3	**-2.3**	Glutamine synthetase
glnH	-1.2	1.0	**-2.1**	Glutamine-binding periplasmic protein precursor

Table 3.2. Contd.

Gene Symbol	Fold change Epi	Fold Change NE	Fold Change IND	Gene Title
glnP	**2.5**	**3.0**	-1.9	Glutamine transport system permease protein *glnP*
gltJ	**3.7**	**4.3**	-1.6	Glutamate/aspartate transport system permease protein *gltJ*
gltK	**2.6**	**2.6**	-1.6	Glutamate/aspartate transport system permease protein *gltK*
gltL	1.4	1.7	-1.9	Glutamate/aspartate transport ATP-binding protein *gltL*
ybeJ	-1.3	-1.1	**-2.5**	Glutamate/aspartate Periplasmic binding protein precursor
Iron Related Genes				
c3773	**2.0**	**2.1**	1.6	Putative iron compound permease protein of ABC transporter family
cydA	**2.0**	**2.8**	-1.1	Cytochrome D ubiquinol oxidase subunit I
cydB	1.9	**2.8**	-1.2	Cytochrome D ubiquinol oxidase subunit II
feoA	**2.5**	**2.6**	-1.3	Ferrous iron transport protein A
feoB	**2.0**	**3.2**	1.0	Ferrous iron transport protein B
fhuB	1.3	**2.5**	1.1	Ferrichrome transport system permease protein *fhuB*
fhuC	1.6	**2.5**	1.0	Ferrichrome transport ATP-binding protein *fhuC*
fhuD	**2.5**	**4.6**	1.1	Ferrichrome-binding periplasmic protein precursor
yodB	**2.5**	**2.6**	-1.3	Cytochrome b561 homolog 1
NADH Dehydrogenase Genes				
nuoA	-1.3	**-2.5**	1.1	NADH dehydrogenase I chain A
nuoB	**-2.0**	**-3.5**	1.0	NADH dehydrogenase I chain B

Table 3.2. Contd.

Gene Symbol	Fold change Epi	Fold Change NE	Fold Change IND	Gene Title
nuoC	-1.7	**-4.0**	-1.1	NADH dehydrogenase I chain C/D
nuoE	**-2.0**	**-4.3**	-1.1	NADH dehydrogenase I chain E
nuoI	-1.1	**-2.5**	1.1	NADH dehydrogenase I chain I
nuoJ	-1.3	**-2.5**	1.3	NADH dehydrogenase I chain J
nuoK	-1.3	**-2.3**	1.4	NADH dehydrogenase I chain K
nuoL	-1.2	**-2.3**	1.4	NADH dehydrogenase I chain L
TCA Genes				
sdhD	**-13.0**	**-21.1**	1.1	Succinate dehydrogenase hydrophobic membrane anchor protein
sdhC	**-12.1**	**-18.4**	1.1	Succinate dehydrogenase cytochrome b-556 subunit
sdhA	**-11.3**	**-16.0**	1.3	Succinate dehydrogenase, catalytic and NAD/flavoprotein subunit
sdhB	**-10.6**	**-12.1**	1.0	Succinate dehydrogenase iron-sulfur protein
sucA	**-7.5**	**-11.3**	1.1	2-oxoglutarate dehydrogenase E1 component
sucB	**-7.0**	**-9.2**	-1.1	Dihydrolipoamide succinyltransferase component of 2-oxoglutarate dehydrogenase complex
sucD	**-6.5**	**-8.6**	1.0	Succinyl-CoA synthetase alpha chain
sucC	**-6.5**	**-8.6**	1.0	Succinyl-CoA synthetase beta chain
acnB	**-2.0**	**-4.3**	1.0	Aconitate hydratase activity
icdA	-1.9	**-2.6**	1.1	Isocitrate dehydrogenase [NADP]
yojH	-1.2	**-2.3**	-1.5	Malate:quinone oxidoreductase
mdh	**-2.0**	**-2.1**	-1.1	Malate dehydrogenase

3.4.2 Gene expression in epi, NE, and indole treated EHEC biofilms

The molecular basis of the effect of epi, NE, and indole on chemotaxis, motility, and biofilm formation was investigated using DNA microarrays. EHEC biofilms were formed in LB glu medium for 7 h on glass wool in the presence of epi, NE, or indole. The glass wool biofilm model was used to mimic surface-associated short-term growth of EHEC, which is similar to the localized adherence required for infection (108). Genes whose expression was altered by at least 2-fold were selected and sorted into functional categories (e.g., metabolism, transport; Table 3.2) and the expression trends with the different stimuli analyzed.

The number of genes differentially expressed in response to epi, NE, and indole treatments were initially compared (Fig. 3.3). A total of 938 and 970 genes were differentially expressed by epi and NE, respectively, with 411 differentially expressed genes common between the two treatments (316 + 80 + 15 genes in Fig. 3.3). In comparison, 163 and 216 EHEC genes were commonly expressed between epi and indole or NE and indole, respectively. Nearly equal numbers of common differentially expressed genes were either similarly (86 out of 163 genes up-regulated by both epi and indole) or divergently (77 out of 163 genes down-regulated by both epi and indole) expressed upon exposure of EHEC to either epi or indole. On the other hand, a majority (197 out of 216) of the common differentially regulated genes between NE and indole were similarly expressed (i.e., genes up-regulated by NE were also up-regulated upon exposure to indole and vice-versa). These results indicate that epi and NE, although similar in structure, exert different effects on EHEC biofilm gene expression.

The common significantly expressed EHEC genes between epi, NE, and indole exposure were further analyzed (i.e., intersection between epi, NE, and indole in Fig. 3.3). Since epi and NE exhibit divergent effects on chemotaxis, motility, and biofilm formation as compared to indole, we sought to classify genes which were either similarly or divergently altered in

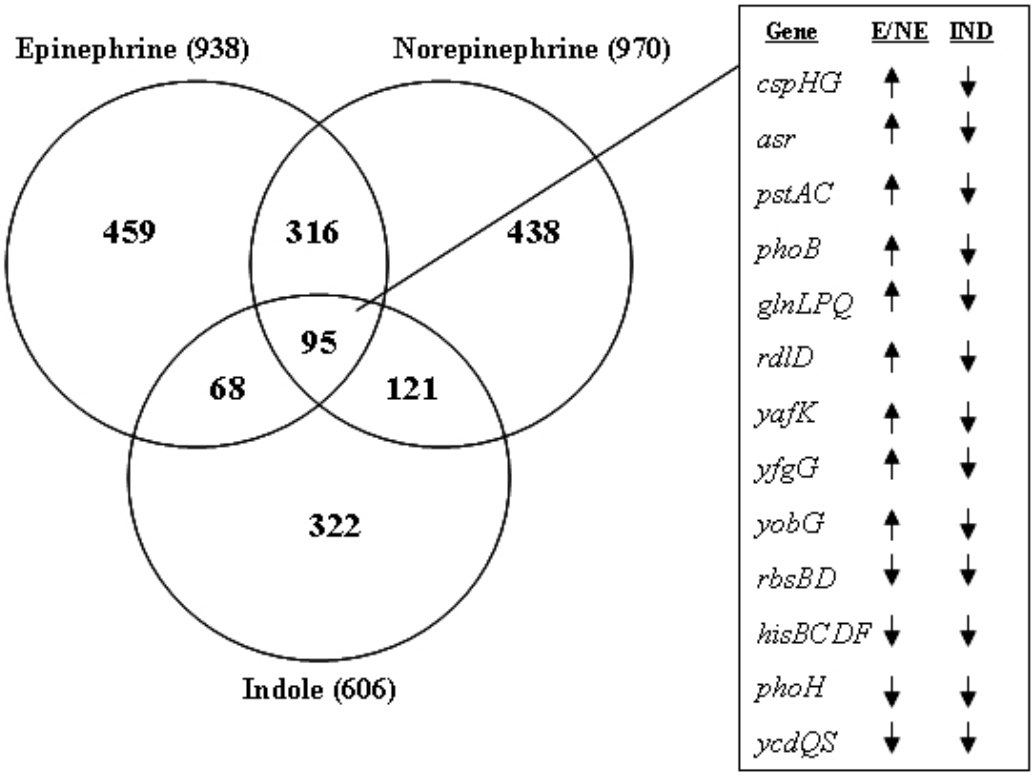

Fig. 3.3. Gene expression in EHEC biofilms upon exposure to epi, NE, or indole. The effect of epi (50 μM), NE (50 μM), and indole (500 μM) on gene expression in EHEC biofilms on glass wool was determined. The number of differentially expressed genes for each molecule, as well as the number of genes common with other molecules, is indicated in the Venn diagram. Genes common between all three molecules are not included in any of the other categories to facilitate interpretation. Annotated genes common to epi, NE, and indole treatments (i.e., divergently expressed between epi/NE and indole) are shown along with arrows indicating increase or decrease in expression. E = epinephrine; N = norepinephrine; IND = Indole.

expression by epi/NE and indole. The addition of epi and NE significantly altered several genes, including those that function in AI-2 uptake, phosphate metabolism, glutamate/glutamine metabolism, cold shock, antisense RNA, hydrogenase activity, phosphotransferase system, TCA cycle, iron uptake and transport, and two component signal transduction systems (Table 3.2).

The expression of genes involved in the transport and uptake of AI-2 were decreased in EHEC biofilms upon exposure to epi and NE. The entire *lsr* operon (*lsrACDBFG*) that encodes an AI-2 uptake and modification system (109-110), as well as regulators of the *lsr* operon (*lsrK* and *lsrR*) demonstrated decrease in expression ranging from 1.4 to 9.8 fold upon exposure to epi and NE (Table 3.3). However, the AI-2 exporter gene, *ydgG* (104), was not significantly altered in expression. The trends observed with the microarrays were further validated using real-time RT-PCR and comparable changes in expression were observed for *lsrA* (-9.8 in microarrays vs. -4.8 with RT-PCR), *lsrB* (-7 in microarrays vs. -2.5 with RT-PCR), and *lsrC* (-4.3 in microarrays vs. -2.4 with RT-PCR). Together, these results suggest that the uptake of AI-2, but not export, was down-regulated by epi and NE in EHEC biofilms.

Genes belonging to three functional groups - cold shock response, phosphate metabolism, and glutamate/glutamine metabolism - were also divergently regulated by indole in EHEC biofilms as compared to epi and NE. For example, the *cspH* gene was up-regulated 22.6-fold by epi and 21.1-fold by NE, but was down-regulated by 2.5-fold upon indole treatment. Changes in the expression of these divergently regulated genes are discussed below.

Cold shock genes: Stress-related cold shock genes were differentially altered in EHEC biofilms by epi, NE, and indole. The data show that cold shock regulator genes (*cspGH*) increased in expression in epi and NE treated biofilms by 6 to 23-fold, while indole decreased the expression of these genes by 2.5 to 4-fold. Earlier work from our laboratory (22) has shown that cold shock genes are up-regulated in developing (7 h), but not mature *E. coli* K12 biofilms.

Table 3.3. Changes in the expression of AI-2 uptake genes in EHEC biofilms after 7 h exposure to epi and NE. Significant changes are in bold

Gene Symbol	Biological Process Description	Fold Change (Array)		Fold Change (RT-PCR)
		Epi	NE	Epi
lsrB	AI-2 transporter	**-7.0**	**-5.3**	**-2.5**
lsrG	Antibiotic biosynthesis	**-3.2**	**-3.0**	-
lsrD	Transport	**-3.2**	-1.4	-
lsrA	Transport	**-9.8**	**-5.3**	**-4.8**
lsrC	Transport	**-4.3**	**-2.3**	**-2.4**
lsrK	Carbohydrate metabolism	**-2.8**	**-2.3**	-
lsrR	Regulation of transcription, DNA-dependent	**-3.7**	**-3.7**	-

The changes in the cold-shock response genes, along with the alterations in biofilm formation (Fig. 3.2A) further support the hypothesis that epi and NE increase EHEC colonization while indole decreases biofilm formation.

Phosphate-related genes: The expression of phosphate-related genes in EHEC biofilms were also divergently regulated upon exposure to epi and NE or indole. Several genes belonging to the *pho* (*phoBRU*) and *pst* (*pstAC*) operons were increased in expression upon exposure to epi or NE whereas the expression of the *pstSCAB* genes and *phoBU* genes was significantly down-regulated in indole-treated biofilms. The phosphate transport system (encoded by the *pstSCAB-phoU* operon) has been previously shown to play an important role in *E. coli* CFT073 virulence and pathogenicity (111). Recently, Buckles et al. (112) have also identified PhoU as a virulence factor in urinary tract colonization. The changes in *pst* and *pho* gene expression observed with epi and NE suggest that these signal molecules increase EHEC virulence while indole inhibits expression of genes involved in virulence.

Glutamate/glutamine genes: The expression of genes involved in glutamate/glutamine biosynthesis and transport were increased in epi and NE treated EHEC biofilms. These included genes involved in glutamate transport (e.g., *gltJ*, *glnP*) that function in importing glutamate into the cell (113-114). A decrease in the expression of these genes was observed with indole; however, these changes in expression were not significant. Genes involved in nitrogen metabolism are known to be involved in virulence of Gram-positive and -negative bacteria (115). Recently, Walters et al. (17) reported that glutamate and oxaloacetate are utilized to generate L-aspartate that is converted to homecysteine and used for autoinducer-3 (AI-3) production. The increase in the expression of genes involved in glutamate intake suggests that epi/NE might stimulate AI-3 production in EHEC during biofilm formation, whereas indole might inhibit the synthesis of AI-3 (although the changes in the expression of *glnP* and *gltJ* are slightly below the

two-fold significance threshold).

3.4.3 Adherence to HeLa cells in the presence of epi, NE, and indole

Based on the chemoattraction of EHEC to epi and NE and repulsion away from indole, we hypothesized that these molecules would also divergently impact EHEC adhesion that leads to virulence and infection. The human cervical carcinoma epithelial cell line, HeLa S3, was used for determining the effect of epi, NE, and indole on EHEC adherence to epithelial cells. Although not of intestinal origin, HeLa cells have been extensively used for studying EHEC infections as they exhibit several classical features of infection including the formation of attaching and effacing lesions (6, 9). Fig. 3.4 shows that exposure to 50 μM of epi or NE for 3 h increased the attachment of EHEC to HeLa cells by 3.4 and 5.2-fold, respectively. On the other hand, adherence to HeLa cells in the presence of 500 μM of indole was reduced by 3.1-fold as compared to untreated controls. These results are consistent with the effect that these molecules have on EHEC chemotaxis, motility, biofilm formation, and gene expression.

3.5 DISCUSSION

The data presented in this report clearly demonstrate that the eukaryotic signaling molecules epi and NE impact EHEC chemotaxis, motility, biofilm formation, gene expression, and attachment to epithelial cells in a manner different from that of the prokaryotic signal indole. The mechanisms utilized by this enteric pathogen to ‘recognize’ its environs and initiate colonization are not fully understood. Kaper and Sperandio (13) have proposed that pathogenic *E. coli* detect quorum sensing molecules from commensal bacteria, as well as other eukaryotic signals in the GI tract, to initiate colonization and infection. Our data provide evidence that EHEC can utilize eukaryotic and prokaryotic signals to ‘sense’ and detect the appropriate

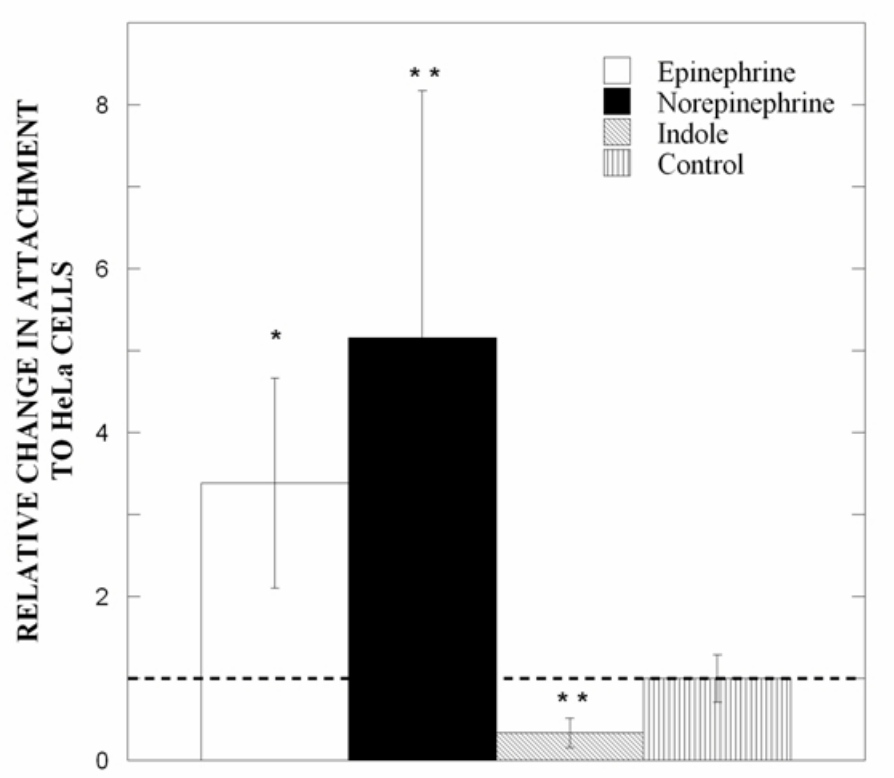

Fig. 3.4. Epi, NE, and indole affect EHEC attachment to HeLa cells. The relative change in EHEC attachment to HeLa cells after 3 h of exposure to epi (50 µM), NE (50 µM), and indole (500 µM) was determined. Cell counts (mean ± one standard deviation) are from duplicate LB agar plates and generated from 5 HeLa cell culture wells. Control indicates EHEC cell counts obtained without addition of any molecule. '*' and '**' indicate statistical significance determined using the Student t-test at $p < 0.01$ and $p < 0.005$, respectively.

location (i.e., large intestine) prior to colonization.

The chemotactic migration of EHEC towards epi and NE is especially intriguing as it suggests that the pathogen has evolved to recognize these signals during host cell infections. Sensing of epi, NE, and indole by EHEC could be the first step in a sequence of events leading to infection, as phenotypes such adherence and colonization, which are down-stream of chemotactic recognition and important for infection, are also up-regulated by epi and NE. Indeed, catecholamines have been shown to increase the adherence of EHEC to intestinal mucosa in different *in vivo* models of infection (4, 97). Our observations on the recognition of epi and NE by EHEC are also in agreement with other reports on epi and NE regulating the expression of virulence genes and infection (16-17), and together, suggest an important role for these molecules in EHEC infections.

Even though the presence and concentration of epi and NE in the intestinal lumen has not been directly measured, it is reasonable to assume that EHEC encounters these molecules during infection. It is well established that approximately 50% of the NE present in the human body is synthesized in the GI tract by the enteric nervous system (116-117). Hence, very high local concentrations of catecholamines exist in the GI tract, which can result in NE leaking into the lumen through diffusion driven by the concentration gradient (118). Evidence towards this has been presented by Chen et al. (119) who demonstrated that addition of 10 μM NE to the contraluminal side of mucosal explants from cecum and colon increases EHEC adherence on the luminal side. The likelihood of NE also being present in the lumen is also supported by the work of Ahlman et al. (120-121) who detected a different neuroendocrine molecule, serotonin, in the intestinal lumen. However, it should be noted that epi is less likely to be present in the intestinal lumen, as there have been no prior reports on epi being generated through the enteric nervous

system or by the mesenteric organs (116). Hence, the concentration gradients driving diffusion of epi in to the lumen will be smaller than that observed with NE.

We restricted our investigation to gene expression changes in a surface-associated (biofilm) model as opposed to planktonic cultures because EHEC is predominantly found in this mode during infections (i.e., localized adherence of microcolonies to epithelial cells). However, very little is known about enterohaemorrhagic and enteropathogenic *E. coli* biofilms *in vivo*. The first report on enteropathogenic *E. coli* biofilm formation *in vitro* was only recently published by Sperandio and co-workers (122). However, the surface-attached growth is a valid model as the microcolonies formed during EHEC infection are also a key element in biofilm formation. Second, genes involved in pathogenic *E. coli* infections (e.g., EspA, BFP) have also been shown to play a key role in biofilm formation (122). Third, the persistent nature of EHEC infections is similar to the antimicrobial resistance demonstrated by surface-associated bacteria; therefore, surface-associated bacteria can be a good model for studying EHEC infections (122). The above lines of evidence suggest surface-associated growth is an important aspect of EHEC pathogenesis.

Our data clearly show that 15 genes (encoding for functions related to virulence and biofilm formation) are divergently regulated between epi/NE and indole. It should also be noted that these signals also exhibited similar effects on the expression of nearly 80 other genes (Fig. 3.3). However, a majority of these similarly-regulated genes are hypothetical proteins, and of the annotated genes, none are related thus far to surface-attachment or virulence. Therefore, based on the available annotation information, we propose that epi/NE and indole play antagonistic roles during EHEC colonization and infection of epithelial cells. Identification and characterization of the 80 similarly regulated genes is needed to generate a comprehensive picture of the role that these molecules play during EHEC infection in the GI tract. Unpublished

data indicate that some of the genes (e.g., *pstA*) identified in our study are important in the EHEC response to NE and in infection, as a EHEC *pstA* mutant does not demonstrate a significant increase in attachment to HeLa cells upon exposure to NE (data not shown).

The changes in the expression of glutamate transport genes suggest an intriguing possibility that epi and NE are involved in up-regulating AI-3 production. Since glutamate is involved in AI-3 synthesis (17), it is possible that this increase in glutamate uptake underlies an increase in AI-3 synthesis, and thereby, virulence. While some genes related to virulence (e.g., *phoU*) were altered in expression, none of the virulence genes (e.g., *eae*) *per se* demonstrated any significant changes in expression upon treatment with epi and NE. These results are in contrast to other studies (4, 118) that have reported increased production of shiga toxins by EHEC upon exposure to catecholamines. However, the experimental conditions between the two studies are sufficiently different (rich LB medium in our study versus serum-based basal medium; gene expression measurement at 7 h in our study versus shiga toxin measurement at 12, 24, and 48 h) and possibly underlie the observed differences. It is also possible that colonization of abiotic surfaces (such as glass wool in our study) does not lead to expression of virulence genes as the cues from epithelial cells may be necessary for induction of the virulence genes may be missing (25). This would also explain the decrease in the expression of curli genes (*csgAB, csgF*) upon exposure to epi and NE, given that curli have been shown to mediate pathogenic *E. coli* internalization (123). Current work in our laboratory focuses on comparing virulence gene expression between EHEC colonization of abiotic and biotic surfaces.

The entire *lsr* operon was down-regulated upon exposure to epi and NE but not indole, which suggests that the uptake of AI-2 was down-regulated upon exposure to epi and NE and does not play a significant role in biofilm formation. However, unpublished data from our lab show that addition of AI-2 increases EHEC biofilm formation by 9.9-fold after 24 h. The

increase in EHEC biofilm upon addition of AI-2 is also consistent with our prior work (20, 104) showing that an AI-2 export deficient K12 mutant (Δ*ydgG*) demonstrates 7000-fold increase in biofilm formation (104). Together, these suggest the possibility that a second AI-2 transporter is present in EHEC (that is not impacted by the addition of epi or NE), as our data (not shown) also show no difference in intracellular AI-2 levels between control and epi/NE treated EHEC. The notion of a second AI-2 transporter is also consistent with that previously proposed by Wang et al. (109) in non-pathogenic *E. coli* and Taga et al. (124) in *S. typhimurium*.

It is interesting to note that some of the genes up-regulated by NE in EHEC biofilms are also similarly altered by other bacterial molecules. Recent work from our laboratory (25) shows that the indole derivative isatin (1-H-indole-2,3-dione) up-regulated the expression of cold-shock response genes (*cspGH*, *deaD*) by 4.6 to 17.1-fold and down-regulated the expression of the AI-2 uptake genes (*lsrACDBFG*) by 10.6 to 61-fold, both of which consistent with the data presented in this study (Table 3.2). Similarly, both NE and isatin down-regulated the expression of genes involved in sulfur metabolism (*cys* genes), which are important in biofilm formation (125). Together, these results suggest commonalities between the effect of NE and isatin on EHEC physiology, especially with respect to AI-2 signaling and biofilm formation.

The consistency with which epi, NE, and indole impact five different responses – chemotaxis, motility, biofilm formation, gene expression, and adherence to HeLa cells – strongly indicates that these three molecules are important determinants of EHEC colonization in the GI tract. It should be noted that at the concentrations used, epi and NE did not increase the growth rate of EHEC, which is in contrast to prior reports describing NE-mediated increase in growth of EHEC and other bacteria (71, 95). However, the similar growth rates observed between control and epi/NE treated cultures further emphasizes the fact that the changes observed in chemotaxis,

motility, biofilm formation and HeLa cell adherence are not an artifact of increased cell density arising from increased growth rate upon exposure to epi/NE.

Our data suggest a complex scenario where the individual signals in the GI tract exert markedly different effects on the different phenotypes, with the net resultant of these interactions determining the extent of colonization and host cell infection. The divergence in the response to epi/NE vs. indole suggests that concentration-dependent interactions between these abundant could be important in GI tract infections. For example, a predominance of epi or NE (such as during stress or after injury) could lead to increased chemotactic migration and colonization of host cells, while excess indole can lead to a decrease in the extent of EHEC colonization. While the current study establishes the response of EHEC to a single concentration of these molecules, the colonizing pathogen is likely to encounter diffusion-driven gradients of different signals in the intestinal lumen. Current work in our laboratory is focusing on presenting different concentration gradients of signaling molecules and their combinations to EHEC and investigating their effect on chemotaxis and colonization.

Based on the divergent regulation of EHEC chemotaxis, motility, and biofilm formation by epi/norpei and indole, we propose a model for EHEC colonization in the GI tract that is dependent on indole concentration (Fig. 3.5). In this model, it is assumed that neuroendocrine signals such as epi and NE are present in the intestinal lumen (with some diffusion-driven gradient) throughout the large intestine while spatial (positional) heterogeneities in the concentration of indole exist in the large intestine due to heterogeneities in the distribution of commensal bacteria (especially that of indole-producing non-pathogenic *E. coli*) (126). We propose that the migration of EHEC to the epithelial cell surface is primarily driven by ‘sensing’ of epi/NE but occurs only in regions of the biofilm where indole concentration is low or below a

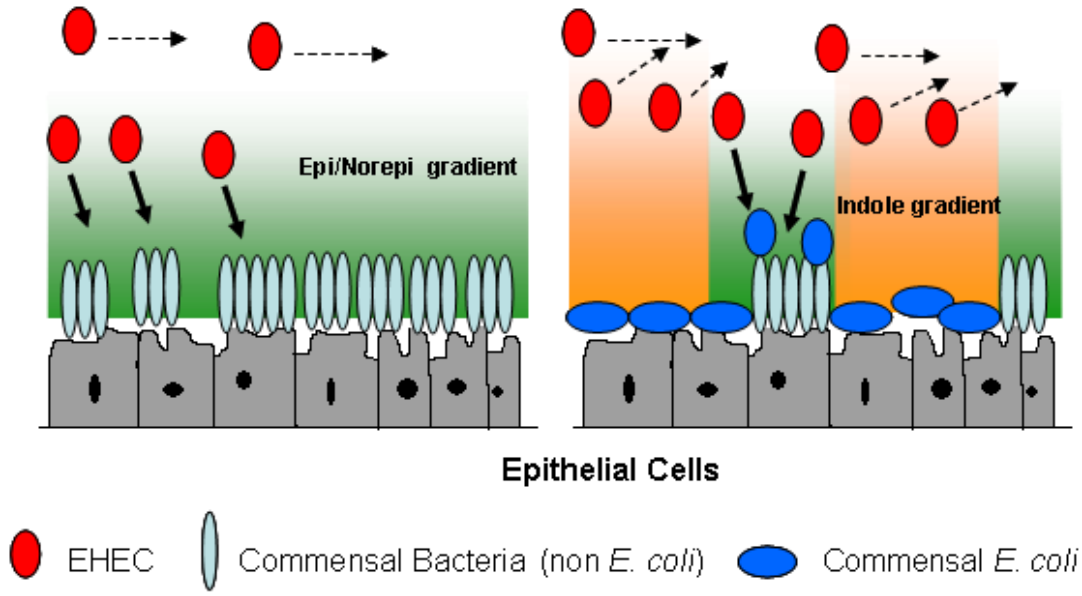

Fig. 3.5. Hypothetical model for EHEC colonization in the GI tract. Gradients of epi and NE influence the chemotactic migration of EHEC to epithelial cell surfaces. Cells that do not encounter high concentrations of epi and NE will continue to move parallel to, and not toward, the epithelial cell surface. (A) In the absence of indole-secreting commensal *E. coli*, colonization of the non-pathogenic biofilm occurs throughout the epithelial cell surface. (B) In the presence of commensal *E. coli*, the pathogen is exposed to gradients of indole which repel it from the host cells. In this scenario, colonization occurs only in regions where non-pathogenic, non-*E. coli* bacteria are present. The direction of migration is indicated by arrows.

critical threshold value. It follows that EHEC colonization occurs to a large extent in regions of the GI tract that are not colonized by non-pathogenic *E. coli* (i.e., regions with low levels of indole). Furthermore, since EHEC itself secretes indole (~500 μM), subsequent colonization will occur only in places that are not already colonized by the pathogen, thereby contributing to further colonization and the spread of infection. Thus, the extent of EHEC colonization is likely to be strongly influenced by the spatial distribution of both eukaryotic signals and indole-producing commensal bacteria in the GI tract.

CHAPTER IV

TEMPORAL REGULATION OF ENTEROHEMORRHAGIC *ESCHERICHIA COLI* VIRULENCE MEDIATED BY AUTOINDUCER-2*

4.1 OVERVIEW

The AI-2 molecule is produced by many bacterial species including various human GI tract commensal bacteria, and has been proposed to be involved in inter-species communication. Since pathogens are likely to encounter AI-2 in the GI tract, we studied the effects of AI-2 on various phenotypes associated with EHEC infections. AI-2 attracted EHEC in agarose plug chemotaxis assays and also increased swimming motility, as well as increased EHEC attachment to HeLa cells. The molecular basis underlying the stimulation of EHEC chemotaxis, motility and colonization by AI-2 was investigated at the transcriptome level using DNA microarrays. We found that exposure to AI-2 altered the expression of 23 LEE genes directly involved in the production of virulence determinants, as well as other genes associated with virulence (e.g., 46 flagellar/fimbrial genes, 24 iron-related genes), in a temporally-defined manner. To our knowledge, this is the first study to report AI-2 mediated regulation of EHEC chemotaxis and colonization, as well as temporal regulation of EHEC transcriptome by AI-2. Our results suggest that AI-2 is an important signal in EHEC infections of the human GI tract.

---

* Reprinted with permission from "Temporal regulation of enterohemorrhagic *Escherichia coli* virulence mediated by Autoinducer-2" by Tarun Bansal, Palmy Jesudhasan, Suresh Pillai, Thomas K. Wood, and Arul Jayaraman, 2008, *Applied Microbiology and Biotechnology,* 78:811-819, Copyright by Springer (www.springerlink.com).

4.2 INTRODUCTION

The GI tract is colonized by approximately ~ 10^{14} bacteria belonging to hundreds of species that exist in a symbiotic relationship with the host without leading to host inflammatory response (5). However, the introduction of pathogens, such as EHEC, into the GI tract disturbs this delicate balance between prokaryotes and eukaryotes (5), and causes bloody diarrhea and HUS (7). Currently EHEC infections are not treated with antibiotics as this has been shown to increase development of HUS in infected children (14), as well as lead to the increased release of shiga-like toxins (10). In the United States there are approximately 70,000 infections annually and 2,000 hospitalizations with an overall cost of $405 million (11), which makes EHEC infections a serious problem.

EHEC infections have been reported to proceed in three stages: migration of the pathogen toward the epithelial cell surface, colonization of epithelial cells, and infection of cells by releasing shiga-like toxins (9). It is becoming increasingly evident that prokaryotic and eukaryotic cell-cell communication signals present in the GI tract impact the different steps involved in EHEC infections. Bacterial signals present in the GI tract include molecules produced by the commensal bacterial flora (e.g., indole, a stationary phase signal secreted by commensal *E. coli*) (41) and those involved in quorum sensing (e.g., AI-2 and AI-3) (127). Recent results from our laboratory have shown that indole attenuates EHEC chemotaxis, motility, biofilm formation, colonization of epithelial cells, and the expression of genes related to virulence (26), suggesting that indole signaling could be important in EHEC infections. Similarly, AI-3 has also been shown to regulate EHEC virulence and flagellar gene expression (16) and function similar to the human hormone epi (17). However, the effect of AI-2, which has been proposed as an inter-species signaling molecule and is produced by many species of commensal bacteria (3), on EHEC virulence and infection has not been fully understood.

AI-2 is synthesized in bacteria through the conversion of *S*-adenosylhomocysteine to *S*-ribosylhomocysteine, and then *S*-ribosylhomocysteine to (*S*)-4,5-dihydroxypentane-2,3-dione (DPD) by the enzymes Pfs and LuxS, respectively (55). DPD spontaneously cyclizes to form a number of molecules, and AI-2 is one of them. While purified AI-2 (DPD) has been shown by us to be directly involved in non-pathogenic *E. coli* biofilm formation (20) and three groups have shown that the inability to form AI-2 stimulates motility (18, 107, 128), its effect on pathogenic *E. coli* has been inconsistent. For example, a recent study (127) reported that addition of AI-2 to a EHEC *luxS* mutant did not significantly alter the expression of virulence genes other than LEE4 and LEE5, and concluded that AI-2 does not impact EHEC virulence. However, this study did not account for temporal regulation of AI-2 uptake and signaling.

The goal of this study was to investigate the effect of AI-2 on phenotypes related to EHEC virulence and infection. Since AI-2 concentration is likely to be high in the human GI tract, we hypothesized that AI-2 will significantly impact EHEC colonization and infection. We studied the relative changes in EHEC chemotaxis, motility and attachment to HeLa cells – important components of EHEC infections – in the presence of AI-2 using a low-nutrient medium that mimics the GI tract environment (24). The temporal response of EHEC gene expression in response to AI-2 exposure was also investigated using a series of DNA microarrays. Our results suggest an important role for AI-2 in EHEC infections. To our knowledge, this is the first study to report AI-2 mediated regulation of EHEC chemotaxis and colonization, and the temporal response of EHEC to AI-2.

4.3 MATERIALS AND METHODS

4.3.1 Bacterial strains, materials and growth

Strain VS94 (EHEC Δ*luxS*) (16) was kindly provided by Dr. V. Sperandio. Plasmids pCM18 (100) and pDS-RedExpress (Clontech, CA) were used to constitutively express GFP and RFP respectively. LB medium was used to grow overnight cultures of bacteria. 10 µg/mL tetracycline, 100 µg/mL kanamycin and 150 µg/mL erythromycin were used for plasmid selection. AI-2 as (*S*)-4,5-dihydroxy-2,3-pentanedione was purchased from Omm Scientific (Dallas, TX).

4.3.2 Agarose plug chemotaxis assay

Chemotaxis assay in agarose plugs was performed as described previously (26). Briefly, an overnight culture of VS94 expressing pCM18 was used to inoculate 10 mL growth medium with erythromycin, and the culture was grown to mid-exponential phase (turbidity of 0.7 at 600 nm). The cells were harvested, washed and resuspended in chemotaxis buffer with kanamycin-killed *E. coli* TG1/pDS-RedExpress cells in a 2:1 ratio and were exposed to a plug containing AI-2. Migration of bacteria was imaged on a Zeiss Axiovert 200 fluorescence microscope (Thornwood, NY) over a period of 20 minutes. Images were analyzed using Zeiss Axiovert software, Version 4.5.

4.3.3 Motility assay

Swimming motility was assayed as previously described (26). Briefly, overnight culture of VS94 was sub-cultured to a turbidity of 0.05 at 600 nm in LB medium and grown to a turbidity of ~ 1.0 at 600 nm at 37°C. AI-2 (1 µM to 100 µM) was added to the motility agar

plates (1% tryptone, 0.25% NaCl, and 0.3% agar), and the sizes of the halos were measured after 8 h. Five motility plates were used for each AI-2 concentration.

4.3.4 *In vitro* adhesion assays

Adhesion of EHEC to HeLa S3 cells was performed using a previously described protocol (26). HeLa S3 cells (ATCC, Manassas, VA) were cultured and propagated in DMEM with 10% heat-inactivated bovine serum according to standard protocols (ATCC). Low-passage-number HeLa cells were cultured in standard 24-well tissue culture plates and grown at 37°C in 5% CO_2 until ~ 80% confluence. HeLa cell monolayers were washed two times with sterile PBS to remove unattached cells, and the growth medium was replaced with antibiotic-free DMEM with 10% bovine serum. Approximately 10^6 cells of a freshly-grown VS94 culture (turbidity of ~ 0.8 at 600 nm) were added to each well and incubated for 3 h at 37°C and 5% CO_2. Loosely attached cells were removed by washing the wells two times with sterile PBS, and the HeLa cells were lysed in the wells using 0.1% Triton X-100 in PBS. The cell suspension in each well was vigorously vortexed, and serial dilutions of the bacteria were plated on LB plates. Colonies were counted after 24 h incubation at 37°C.

4.3.5 AI-2 uptake assay

Overnight cultures of VS94 were diluted in Standard American Petroleum Institute (SAPI) medium (24) to a turbidity of 0.1 at 600 nm. SAPI medium contains limited nutrients (2.77 mM dextrose, 6.25 mM ammonium nitrate, 1.84 mM monobasic potassium phosphate, 3.35 mM potassium chloride, 1.01 mM magnesium sulfate and 10 mM HEPES); hence, it was used here to mimic the *in vivo* milieu of the human GI tract (24). The medium pH was adjusted to 7.5 and filter-sterilized. 30% (v/v) bovine serum was then added. The cells were grown to a

turbidity of approximately 0.5 at 600 nm at 37^{o}C before adding 100 µM AI-2. Turbidity was measured and supernatants were collected every hour for 7 h after addition of AI-2. Three independent cultures were used, and the *V. harveyi* autoinducer assay was performed as described previously (129). Briefly, an overnight culture of *V. harveyi* was diluted 1:5000 in fresh AB medium, mixed with supernatants in a ratio 9:1, and grown for 4 h at 30^{o}C with shaking. Luminescence was then measured using TD-20e luminometer (Turner Biosystems, Sunnyvale, CA) to determine the amount of extracellular AI-2 remaining at each time-point.

4.3.6 RNA isolation and DNA microarrays

Overnight cultures of VS94 were diluted in SAPI medium to a turbidity of 0.1 at 600 nm. The cells were allowed to grow to a turbidity of 0.5 at 600 nm at 37^{o}C and 100 µM AI-2 was added to the culture. In the control flasks, no AI-2 was added. The cultures were then allowed to grow for 3.5 h, 4 h, 4.5 h or 5.5 h before cell pellets were collected by centrifugation and stored at -80^{o}C.

Total RNA was isolated from the cell pellets, and RNA quality was assessed using gel electrophoresis. *E. coli* Genome 2.0 arrays (Affymetrix, California) containing 10,208 probe sets for all 20,366 genes present in four strains of *E. coli*, including EHEC, were used to profile changes in gene expression using RNA samples for each treatment. Hybridization was performed for 16 h, and the total cell intensity was scaled automatically in the software to an average value of 500. The data were inspected for quality and analyzed according to the procedures described by the manufacturer (Affymetrix Data Analysis Fundamentals) which include using premixed polyadenylated transcripts of the *B. subtilis* genes (*lys*, *phe*, *thr*, and *dap*) at different concentrations. Genes were identified as differentially expressed if the expression

Table 4.1. Summary of changes in VS94 gene expression in presence of AI-2. Relative changes less than 1 indicate the genes were repressed in presence of AI-2. Relative changes greater than 1 indicate genes were induced in presence of AI-2

Gene	Relative Change (AI-2/control)				Function
	3.5 h	4 h	4.5 h	5.5 h	
AI-2 uptake operon					
lsrC	8.57	13.00	9.19	1.23	AI-2 transporter: putative ABC transport system permease protein
lsrB	7.46	10.56	6.50	1.15	Putative LACI-type transcriptional regulator
lsrG	7.46	8.00	6.06	1.00	Autoinducer-2 (AI-2) modifying protein LsrG
lsrK	7.46	6.50	5.28	1.32	AI-2 kinase
lsrA	7.46	11.31	8.00	1.23	Fused AI-2 transporter subunits of ABC superfamily
yneB	6.50	6.06	6.06	1.15	putative aldolase
lsrD	6.50	8.57	8.57	1.14	AI-2 transporter: putative ABC transport system permease protein
lsrR	6.06	8.00	6.50	1.23	*lsr* operon transcriptional repressor: putative transcriptional regulator, *sorC* family
Virulence/LEE genes					
eae	0.81	0.87	2.00	1.15	Intimin adherence protein
espF	0.71	0.87	1.52	1.15	Putative secreted protein encoded by cryptic prophage CP-933M
espA	0.76	0.66	1.62	1.23	Secreted protein EspA
sepQ	1.07	0.81	1.62	1.15	Type III secretion system SepQ protein
sepL	0.81	0.81	1.74	1.07	Type III secretion system SepL protein
escS	0.81	0.66	1.87	1.23	Transport
escU	0.93	0.68	1.87	1.15	Transport
escC	0.93	0.87	1.74	1.23	Protein transporter activity
cesD	0.87	0.76	1.87	1.15	Response to stress

Table 4.1. Contd.

Gene	Relative Change (AI-2/control)				Function
	3.5 h	4 h	4.5 h	5.5 h	
escT	0.87	0.71	1.74	1.15	Protein targeting
escV	1.00	0.81	1.62	1.23	Protein secretion
escR	0.87	0.76	1.62	1.15	Type III protein (virulence-related) secretor activity
escN	1.07	0.81	1.52	1.32	Defense response
escF	0.71	0.76	1.74	1.07	Pathogenesis
eaeH	0.57	0.66	2.00	1.23	Attaching and effacing protein, pathogenesis factor
ECs3718	0.81	0.76	1.52	1.15	Pathogenesis
ECs1092	0.71	0.93	1.62	1.23	Viral envelope fusion with host membrane
ECs2183	0.62	1.00	1.74	1.23	Viral envelope fusion with host membrane
ECs1535	0.71	1.00	1.52	1.15	Viral envelope fusion with host membrane
Z4190	0.93	0.71	2.00	1.23	Type III protein (virulence-related) secretor activity
Z4189	0.93	0.88	1.87	1.07	Type III protein (virulence-related) secretor activity
Z4196	0.81	0.76	1.87	1.23	Type III protein (virulence-related) secretor activity
Z4180	1.23	0.81	1.87	1.32	Type III protein (virulence-related) secretor activity
Flagellar/fimbrial genes					
fliR	0.57	0.66	1.74	1.00	Flagellar biosynthetic protein *fliR*
fliQ	0.57	0.87	1.87	1.07	Flagellar biosynthetic protein *fliQ*
fliP	0.57	0.81	1.74	1.15	Flagellar biosynthetic protein *fliP* precursor
fliN	0.66	0.87	1.87	1.23	Flagellar motor switch protein *fliN*
fliL	0.62	0.93	1.74	1.15	Flagellar *fliL* protein

Table 4.1. Contd.

Gene	Relative Change (AI-2/control)				Function
	3.5 h	4 h	4.5 h	5.5 h	
fliK	0.57	0.76	1.52	1.15	Flagellar hook-length control protein
fliI	0.54	0.87	1.74	1.23	Flagellum-specific ATP synthase
fliG	0.62	0.71	1.74	1.32	Flagellar motor switch protein *fliG*
fliF	0.66	0.76	1.74	1.15	Flagellar M-ring protein
fliA	0.66	0.81	1.62	1.15	RNA polymerase sigma factor for flagellar operon
flhE	0.66	0.76	1.74	1.23	Flagellar protein
flgK	0.57	0.81	1.52	1.15	Flagellar hook-associated protein 1
flgJ	0.62	0.93	1.52	1.15	Peptidoglycan hydrolase *flgJ*
flgH	0.54	0.87	1.62	1.23	Flagellar L-ring protein precursor
flgG	0.57	0.87	1.62	1.07	Flagellar basal-body rod protein *flgG*
flgB	0.54	0.76	1.62	1.15	Flagellar basal-body rod protein *flgB*
fimZ	0.62	0.76	1.87	1.23	Fimbrial protein Z, putative transcriptional regulator of fimbrial expression (LuxR/UhpA family)
fimG	0.57	0.76	1.52	1.15	FimG protein precursor
fimF	0.66	0.81	1.62	1.41	FimF protein precursor
fimD	0.54	0.87	1.52	1.15	Outer membrane usher protein *fimD* precursor
fimC	0.66	0.66	1.62	1.23	Chaperone protein *fimC* precursor
sfmH	0.62	0.81	2.00	1.23	Fimbrial assembly protein
sfmF	0.66	0.76	1.62	1.15	Putative fimbrial-like protein
sfmD	0.57	0.87	1.62	1.32	Putative outer membrane protein
sfmC	0.44	0.81	1.87	1.23	Putative chaperone
sfmA	0.62	0.87	1.52	1.15	Putative fimbrial-like protein
c1936	0.54	0.93	2.00	1.00	Type-1 fimbrial protein, A chain precursor
c0430	0.57	0.93	1.62	1.15	Type-1 fimbrial regulatory protein *fimB*

Table 4.1. Contd.

Gene	Relative Change (AI-2/control)				Function
	3.5 h	4 h	4.5 h	5.5 h	
ycbV	0.62	0.87	1.74	1.15	Putative fimbrial-like protein
ycbU	0.62	1.00	1.62	1.07	Putative fimbrial-like protein
ycbQ	0.62	0.76	1.62	1.15	Putative fimbrial-like protein
ycbR	0.62	0.93	1.62	1.07	Putative fimbrial chaperone
Z0615	0.57	0.93	1.52	1.23	Cell adhesion
yadN	0.54	0.81	1.74	1.15	Cell adhesion
Z3597	0.62	0.93	1.74	1.15	Cell adhesion
Z3601	0.62	0.76	1.52	1.23	Cell adhesion
Z4971	0.62	0.71	1.62	1.07	Cell adhesion
Z3598	0.62	0.81	1.74	1.23	Cell adhesion
Z5225	0.62	0.87	1.87	1.07	Cell adhesion
Z3135	0.66	0.87	1.52	1.07	Cell adhesion
yehD	0.66	0.76	1.62	1.07	Cell adhesion
Z3596	0.66	0.87	1.74	1.23	Cell adhesion
Z1538	0.66	0.87	1.62	1.15	Cell adhesion
flgI	0.62	0.76	1.62	1.00	Ciliary or flagellar motility
ydeS	0.62	0.81	2.00	1.15	Hypothetical fimbrial-like protein *ydeS* precursor
ydeQ	0.66	0.87	1.74	1.15	Hypothetical fimbrial-like protein *ydeQ* precursor
Iron related genes					
napH	0.57	0.81	1.74	1.15	Ferredoxin-type protein *napH*
napG	0.66	0.76	1.87	1.32	Ferredoxin-type protein *napG*
napF	0.54	0.87	1.62	1.07	Ferredoxin-type protein *napF*

Table 4.1. Contd.

Gene	Relative Change (AI-2/control)				Function
	3.5 h	4 h	4.5 h	5.5 h	
napB	0.66	0.76	1.52	1.41	Diheme cytochrome-C *napB* precursor
fixX	0.54	0.81	1.74	1.23	Ferredoxin-like protein
fixC	0.66	0.76	1.62	1.15	FixC protein
fixB	0.62	0.81	1.52	1.23	Probable flavoprotein subunit, carnitine metabolism
fixA	0.57	0.76	1.62	1.15	FixA protein
c1650	0.50	0.87	1.62	1.23	Putative iron compound ABC transporter, ATP-binding protein
fepE	0.62	0.81	1.74	1.07	Ferric enterobactin (enterochelin) transport
ygcO	0.62	0.93	1.52	1.23	Ferredoxin-like protein *ygcO*
hcaC	0.62	0.76	1.74	1.15	Ferredoxin subunit of phenylpropionate dioxygenase
c2068	0.62	0.81	1.62	1.07	Putative ferredoxin-like protein *ydhY*
c2065	0.66	0.87	1.52	0.87	Putative ferredoxin-like protein *ydhX*
c1652	0.62	0.76	1.87	1.15	Hypothetical protein
ynfE	0.66	0.71	1.74	1.15	Putative dimethyl sulfoxide reductase chain *ynfE* precursor
ybjW	0.57	1.00	1.74	1.15	Prismane protein homolog
c3734	0.62	0.87	1.52	1.32	Hydrogenase-2 small chain precursor
nrfB	0.57	0.81	1.87	1.41	Cytochrome C-type protein *nrfB* precursor
dmsA	0.66	0.87	1.62	1.00	Anaerobic dimethyl sulfoxide reductase chain A precursor
hcaE	0.57	0.66	1.52	1.23	3-phenylpropionate dioxygenase, alpha subunit
mhpB	0.57	0.81	1.62	1.32	2,3-dihydroxyphenylpropionate 1,2-dioxygenase
napA	0.62	0.81	1.52	1.32	Iron ion binding
Z3785	0.66	0.87	1.52	1.07	Iron ion binding

Table 4.1. Contd.

Gene	Relative Change (AI-2/control)				Function
	3.5 h	4 h	4.5 h	5.5 h	
Colanic acid genes					
wcaJ	0.66	0.66	1.62	1.23	Putative colanic biosynthesis UDP-glucose lipid carrier transferase
wcaH	0.62	0.87	1.52	1.23	GDP-mannose mannosyl hydrolase
wcaG	0.57	0.81	1.52	1.32	GDP-4-keto-6-L-galactose reductase
wcaF	0.50	1.07	2.14	1.23	Putative colanic acid biosynthesis acetyltransferase *wcaF*
wcaE	0.57	0.87	2.00	1.00	Putative colanic acid biosynthesis glycosyl transferase *wcaE*
wcaC	0.54	0.87	1.87	1.15	Putative colanic acid biosynthesis glycosyl transferase *wcaC*
wcaB	0.54	1.00	1.52	1.07	Putative colanic acid biosynthesis acetyltransferase *wcaB*
wcaA	0.50	0.66	1.52	1.15	Putative colanic acid biosynthesis glycosyl transferase *wcaA*
Galactitol operon					
agaZ	0.62	0.71	2.00	1.32	Putative tagatose 6-phosphate kinase *agaZ*
agaY	0.57	0.62	1.74	1.41	Tagatose-bisphosphate aldolase *agaY*
agaV	0.62	0.87	1.62	1.23	PTS system, N-acetylgalactosamine-specific IIB component 2
agaI	0.62	0.81	1.62	1.23	Putative galactosamine-6-phosphate isomerase
agaI	0.62	1.00	1.62	1.07	Putative galactosamine-6-phosphate isomerase
agaC	0.54	0.87	1.62	1.23	PTS system, N-acetylgalactosamine-specific IIC component 1
agaB	0.54	0.81	1.52	1.07	PTS system, N-acetylgalactosamine-specific IIB component 1

Table 4.1. Contd.

Gene	Relative Change (AI-2/control)				Function
	3.5 h	4 h	4.5 h	5.5 h	
gatZ	0.66	0.81	1.74	1.15	Putative tagatose 6-phosphate kinase 1
gatD	0.50	0.81	1.52	0.93	Galactitol-1-phosphate dehydrogenase
gatB	0.66	0.66	1.87	1.15	PTS system, galactitol-specific IIB component
gatA	0.62	0.87	1.87	1.23	PTS system, galactitol-specific IIA component
Cell wall/cycle related genes					
Z1537	0.57	0.87	1.52	1.15	Cell wall organization and biogenesis
Z5223	0.66	0.66	1.62	1.15	Cell wall organization and biogenesis
Z2086	0.57	0.81	2.00	1.00	Cell division
Z3128	0.66	0.71	1.87	1.32	Cell division
kil	0.54	0.71	1.62	1.15	Kil protein (killing function) of lambdoid prophage Rac
Two-component signal transduction genes					
uhpB	0.66	0.76	2.14	1.15	Sensor protein *uhpB*
yqeI	0.66	0.81	1.74	1.07	Putative sensory transducer
rtcR	0.57	0.76	2.00	1.32	Two-component signal transduction system (phosphorelay)
torS	0.54	0.76	1.62	1.23	Two-component sensor molecule activity
Hydrogenase genes					
hyfR	0.57	0.87	1.52	1.32	Putative 2-component regulator, interaction with sigma 54
hyfI	0.57	0.87	1.52	1.23	Hydrogenase 4 Fe-S subunit
hyfG	0.62	0.81	1.52	1.15	Hydrogenase 4 subunit
hyfE	0.57	0.93	1.52	1.15	Hydrogenase 4 membrane subunit

Table 4.1. Contd.

Gene	Relative Change (AI-2/control)				Function
	3.5 h	4 h	4.5 h	5.5 h	
hyfD	0.57	0.87	1.62	1.32	Hydrogenase 4 membrane subunit
hyfC	0.54	0.81	1.74	1.23	Hydrogenase 4 membrane subunit
hyfA	0.54	0.71	1.62	1.32	Hydrogenase 4 Fe-S subunit
***hyc* operon**					
hycG	0.62	0.71	1.52	1.32	Formate hydrogenlyase subunit 7
hycF	0.54	0.76	1.62	1.15	Formate hydrogenlyase subunit 6
hycE	0.62	0.76	1.52	1.15	Formate hydrogenlyase subunit 5 precursor
hycD	0.62	0.81	1.87	1.00	Formate hydrogenlyase subunit 4
hycC	0.54	0.87	1.62	1.07	Hydrogenase 3, membrane subunit (part of FHL complex)
hycA	0.54	0.71	1.62	1.23	Formate hydrogenlyase regulatory protein *hycA*
Ethanolamine genes					
eutJ	0.50	0.81	1.74	1.15	Ethanolamine utilization protein *eutJ*
eutI	0.62	0.81	1.74	1.23	Ethanolamine utilization protein *eutD*
eutG	0.62	0.76	1.62	1.32	Ethanolamine utilization; homolog of *Salmonella* enzyme, similar to iron-containing alcohol dehydrogenase
eutE	0.57	0.66	1.52	1.32	Ethanolamine utilization protein *eutE*
c2987	0.62	0.71	1.62	1.15	Ethanolamine utilization protein *eutS*
c2985	0.62	0.87	1.52	1.32	Ethanolamine utilization protein *eutQ*
c2986	0.62	1.15	1.62	1.15	Ethanolamine utilization protein *eutP*
cchB	0.54	0.81	1.62	1.23	Ethanolamine utilization protein *eutN*
Z3715	0.62	0.76	1.74	1.15	Ethanolamine metabolism

Table 4.1. Contd.

Gene	Relative Change (AI-2/control)				Function
	3.5 h	4 h	4.5 h	5.5 h	
Threonine genes					
tdcR	0.62	0.66	1.62	1.07	Threonine dehydratase operon activator protein
tdcD	0.66	0.66	1.87	1.15	Propionate kinase/acetate kinase II, anaerobic
tdcB	0.66	0.76	1.74	1.15	Threonine dehydratase catabolic
tdcA	0.62	0.81	1.62	1.15	*tdc* operon transcriptional activator
Sorbitol genes					
srlD	0.57	0.81	1.52	1.32	Sorbitol-6-phosphate 2-dehydrogenase
srlB	0.50	0.87	2.00	1.32	PTS system, glucitol/sorbitol-specific IIA component
srlA	0.54	0.93	1.62	1.07	PTS family enzyme IIC, glucitol/sorbitol-specific
srlA	0.57	0.87	1.62	1.07	PTS system, glucitol/sorbitol-specific IIC2 component
Phosphonate genes					
phnJ	0.66	0.87	1.87	1.07	Conserved protein in *phn* operon
phnH	0.47	1.00	2.00	1.07	PhnH protein
phnF	0.47	0.76	1.87	1.23	Probable transcriptional regulator *phnF*
phnE	0.47	0.76	2.00	1.15	Membrane channel protein component of Pn transporter
phnE	0.62	0.93	1.52	1.23	Membrane channel protein component of Pn transporter
phnD	0.62	0.76	1.87	1.32	Phosphonates-binding periplasmic protein precursor

Table 4.1. Contd.

Gene	Relative Change (AI-2/control)				Function
	3.5 h	4 h	4.5 h	5.5 h	
Citrate genes					
citT	0.54	0.66	2.14	1.15	Citrate carrier
citG	0.54	0.81	2.30	1.32	2-(5"-triphosphoribosyl)-3'-dephosphocoenzyme-A synthase
citF	0.57	0.76	1.74	1.41	Citrate lyase alpha chain
citE	0.62	0.66	1.62	1.23	Citrate lyase beta chain
citD	0.44	0.71	1.74	1.23	Citrate lyase acyl carrier protein (gamma chain)
Sodium ion transport genes					
ygjE	0.57	0.81	1.52	1.23	Putative tartrate carrier/transporter
yihO	0.66	0.71	1.52	1.07	Putative permease
ybhI	0.44	0.93	2.00	1.15	Putative membrane pump protein
Z5001	0.50	0.76	1.87	1.23	Sodium ion transport
yihP	0.54	1.00	1.74	1.15	Sodium ion transport

ratio (between AI-2 and the control cells at different time-points) was greater than 1.5 (based on the standard deviation between values measuring relative changes in expression) (107) and if the change in the *P* value was less than 0.05. The differentially expressed genes were annotated using gene ontology definitions available in the Affymetrix NetAffx Analysis Center (http://www.affymetrix.com/analysis/index.affx). The expression data have been deposited in the NCBI Gene Expression Omnibus (GEO; http://www.ncbi.nlm.nih.gov/geo/) and are accessible through GEO Series accession number GSE9388.

A total of eight microarrays were used in this study at the four time-points for samples without and with externally added 100 μM AI-2. The genes were sorted into various functional categories (Table 4.1), and the role of AI-2 in regulation of these genes was analyzed.

4.4 RESULTS

4.4.1 Effect of AI-2 on VS94 chemotaxis, motility and colonization

A two-fluorophore agarose plug assay was used to determine the effect of AI-2 on EHEC chemotaxis. AI-2 attracted VS94 in a concentration-dependent manner, where migration towards AI-2 was increasingly pronounced as the concentration of AI-2 in the plug was increased to 500 μM (Fig. 4.1B); i.e., more live (green) cells move to the plug containing AI-2 than dead cells (red). When casamino acids (positive control) were used in the plug, VS94 was similarly attracted (Fig. 4.1C); whereas exposure to nickel sulfate (negative control) caused VS94 to move away from the plug (Fig. 4.1D). Exposure to no chemical (experimental control) elicited no response from VS94 (Fig. 4.1A). Motility assays showed that low concentrations of AI-2 (1 μM) did not evoke a response from the pathogen while AI-2 at 100 μM increased the swimming motility by 1.3-fold (Fig. 4.2A). Since, AI-2 impacted EHEC motility and

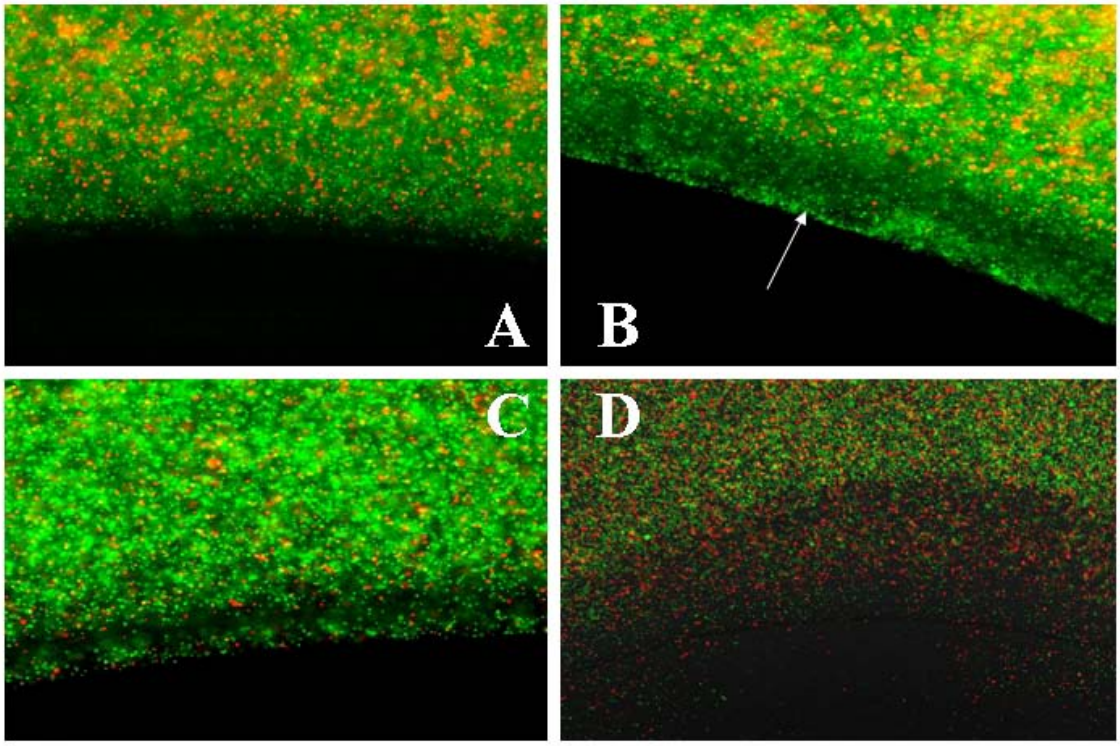

Fig. 4.1. Agarose plug chemotaxis assay. Response of VS94 to various chemicals was observed using a modified agarose plug assay in which dead cells are red (RFP) and live cells are green (GFP). Fluorescent images are shown from: experimental control (no AI-2) (A), AI-2 (500 μM) (B), casamino acids (positive control) (C) and nickel sulfate (negative control) (D). Data are a representative image from three independent experiments. Arrow indicates chemo-attractant ring (B).

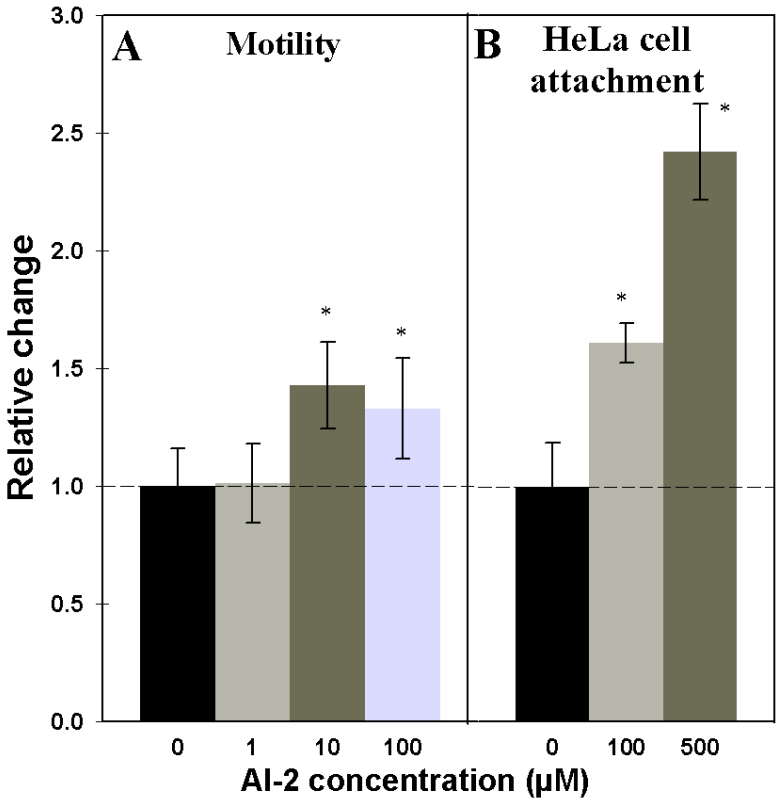

Fig. 4.2. AI-2 effects on VS94 motility and attachment to HeLa cells. Relative change in VS94 motility in the presence of AI-2 (A). Motility data are mean ± one standard deviation for 5 plates for each concentration. Relative change in VS94 attachment to HeLa cells in the presence of AI-2 (B). Data are from 6 HeLa cell culture wells for each concentration. '*' indicates statistical significance determined using student t-test at $p < 0.01$.

chemotaxis; we also tested the effect of presence of AI-2 on EHEC adherence to HeLa cells. Consistent with the changes in chemotaxis and motility, AI-2 at concentrations of 100 µM and 500 µM caused a statistically significant increase in attachment of VS94 to HeLa cells by 1.6-fold and 2.4-fold, respectively (Fig. 4.2B). Hence, AI-2 increases EHEC chemotaxis, motility, and attachment to HeLa cells. These are the first results to show regulation of EHEC chemotaxis and colonization by AI-2.

4.4.2 Uptake of AI-2 in VS94

As a first step towards determining the genes that are altered in expression by AI-2, we investigated the time at which externally added AI-2 is imported by the EHEC *luxS* mutant. Extracellular AI-2 levels were determined at different time-points corresponding to various growth phases of VS94 using the AI-2 bioassay (129). The concentration of AI-2 in the GI tract is not known; therefore, experiments were performed with 100 µM AI-2 as this concentration was sufficient to increase chemotaxis, motility, and attachment of VS94, and has also been used in a recent study (127). Our data show that ~ 99% of the externally added AI-2 was still present in the medium after 3 h. However, after 4 h, the extracellular AI-2 concentration dropped precipitously to less than 5% of the initial value (Fig. 4.3); this indicates that AI-2 is imported by VS94 between 3 and 4 h after addition. Based on these results, transcriptome analysis were performed at different time-points including when extracellular AI-2 was actively being absorbed by the cells (3.5 h), was reduced to zero (4 h), and was likely processed and cleared from the cells (4.5 h and 5.5 h) (110).

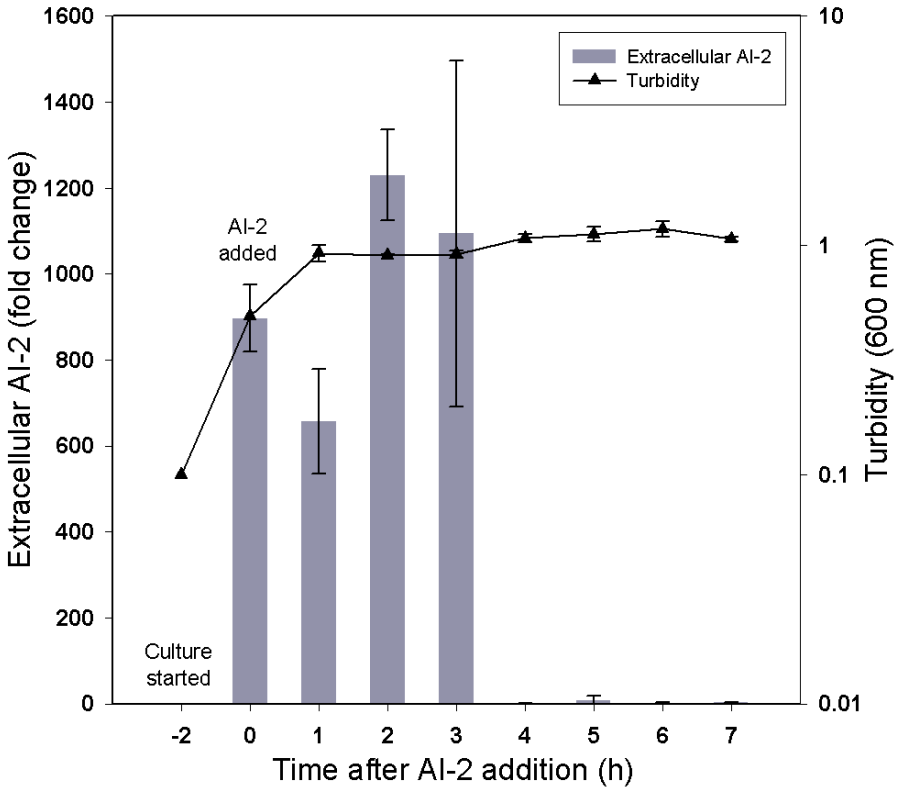

Fig. 4.3. AI-2 uptake assay. VS94 was grown in SAPI medium to a turbidity of 0.5 at 600 nm and 100 µM AI-2 was added. Supernatants were collected, and the *V. harveyi* autoinducer assay was performed to determine amount of extracellular AI-2 remaining. Three independent cultures were used to generate the AI-2 uptake profile.

4.4.3 Transcriptome profiling of the effect of AI-2

We investigated the molecular basis underlying the effect of AI-2 on VS94 chemotaxis, motility and attachment to epithelial cells using DNA microarrays. VS94 was grown both in the absence (negative control) and presence of 100 μM AI-2 and cells were isolated at various times based on the AI-2 uptake assay (Fig. 4.3). Genes whose expression was altered by 1.5-fold (based on the standard deviation of our data (107) which was less than 1.5) in presence of AI-2 were selected and sorted into operons or various functional groups (e.g., virulence genes, flagellar genes, iron uptake genes etc.; Table 4.1), and the temporal expression trends were analyzed (Fig. 4.4).

The data show that after 3.5 h of exposure to AI-2, 1441 genes were down-regulated and 127 genes were up-regulated as compared to the negative control with no AI-2. The genes that were down-regulated included flagellar and fimbrial genes (average fold-change of 0.60-fold for 46 genes), iron uptake genes (average fold-change of 0.61-fold for 24 genes) and operons related to biofilm formation, galactitol (average fold-change of 0.59-fold for 11 genes) and colanic acid operon (average fold-change of 0.56-fold for eight genes). The *lsr* operon, involved in AI-2 uptake (110, 130), was the most-induced operon at this time point (average fold-change of 6 to 9-fold).

At 4 h, the gene expression data showed that fewer genes were significantly altered in expression in VS94 exposed to AI-2 as compared to the negative control with no AI-2. The expression of 48 genes was significantly induced while 145 genes were down-regulated after 4 h. As expected, the *lsr* operon was again induced by 6- to 13-fold, but all the other operons that were down-regulated at 3.5 h (e.g., LEE genes, flagella genes etc.), were unchanged from the negative control.

In contrast to the gene expression data at 3.5 h, a significant number of genes (1619

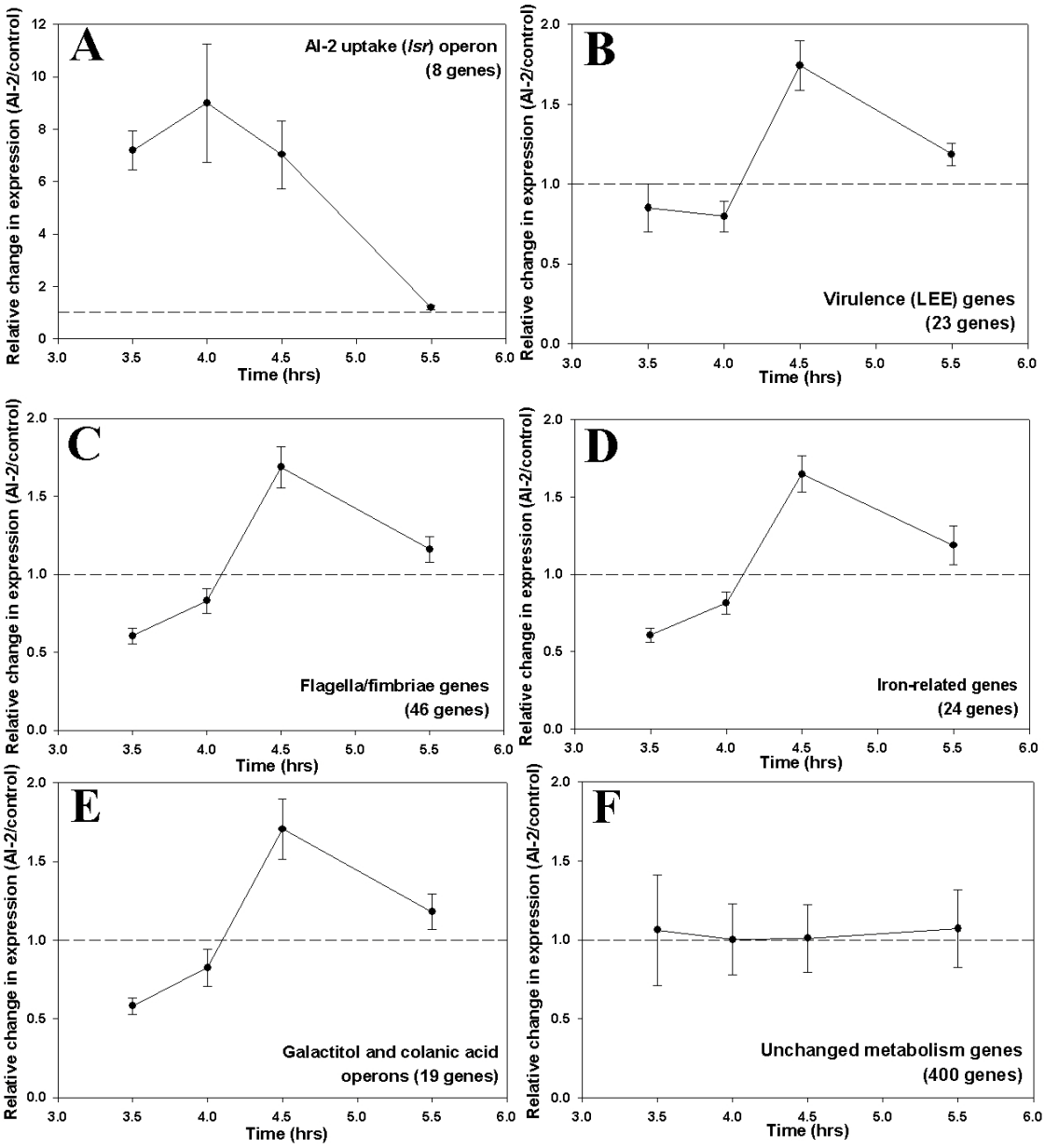

Fig. 4.4. Changes in VS94 gene expression with AI-2 as a function of time. Effect of AI-2 (100 μM) on genes related to the *lsr* operon (a), virulence (b), flagella/fimbriae (c), iron (d), biofilm (e), and metabolism (f).

genes) were up-regulated at 4.5 h in the presence of AI-2, while only 71 genes were repressed compared to the negative control with no AI-2. The *lsr* operon was induced (5- to 9-fold) along genes related to the flagella, iron uptake, and biofilm formation. Most importantly, 23 LEE genes that are involved in EHEC virulence (36) were also significantly induced (average fold-change of 1.74-fold) at this time point. At 5.5 h, after all the extracellular AI-2 had been taken up by VS94 cells (Fig. 4.3), only 207 genes were found to be repressed and 64 genes were induced by AI-2 as compared to the negative control. The *lsr* operon was no longer differentially expressed as no more extracellular AI-2 was available for uptake.

4.5 DISCUSSION

It is becoming increasingly evident that the signaling environment in the GI tract is an important determinant of pathogen colonization and infection. This is not surprising as the GI tract is colonized by hundreds of bacterial species (5) that produce a diverse range of signals. We (26) have recently demonstrated for the first time that the bacterial signal indole is important in EHEC infections by demonstrating that indole down-regulated EHEC chemotaxis, motility, biofilm formation, and adherence to epithelial cells in a manner directly opposite to that observed with the eukaryotic hormones epi and NE. Here we demonstrate that the bacterial signal quorum sensing signal AI-2 is also important in EHEC infections.

It is highly likely that EHEC encounters AI-2 in the GI tract as this inter-species communication signal is produced by several commensal bacterial species that reside in the GI tract (3). Although the concentration of AI-2 in the GI tract is not known, unpublished data from our laboratory show that the concentration used in this study (100 μM) is comparable to that produced by ~ 10^8 cells/mL of non-pathogenic *E. coli*, which is the reported density of commensal *E. coli* in the GI tract (131-133). However, this only provides an approximate

estimate of *in vivo* AI-2 levels as commensal *E. coli* constitutes only 1% of the GI tract flora (131, 133), and other commensal bacteria present in the GI tract can also synthesize and utilize AI-2.

The chemotactic recognition of AI-2 and the increase in motility by EHEC in the presence of AI-2 suggest that this signal is involved in the initial migration of EHEC to epithelial cells. Consistent with this increase in chemotaxis and motility, the presence of AI-2 also causes an increase in adherence to HeLa cells. Given the direct correlation between colonization to epithelial cells and increased virulence (24, 72), our data strongly suggests that the presence of AI-2 leads to increased EHEC colonization of host cells and virulence. This is also corroborated by the gene expression data showing that genes involved in bacterial colonization and biofilm formation (colonic acid and galactitol transport genes) are up-regulated by AI-2 (Fig. 4.4E). Colanic acid is a capsular exopolysaccharide that is involved in colonization (134). Similarly, genes associated with galactitol transport are important during early developmental stages of bacterial colonization of abiotic surfaces (135). The up-regulation of these genes is consistent with increased attachment of EHEC to HeLa cells in our experiments.

The regulation of virulence genes (LEE genes) and several other operons important in virulence strongly suggests the importance of AI-2 in EHEC infections. Several studies (20, 107, 127-128, 136) have used whole transcriptome analysis to understand the effect of AI-2 on gene expression in both non-pathogenic and pathogenic bacteria. While the role of AI-2 in non-pathogenic *E. coli* biofilm formation has been established, its effect on EHEC phenotypes is less well understood. One study (136) recently observed that AI-2 down-regulated several virulence genes including *rpoS* (positive regulator of LEE3 operon) and *prgH* (cell invasion protein) in *Salmonella enterica* serotype Typhimurium *delta luxS*. However, another recent study (127) observed that several metabolism genes, but only two virulence genes, *espA* and *eae*, belonging

to LEE4 and LEE5 respectively, were altered in expression when VS94 was exposed to AI-2, and concluded that AI-2 is not involved in EHEC virulence. On the other hand, our results clearly show that LEE genes and other operons involved in virulence are up-regulated in VS94 upon exposure to AI-2 (Fig. 4.5). Irrespective of the effect exerted by AI-2 (i.e., up-regulation or down-regulation of virulence) or the extent to which virulence genes were altered in expression, our data and these studies clearly indicate that AI-2 is an important signal in GI tract infections.

A notable difference between this study and prior work (127) is that we specifically account for temporal aspects of AI-2 signaling. This is important as several groups have demonstrated that AI-2 is taken up by bacterial cells only during the early stationary phase of growth (109-110) and is rapidly phosphorylated and cleared from the system (110). Therefore, it is possible that the effects of AI-2 on virulence gene expression were not evident at the single time points at which transcriptome analysis was performed in these studies (127).

The addition of AI-2 induced the expression of 23 virulence genes (belonging to all five LEE operons – LEE1 through LEE5) by an average of 2-fold (Fig. 4.4B) after 4.5 h. Induction of flagellar and fimbrial genes has been associated previously with virulence (137) and in our studies, we also observed that 46 fimbrial genes were regulated by AI-2 over time (Fig. 4.4C). The same was true for 24 iron-related genes (Fig. 4.4D). Iron has been reported to increase virulence of certain strains of *E. coli* along with other species such as *Vibrio*, *Neisseria* and *Hemophilus* through the production of cytotoxins and leukotoxins (138). Together, the transcriptome profiling data strongly support our hypothesis that AI-2 is involved the regulation of EHEC virulence. The temporal aspect of AI-2 signaling in virulence gene expression is not a non-specific effect that is seen with all genes, as approximately 400 genes involved in phenotypes other than virulence were not altered in expression at any of the 4 time-points at

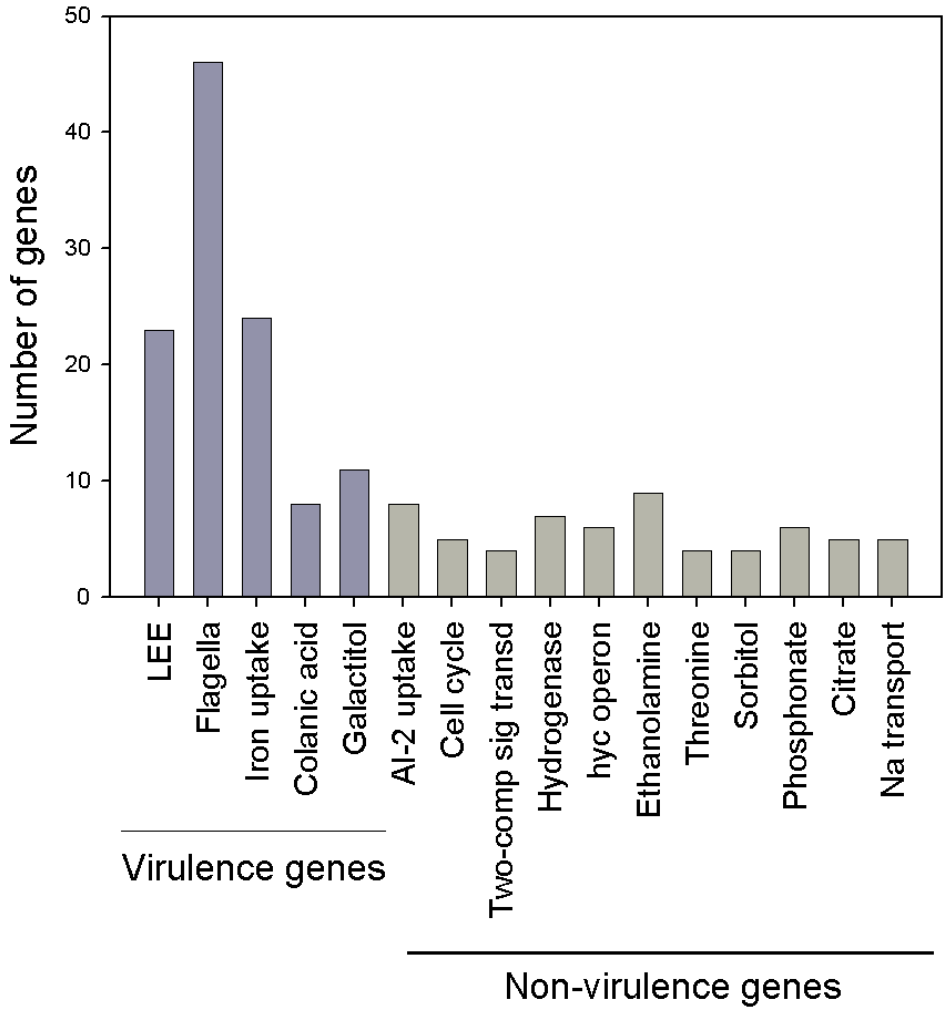

Fig. 4.5. Overall changes in VS94 gene expression in presence of AI-2. Genes significantly regulated by AI-2 were divided into two groups – virulence related and non-virulence related. The genes were further classified based on operons and functions.

which transcriptome analysis was performed (Fig. 4.4F).

The regulation of EHEC virulence by AI-2 was temporally regulated, as LEE genes and other genes related with virulence were down-regulated in AI-2 exposed cells at 3.5 and 4 h. This is intriguing as the AI-2 uptake data clearly show that almost all of the externally added AI-2 is still present in the culture supernatant at this time point (Fig. 4.3). One possible explanation for this observation could be that additional mechanism(s) for AI-2 signal recognition exist. For example, AI-2 could be sensed by a membrane-bound receptor that transduces, but not transports into the cell, the AI-2 signal. The idea of a *lsr*-independent AI-2 recognition mechanism has also been proposed (109, 124). These observations could also reflect the need for a different signal for AI-2 to up-regulate virulence, in the absence of which AI-2 down-regulates certain phenotypes. Taken together, our data suggest that AI-2 signaling in EHEC is tightly regulated, which is reasonable considering that AI-2 is likely to be abundant in the GI tract and the additional layers of regulation likely prevent early up-regulation of virulence genes (i.e., prior to colonization).

The choice of growth medium could explain the contradiction between our results and the work of Kendall et al. (127) on the effects of AI-2 on EHEC virulence. In our study, we used serum supplemented-SAPI medium which has limited nutrients in an effort to mimic the *in vivo* milieu of human GI tract (139). More importantly, SAPI medium also contains ~ 10-fold less glucose than standard glucose supplemented DMEM medium which was used in Kendall et al. (127). The presence of glucose in culture is important as it is well established that AI-2 uptake is regulated by catabolite repression in the presence of glucose through down-regulation of the *lsr* operon (109-110); hence, glucose can mask the impact of AI-2 on gene expression.

The validity of our data is clearly evident from the temporal expression pattern of the *lsr* operon which consists of eight genes that are involved in uptake of extracellular AI-2 during the

stationary phase. These genes were all up-regulated between 6- and 12-fold at the first three time-points, (i.e., only when extracellular AI-2 was available) but not at 5.5 h since no extracellular AI-2 was remaining at that time point (Fig. 4.4A). The transcriptome analysis data revealed that, in addition to altering the expression of genes involved in virulence, AI-2 also controlled the expression of genes involved in other phenotypes and functions (e.g., metabolism). In this regard, our data is consistent with that of several prior reports that have reported on the role of AI-2 in metabolism (127, 130).

Although the relative changes in expression of genes other than the *lsr* operon are not very high, they are statistically significant. Furthermore, it should also be noted that entire operons associated with these phenotypes were differentially expressed. For example, 23 LEE genes were differentially expressed at 4.5 h after AI-2 addition, as were 46 flagellar and fimbrial genes, 24 iron related genes, and 19 genes associated with colonization. A possible reason for the relatively small changes in expression of the virulence genes could be the choice of the experimental system. Although we used a *luxS* mutant that does not produce AI-2 to study the effect of external addition of AI-2, AI-3 synthesis is not affected in these cells as it has been reported to take place independent of *luxS* (17). Since AI-3 has been reported to be involved in EHEC virulence (127), the reduced fold-change in AI-2 treated cells relative to control could be a result of high levels of AI-3-mediated virulence gene expression in the control cells.

In summary, we show here that AI-2 is an important determinant of EHEC virulence and infection. Phenotypic assays for chemotaxis, motility, and colonization clearly demonstrate the importance of AI-2 in EHEC pathogenesis, and are strongly supported by the gene expression data. To our knowledge, this is the first temporal study of EHEC gene expression in presence of AI-2.

CHAPTER V

THE BACTERIAL SIGNAL INDOLE INCREASES EPITHELIAL CELL TIGHT JUNCTION RESISTANCE AND ATTENUATES INDICATORS OF INFLAMMATION*

5.1 OVERVIEW

Inter-kingdom signaling is established in the GI tract in that human hormones trigger responses in bacteria; here we show the corollary is true, that a specific bacterial signal, indole, triggers responses in epithelial cells. Our prior work has shown that indole, secreted by commensal *E. coli* and detected in human feces, reduces pathogenic *E. coli* chemotaxis, motility, and attachment to epithelial cells. However, the effect of indole on intestinal epithelial cells is not known. Since intestinal epithelial cells are likely to be exposed continuously to indole, we hypothesized that indole may be beneficial for these cells, and investigated changes in gene expression with the human enterocyte cell line HCT-8 upon exposure to indole. Exposure to physiologically-relevant amounts of indole increased expression of genes involved in strengthening the mucosal barrier and mucin production, which were consistent with an increase in the trans-epithelial resistance of HCT-8 cells. Indole also decreased TNF-α-mediated activation of NF-κB, expression of the pro-inflammatory chemokine IL-8, and the attachment of pathogenic *E. coli* to HCT-8 cells, as well as increased expression of the anti-inflammatory cytokine IL-10. The changes in trans-epithelial resistance and NF-κB activation were specific to

* Reprinted with permission from "The bacterial signal indole increases epithelial cell tight junction resistance and attenuates indicators of inflammation" by Tarun Bansal, Robert C. Alaniz, Thomas K. Wood, and Arul Jayaraman, 2010, *Proceedings of the National Academy of Sciences of the United States of America,*107:228-233, Copyright by the National Academy of Sciences.

indole, as other indole-like molecules did not elicit a similar response. Our results are similar to that observed with probiotic strains, and suggest that indole could be important in the intestinal epithelial cells response to gastrointestinal tract pathogens. To our knowledge, this is the first report of a specific bacterial signal that is recognized as a beneficial cue by human cells.

5.2 INTRODUCTION

The human GI tract is rich in a diverse range of signaling molecules. A wide range of bacterial signals (e.g., AI-2, AI-3, and indole) (28) are produced by the ~10^{14} non-pathogenic commensal bacteria that co-exist with host cells in the GI tract, while neuroendocrine hormones (e.g., NE, dopamine) are also synthesized *in situ* in the GI tract via the enteric nervous system. The close proximity of bacteria and the host cells in the GI tract, as well as the high local concentrations of the signals they secrete, has led to a signal-centric paradigm wherein GI tract signals are considered to be important mediators of homeostasis and infections through intra-kingdom (i.e., recognition of bacterial signals by other bacteria) and/or inter-kingdom (i.e., recognition of host signals by bacteria and vice-versa) signaling and communication.

Inter-kingdom recognition of hormones by pathogens was first demonstrated by Lyte et al. (24). Subsequently, Sperandio et al. (16) showed that EHEC virulence is increased upon exposure to epi and NE, and epi binds and signals through the QseC receptor (99). Work from our group (26) has also shown that epi and NE increase EHEC chemotaxis, motility, adherence to epithelial cells, and virulence gene expression. While these studies provide evidence for the recognition of human hormones by pathogens, the converse (i.e., recognition of bacterial specific signaling molecules by intestinal epithelial cells and their role in GI tract function) has not been fully investigated. While several studies have shown that culture supernatants from probiotic strains attenuate pathogen infection (140-141), modulate inflammation in dendritic cells (142)

and Caco-2 cells (143), and increase intestinal epithelial cell barrier function (144), the specific molecules contributing to these responses and the mechanisms involved are not known. In fact, most individual bacterial signals have been shown to be deleterious to host cells; for example, the *P. aeruginosa* quorum sensing signaling molecule *N*-(3-oxododecanoyl)-*L*-homoserine lactone (3OC12-HSL) disrupts epithelial barrier integrity in Caco-2 cells (145), increases the expression of pro-inflammatory cytokines in murine fibroblasts and human lung epithelial cells (146), and disrupts NF-κB signaling to promote persistence of a local *P. aeruginosa* infection (65). Therefore, mechanisms underlying inter-kingdom recognition of bacterial signals by eukaryotic cells remain poorly understood.

Indole is produced in *E. coli* from *L*-tryptophan via tryptophan indole-lyase or tryptophanase (encoded by *tnaA*) (41). Prior work from our laboratory has shown that indole is an extracellular signal, represses *E. coli* K-12 biofilm formation through the sensor of quorum sensing signals, SdiA (41), is more effective in repressing *E. coli* K-12 biofilm at low temperatures, i.e., 25^{o}C and 30^{o}C (47), and exerts the opposite effect as epi and NE on EHEC chemotaxis, motility, adherence to epithelial cells, and virulence gene expression, at 37^{o}C (26).

Since commensal *E. coli* produce as much as 600 μM of indole in suspension cultures (22) and indole has been detected in human feces at comparable concentrations (~ 250 - 1100 μM) (44-45), it is likely that intestinal epithelial cells are continually exposed to high concentrations of indole. Therefore, we hypothesized that indole is recognized as an inter-kingdom signal in intestinal epithelial cells. Measurements of changes in gene expression in HCT-8 intestinal epithelial cells and phenotypic measurements of trans-epithelial resistance, NF-κB activation, IL-8 and IL-10 secretion, and EHEC attachment, show that indole modulates expression of pro-inflammatory genes, increases expression of anti-inflammatory genes,

strengthens epithelial cell barrier properties, and decreases pathogen colonization. Our data strongly suggest indole is a beneficial inter-kingdom signal for intestinal epithelial cells.

5.3 MATERIALS AND METHODS

5.3.1 Growth and maintenance of HCT-8 cells

The human colon-cancer cell line HCT-8 (ATCC, Manassas, VA), derived from enterocytes at the junction of the large and small bowel, was maintained in RPMI (Roswell Park Memorial Institute) 1640 medium with 10% horse serum, 1 mM sodium pyruvate, 10 mM HEPES, 100 U/ml penicillin and 100 µg/ml streptomycin, at 37°C in 5% CO_2, according to standard ATCC protocols (henceforth referred to as RPMI medium).

5.3.2 RNA isolation and microarrays

HCT-8 cells were grown in monolayers in standard tissue-culture T-25 flasks to ~ 80% confluence. Cells were washed twice with sterile phosphate buffered saline (PBS; 9 g/liter NaCl, 0.795 g/liter Na_2HPO_4, 0.144 g/liter KH_2PO_4) and exposed to 1 mM indole (Acros Organics, New Jersey, NJ; stock solution of 250 mM in DMF) in triplicate for 4 h or 24 h. This concentration of indole was chosen based on detection of 30 – 130 µg indole/g fecal matter (44-45) (or ~ 250 – 1100 µM, assuming a feces density of 1 g/cm^3 (147)). Control cells were exposed to same volume of solvent, dimethyl formamide (DMF). At the end of exposure, cells were washed twice with PBS, detached from the flasks using trypsin-EDTA, centrifuged and stored at -80°C. RNA was isolated using Qiagen RNeasy Mini Kit (Valencia, CA) and the quality of RNA assessed using gel electrophoresis (gel images were observed for high and low molecular weight smears, which indicate DNA and RNase contamination, respectively) and

spectrophotometrically (A_{260}/A_{280} ratio between 1.9 and 2.1). Reverse transcription, cDNA labeling, hybridization of arrays, and scanning were performed using standard protocols at The Center for Environmental and Rural Health (CERH) Genomics core facility at Texas A&M University. Following quality assessment on an Agilent Bioanalyzer, 2 µg total RNA was used to generate biotin-labeled cRNA via a modified Eberwine RNA amplification protocol using the CodeLink iExpress Kit (Applied Microarrays Inc, Tempe, AZ). Labeled cRNA was hybridized to CodeLink Human genome arrays (Catalog # 300026) for 18 h followed by washing, staining, and scanning according to the standard CodeLink protocol. Array images were processed using CodeLink system software and global median normalization was used to generate normalized expression values. A total of nine arrays were performed with three arrays each for control and exposure to indole at 4 h and 24 h.

Pair-wise comparison between control and indole-treated cells and identification of differentially-expressed genes was carried out using a sequential three-step procedure. First, only those transcripts that were detected in all six arrays (three arrays each for control and indole) were selected for further analysis. Second, the data were filtered for quality and only those signals that were classified as "G" (good) by the Codelink analysis software in all six arrays were processed further. Third, transcripts exhibiting a statistically significant change in expression in indole-treated arrays with respect to control were identified using the Student's T-test at a significance level of $p < 0.01$. Using this approach, 523 and 4102 genes were differentially expressed upon indole exposure after 4h and 24 h, respectively.

The microarray data have been deposited in the Gene Expression Omnibus (GEO) database; accession number GSE14379 (www.ncbi.nlm.nih.gov/geo).

5.3.3 *In vitro* colonization assays

Adhesion of EHEC to HCT-8 cells was performed using a previously described protocol (26). Low-passage-number HCT-8 cells were cultured in standard 24-well tissue culture plates and grown at 37°C in 5% CO_2 until ~ 80% confluence. Indole (1 mM final concentration) was added to some wells 24 h prior to the experiment. After the pre-incubation, HCT-8 cell monolayer was washed two times with PBS to remove traces of indole, and antibiotic-free RPMI with 10% heat-inactivated horse serum was added. Approximately 10^7 cells of a freshly-grown EHEC culture (turbidity of ~ 0.8 at 600 nm) were added to each well along with 500 µM NE and incubated for 3 h at 37°C and 5% CO_2 as previously described (26). Loosely attached bacteria were removed by washing the wells twice with PBS, and the HCT-8 cells were lysed in the wells using 0.1% Triton X-100 in PBS. The cell suspension in each well was vigorously vortexed, and serial dilutions of the bacteria were grown on LB-agar plates. Colonies were counted after 24 h incubation at 37°C.

5.3.4 Reporter lentivirus and NF-κB activity measurements

HCT-8 cells were transduced with a NF-κB reporter lentivirus (kind gift of Prof. Stelios Andreadis, SUNY Buffalo). The 3rd generation lentiviral plasmid contains a fluorescent protein (ZsGreen-DR) that is under the control of an inducible phosphoglycerate kinase (PGK) promoter and tandem repeats of the NF-κB binding sequence (response element). Binding of NF-κB to its response element results in transcription of the ZsGreen-DR protein, and can be used to monitor activation of NF-κB. In addition, the reporter plasmid also contains a DsRed2 fluorescent protein under control of a cytomegalovirus (CMV) constitutive promoter for monitoring transduction efficiency. Details on construction of the lentivirus reporter plasmid are described in Tian and Andreadis (148). Lentiviral particles were produced by co-transfection of the NF-κB reporter

plasmid and three other plasmids (plasmid pMDL-g/p, plasmid pSRV-rev and plasmid pMDG-VSVG) into 293T/17 cells. Virus particles in the supernatant were harvested after 24 h, pelleted by ultracentrifugation (50,000 *g* at 4^{o}C for 2 h), and resuspended in Dulbecco's Modified Eagle Medium (DMEM) supplemented with 10% fetal bovine serum.

For transduction, HCT-8 cells were seeded at low density (~ 30,000 cells/well in a 24-well plate; ~ 30% confluence) and incubated for 24 h at 37°C and 5% CO_2. Next day, the reporter lentivirus was diluted 10-fold in RPMI medium and 8 µg/ml Polybrene (hexadimethrine bromide) was added to lentivirus solution. To each well, 200 µl of the lentivirus-polybrene mixture was added and the plate was incubated for 24 h at 37°C and 5% CO_2. The supernatant was removed, fresh RPMI medium was added, and the cells maintained in culture for a further 3-5 days. The transduction efficiency (determined using expression of the DsRed2 fluorescent protein) was ~ 70%.

Reporter cells transduced with the lentivirus were then exposed to different bicyclic-aromatics for 4 h, followed by incubation with 40 ng/mL of TNF-α to activate NF-κB. The different compounds and the concentrations used were: indole (1 mM), and 250 µM each of indole-2,3-dione, 2-hydroxyindole, 5-hydroxyindole, 7-hydroxyindole, and indole-3-acetic acid. These concentrations were chosen based on preliminary data from our lab on the toxicity of these compounds to HCT-8 cells. Expression of the NF-κB-driven ZsGreen-DR fluorescent protein was monitored using a Zeiss Axiovert 200 fluorescence microscope (Thornwood, NY). Positive control was cells exposed to TNF-α, while the negative control cells were not exposed to either TNF-α or bicyclic aromatics. The cells were positioned on an automated stage on microscope, enclosed in an incubated chamber at 37^{o}C and 5% CO_2, and fluorescence and transmitted light images taken at different time points. For experiments with indole, images were taken every hour for 18 h, whereas for experiments with the other compounds, images were

obtained at a single time point after 18 h. For all experiments, images were taken at the exact same spot at every time using the mark-and-find feature of the microscope; thus, eliminating any user bias. Fluorescent images were analyzed using an in-house developed image analysis program developed in MatLab (The MathWorks Inc; Natick, MA) (149).

5.3.5 Trans-epithelial resistance (TER) measurements

Approximately 10^5 HCT-8 cells were grown on 0.33 cm^2 0.4 µm Transwell filter units (Costar, Cambridge, MA) for TER measurement (150), with 100 µl and 600 µl RPMI medium added to the apical side and basolateral sides, respectively. Polarization of HCT-8 cells was observed using a volt-ohmmeter (World Precision Instruments, Sarasota, FL). Cells were considered to be polarized when the TER was ~ 500 $\Omega.cm^2$ (typically after 5-6 days in culture) (150). After verification of polarization, different bicyclic aromatics were added to both apical and basolateral chambers and the TER was monitored. The different compounds and the concentrations used were: indole (1 mM), and 250 µM each of indole-2,3-dione, 2-hydroxyindole, 5-hydroxyindole, 7-hydroxyindole, and indole-3-acetic acid. For experiments with indole, TER was monitored at different time points, while the TER upon exposure to the other compounds was measured at a single time point after 24 h. The change in TER upon exposure to bicyclic aromatics was calculated relative to control cells (exposed to DMF only).

5.3.6 Extracellular indole assay

Extracellular indole assay was performed as described previously (25). Briefly, HCT-8 cells were grown in 24-well plates till ~ 80% confluence. To cells in three wells, 1 mM indole was added and to cells in three wells, no indole was added (negative control). Also, to three empty wells, 1 mM indole was added to RPMI medium alone, as positive control. The plate was

then incubated for 24 h and the supernatants from all the wells were collected. Extracellular indole was measured by mixing 500 µl supernatant with 200 µl Kovac's reagent. The pink-colored solution, arising from the reaction of p-dimethylaminobenzaldehyde with indole, was diluted in HCl-amyl alcohol mixture and the absorbance was measured at 540 nm. Indole concentrations were determined according to standard concentration curves.

5.3.7 HCT-8 viability assay

HCT-8 cells were grown in 24-well plates till ~ 80% confluence and washed once with PBS prior to the experiment. Indole (1 mM) in fresh RPMI media was added to triplicate wells while the same volume of DMF was added to the negative control wells. The plate was incubated at 37^{o}C and 5% CO_2 for 24 h. Next day, the cells were washed twice with PBS and detached from the surface using 100 µl of trypsin-EDTA. The cells were then resuspended in 500 µl RPMI medium and an equal volume of 0.4% trypan blue solution (Mediatech Inc, Manassas, VA) was added to cells. The cells were then incubated at room temperature for 2 minutes, and the number of live (transparent) and dead (blue) cells in 10 µl of this solution was counted using a hemocytometer (Hausser Scientific, Horsham, PA) at 25X magnification. For each sample, cells present in five 1 mm x 1 mm squares were counted and used for calculating the cell density.

5.3.8 Quantitative RT-PCR

DNA microarray data was corroborated using qRT-PCR (26). The primers were designed using PrimerQuest online software (Table 5.1). qRT-PCR was performed using iScript one-step RT-PCR kit with SYBR green (Bio-Rad Laboratories, CA) on a MyiQ single-color real-time PCR detection system (Bio-Rad Laboratories). The threshold cycles, as calculated by

the MyiQ optical system software (Bio-Rad Laboratories), were used to determine the relative changes between the samples. The experiments were run in triplicate in 20 µl reactions and 50 ng of total RNA was used for each reaction, with the final forward and reverse primer concentrations at 0.15 µM each. After amplification, template specificity was ensured through melting curve analysis. 18S RNA was used as the housekeeping gene for normalizing the data.

5.3.9 IL-8 Enzyme linked immunosorbent assay (ELISA)

IL-8 concentration in the HCT-8 cell supernatants was determined using a commercially available human IL-8 ELISA kit (Pierce Biotechnology Inc., Rockford, IL) according to manufacturer's instructions. HCT-8 cells were exposed to solvent (control) or 1 mM indole for either 4 h or 24 h and the supernatants were collected. To some wells, 1 mM indole was added for 4 h and then 20 ng/ml TNF-α was added to stimulate IL-8 production. 4 h later, supernatants from those cells were collected. IL-8 standard supplied by manufacturer was diluted serially at 1000, 400, 160, 64, 25.6, and 0 pg/ml, and was used to determine the concentration of IL-8 released by cells. The assay range is 25.6-1000 pg/ml and the sensitivity is < 2 pg/ml. The assay was performed with three biological replicates per condition. The samples were diluted as required to maintain IL-8 concentration in the assay range.

5.3.10 Flow cytometry and intracellular cytokine staining

Changes in IL-10 production in response to indole or DMF (solvent control) were determined using intracellular cytokine staining as previously described (151). Briefly, confluent monolayers of HCT-8 cells in a 24-well plate were exposed to 1 mM indole or solvent for 24 h. BD GolgiPlug (BD Biosciences, San Jose, CA), a protein transport inhibitor containing brefeldin A, was added to the cells for the final 6 h of incubation, at a 1000-fold final dilution. Cells were

Table 5.1. Sequences of primers used for RT-PCR

Gene	Forward Primer (5'-3')	Reverse Primer (5'-3')
ISGF3G	TCCATTCAGACATTGGGAGCAGCA	AGATGAAGGTGAGCAGCAGTGAGT
CXCL5	ATCCTCCAATCTTCGCTCCTCCAA	AAACAAACGCAACGCAGCTCTCTC
IL-8	TTGAGGCCAAGGGCCAAGAGAATA	AAACCAAGGCACAGTGGAACAAGG
Pre-IL-1	AATGATCAGTACCTCACGGCTGCT	TGGTCTTCATCTTGGGCAGTCACA
Cldn3	AGATGCAGTGCAAGGTGTACGACTC	TGCCACGATGGTGATCTTGGCCTT
ZO3	TGCTGAGATGCCTGACCAGTTTGA	AGTACTGCACATAGTTGAGGCGCT
Muc13	CCTGGGCAAACATTGCTCTTGAGT	TTGCAAGCTCTGGGCTGTTCAAAG
18S	TCAACTTTCGATGGTAGTCGCCGT	ACTCATTCCAATTACAGGGCCTCG

washed twice with PBS, detached from the surface using trypsin-EDTA, resuspended in RPMI, and added to 96-well round-bottom plates. After two washes in PBS supplemented with 0.5% bovine serum albumin, cells were fixed on ice with 4% paraformaldehyde, permeabilized with Perm/Wash buffer (BD Biosciences), followed by staining with phycoerythrin (PE) labeled anti-human IL-10 antibody (eBioscience Inc., San Diego, CA) for 2 h. Cells were resuspended in PBSA and stored in the dark at 4^{o}C until analysis. Unstained cells were used as negative control. Data (8000 events/sample) were acquired on BD FACSAriaII cell sorter system (BD Biosciences) and analyzed using FlowJo software (Tree Star Inc., Ashland, OR).

5.4 RESULTS

5.4.1 HCT-8 intestinal epithelial cell transcriptome profiling upon exposure to indole

To investigate whether indole affects cells of the GI tract, changes in intestinal epithelial cell gene expression upon exposure to 1 mM indole for 4 h and 24 h were determined using whole-transcriptome profiling. Genes exhibiting a statistically significant change ($p < 0.01$) in expression relative to untreated controls were used to populate the Kyoto Encyclopedia of Genes and Genomes (KEGG) pathways with the Pathway Express software (152). Exposure to indole for 4 h resulted in the differential expression of 523 genes, of which 476 genes were induced and 47 genes were repressed. Importantly, no single pathway or ontology classification was dominant in the differentially expressed genes. On the other hand, approximately 8% (4102 genes; 3083 annotated) of the HCT-8 transcriptome was differentially expressed after 24 h exposure to indole. Although several pathways were populated by this approach, (e.g., metabolism, transport, protein modification, etc) (Fig. 5.1), we limit our discussion to specific pathways - epithelial cell structure and organization, inflammation, and infection – that are

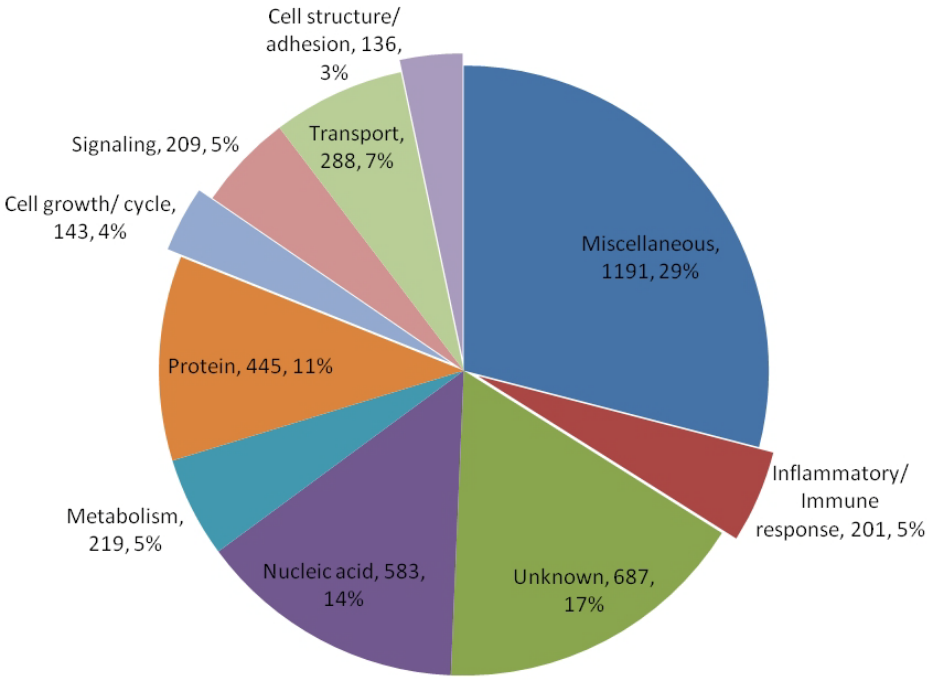

Fig. 5.1. Classification of genes differentially expressed upon indole exposure. Differentially expressed genes were identified from the microarray data (control and 24 h indole exposure) as described in the supporting information, and classified into various functional categories. The three entries in each data label represent, in order, "functional category, number of genes differentially expressed, and % of total differentially expressed genes'.

Table 5.2. Classification of genes differentially regulated by 1 mM indole at 24 h

Classification	Pathway*	Total genes in pathway	Genes regulated by indole
Cell structure/adhesion	Adherens junction	75	19
	Cell adhesion molecules (CAMs)	133	38
	Gap junction	96	17
	Regulation of actin cytoskeleton	211	50
	Tight junction	135	29
	Cytokine-cytokine receptor interaction	259	45
Inflammatory/ immune response	Jak-STAT signaling pathway	153	38
	MAPK signaling pathway	265	48
	Phosphatidylinositol signaling system	77	22
	Toll-like receptor signaling pathway	102	27
Cell growth/cycle	Apoptosis	84	23
	Cell cycle	112	25

* Epithelial cell pathways were determined by Pathway Express.

related to pathogen colonization in the GI tract (Table 5.2). The entire list of differentially expressed genes, with fold-changes in expression, is included as Table 5.3.

5.4.2 Changes in epithelial cell barrier properties and colonization

Indole significantly induced several genes involved in the maintenance of epithelial cell structure and function. These included genes responsible for tight junction organization, actin cytoskeleton, mucin production, and adherens junction, which together suggest strengthening of epithelial cell barrier properties. Coordinated induction of seven claudin genes (Table 5.3) suggested that 24 h exposure to indole increases paracellular resistance (Fig. 5.2A). The decrease in the expression of the pore-forming cldn2, which increases paracellular cation permeability (153), also further supports that indole mediates an increase in paracellular resistance. Tight junction proteins TJP1, TJP3 and TJP4, which are downstream of claudin-mediated tight junction regulation (Fig. 5.2A), and gap junction proteins GJE1, GJB3, GJB4, and GJA8 were also induced by indole. Exposure to indole also induced the expression of 50 cytoskeleton genes (e.g., actinin, cingulin, syntrophin), and the coordinated induction of several cytoskeleton gene families suggests fortification of the actin cytoskeleton upon exposure to indole. Similarly, genes involved in the production of mucins (muc1, muc3, muc13, muc20, and mucin and cadherin-like transcript variant 4), high molecular weight glycoproteins secreted by intestinal epithelial cells (154) and integral to epithelial cell defense, were also induced in expression upon exposure to indole. Together, these transcriptome changes suggest indole promotes intestinal epithelial cell barrier function and increases resistance to pathogen colonization.

Table 5.3. Partial list of genes differentially regulated by 1 mM indole at 24 h

NCBI Accession	Control Average	Indole Average	Fold Change (ind/cont)	*p*-value	Description
Immune/Inflammatory response (201)					
NM_003733.2	247.0	364.7	1.5	0.0027	2'-5'-oligoadenylate synthetase-like (OASL), transcript variant 1
NM_006422.2	141.6	247.0	1.7	0.0057	A kinase (PRKA) anchor protein 3 (AKAP3)
NM_000681.2	563.1	1029.9	1.8	0.0037	Adrenergic, alpha-2A-, receptor (ADRA2A)
NM_015158.1	97.0	176.1	1.8	0.0018	Ankyrin repeat domain 15 (ANKRD15), transcript variant 1
NM_020427.2	205.1	348.9	1.7	0.0024	ARS component B (ARS)
NM_012070.2	123.8	249.9	2.0	0.0053	Attractin (ATRN), transcript variant 3
NM_001144.3	423.0	903.1	2.1	0.0017	Autocrine motility factor receptor (AMFR), transcript variant 1
NM_139317.1	55.1	84.3	1.5	0.0087	Baculoviral IAP repeat-containing 7 (livin) (BIRC7), transcript variant 1
NM_013314.2	254.0	403.0	1.6	0.0102	B-cell linker (BLNK)
NM_004282.2	2510.0	1791.0	-1.4	0.0080	BCL2-associated athanogene 2 (BAG2)
NM_004048.2	854.1	1616.1	1.9	0.0043	Beta-2-microglobulin (B2M)
NM_006129.2	387.3	727.6	1.9	0.0044	Bone morphogenetic protein 1 (BMP1), transcript variant BMP1-3
NM_006129.2	98.5	202.8	2.1	0.0006	Bone morphogenetic protein 1 (BMP1), transcript variant BMP1-3
NM_005448.1	184.9	391.4	2.1	0.0000	Bone morphogenetic protein 15 (BMP15)
NM_000710.2	26.3	65.5	2.5	0.0010	Bradykinin receptor B1 (BDKRB1)
NM_032966.1	233.6	662.5	2.8	0.0003	Burkitt lymphoma receptor 1, GTP binding protein (chemokine (C-X-C motif) receptor 5) (BLR1), transcript variant 2
NM_006077.1	795.3	1515.6	1.9	0.0020	Calcium binding atopy-related autoantigen 1 (CBARA1)
NM_001841.1	135.3	331.0	2.4	0.0005	Cannabinoid receptor 2 (macrophage) (CNR2)
NM_001712.2	97.1	170.4	1.8	0.0031	Carcinoembryonic antigen-related cell adhesion molecule 1 (biliary glycoprotein) (CEACAM1)
NM_006016.3	2895.0	4996.0	1.7	0.0080	CD164 antigen, sialomucin (CD164)
NM_001764.1	29.5	78.4	2.7	0.0095	CD1B antigen, b polypeptide (CD1B)
NM_001765.1	484.8	866.7	1.8	0.0020	CD1C antigen, c polypeptide (CD1C)

Table 5.3. Contd.

NCBI Accession	Control Average	Indole Average	Fold Change (ind/cont)	*p*-value	Description
NM_013230.1	1225.6	3106.5	2.5	0.0014	CD24 antigen (small cell lung carcinoma cluster 4 antigen) (CD24)
NM_203331.1	2102.6	4271.9	2.0	0.0056	CD59 antigen p18-20 (antigen identified by monoclonal antibodies 163A5, EJ16, EJ30, EL32 and G344) (CD59), transcript variant 4
NM_203331.1	928.3	1887.8	2.0	0.0003	CD59 antigen p18-20 (antigen identified by monoclonal antibodies 163A5, EJ16, EJ30, EL32 and G344) (CD59), transcript variant 4
NM_203331.1	52.8	137.8	2.6	0.0035	CD59 antigen p18-20 (antigen identified by monoclonal antibodies 163A5, EJ16, EJ30, EL32 and G344) (CD59), transcript variant 4
NM_006725.1	152.8	352.0	2.3	0.0023	CD6 antigen (CD6)
NM_004355.1	23.0	52.6	2.3	0.0007	CD74 antigen (invariant polypeptide of major histocompatibility complex, class II antigen-associated) (CD74)
NM_001768.4	226.5	423.8	1.9	0.0003	CD8 antigen, alpha polypeptide (p32) (CD8A), transcript variant 1
NM_001784.2	785.7	1509.1	1.9	0.0029	CD97 antigen (CD97), transcript variant 2
NM_016174.3	289.8	658.9	2.3	0.0019	Cerebral endothelial cell adhesion molecule 1 (CEECAM1)
NM_002995.1	421.1	636.9	1.5	0.0025	Chemokine (C motif) ligand 1 (XCL1)
NM_005283.1	41.8	88.5	2.1	0.0060	Chemokine (C motif) receptor 1 (XCR1)
NM_004590.2	65.8	124.1	1.9	0.0019	Chemokine (C-C motif) ligand 16 (CCL16)
NM_005624.2	62.1	399.5	6.4	0.0000	Chemokine (C-C motif) ligand 25 (CCL25), transcript variant 1
NM_002984.1	72.7	138.5	1.9	0.0063	Chemokine (C-C motif) ligand 4 (CCL4)
NM_001838.2	905.8	1477.9	1.6	0.0072	Chemokine (C-C motif) receptor 7 (CCR7)
NM_002996.1	145.0	304.1	2.1	0.0076	Chemokine (C-X3-C motif) ligand 1 (CX3CL1)
NM_002090.1	269.8	441.0	1.6	0.0018	Chemokine (C-X-C motif) ligand 3 (CXCL3)
NM_002994.3	954.1	182.9	-5.2	0.0059	Chemokine (C-X-C motif) ligand 5 (CXCL5)
NM_001504.1	131.7	244.1	1.9	0.0000	Chemokine (C-X-C motif) receptor 3 (CXCR3)
NM_006564.1	30.0	56.5	1.9	0.0029	Chemokine (C-X-C motif) receptor 6 (CXCR6)

Table 5.3. Contd.

NCBI Accession	Control Average	Indole Average	Fold Change (ind/cont)	*p*-value	Description
NM_144601.2	271.5	450.1	1.7	0.0017	Chemokine-like factor super family 3 (CKLFSF3), transcript variant 1
NM_178818.2	216.4	261.3	1.2	0.0044	Chemokine-like factor super family 4 (CKLFSF4), transcript variant 1
NM_138460.2	418.9	813.0	1.9	0.0002	Chemokine-like factor super family 5 (CKLFSF5), transcript variant 1
NM_020644.1	3965.0	6005.3	1.5	0.0035	Chromosome 11 open reading frame 15 (c11orf15)
NM_000759.2	616.4	997.0	1.6	0.0015	Colony stimulating factor 3 (granulocyte) (CSF3), transcript variant 1
NM_000760.2	42.2	67.3	1.6	0.0027	Colony stimulating factor 3 receptor (granulocyte) (CSF3R), transcript variant 1
NM_020428.2	380.0	971.5	2.6	0.0077	CTL2 gene (CTL2)
NM_022570.3	90.6	156.4	1.7	0.0064	C-type (calcium dependent, carbohydrate-recognition domain) lectin, superfamily member 12 (CLECSF12), transcript variant 2
NM_004935.2	1988.4	3431.6	1.7	0.0019	Cyclin-dependent kinase 5 (CDK5)
NM_004935.2	1745.1	2910.9	1.7	0.0075	Cyclin-dependent kinase 5 (CDK5)
NM_014376.1	164.0	365.5	2.2	0.0045	Cytoplasmic FMR1 interacting protein 2 (CYFIP2)
NM_001380.2	398.2	692.4	1.7	0.0039	Dedicator of cytokinesis 1 (DOCK1), mrna
NM_001379.1	289.4	164.3	-1.8	0.0073	DNA (cytosine-5-)-methyltransferase 1 (DNMT1)
NM_004417.2	217.7	468.3	2.2	0.0084	Dual specificity phosphatase 1 (DUSP1)
NM_007207.3	92.4	174.6	1.9	0.0036	Dual specificity phosphatase 10 (DUSP10), transcript variant 1
NM_030640.1	396.2	631.5	1.6	0.0061	Dual specificity phosphatase 16 (DUSP16)
NM_152511.2	170.1	374.7	2.2	0.0034	Dual specificity phosphatase 18 (DUSP18)
NM_020185.3	776.5	1305.7	1.7	0.0015	Dual specificity phosphatase 22 (DUSP22)
NM_004090.2	121.8	332.4	2.7	0.0035	Dual specificity phosphatase 3 (vaccinia virus phosphatase VH1-related) (DUSP3)
NM_016946.3	1140.3	1939.9	1.7	0.0001	F11 receptor (F11R), transcript variant 1
NM_032036.2	1162.1	2741.3	2.4	0.0005	Family with sequence similarity 14, member A (FAM14A), mrna
NM_004107.3	175.3	422.4	2.4	0.0012	Fc fragment of igg, receptor, transporter, alpha (FCGRT)

Table 5.3. Contd.

NCBI Accession	Control Average	Indole Average	Fold Change (ind/cont)	*p*-value	Description
NM_001456.1	911.1	1665.2	1.8	0.0054	Filamin A, alpha (actin binding protein 280) (FLNA)
AK090439.1	142.5	275.1	1.9	0.0034	FLJ00359 protein
AK090461.1	128.1	197.9	1.5	0.0083	FLJ00382 protein
NM_004778.1	131.7	225.2	1.7	0.0043	G protein-coupled receptor 44 (GPR44)
NM_000853.1	821.5	1637.8	2.0	0.0005	Glutathione S-transferase theta 1 (GSTT1)
NM_000853.1	513.6	1231.2	2.4	0.0031	Glutathione S-transferase theta 1 (GSTT1)
NM_015675.1	646.6	1065.5	1.6	0.0065	Growth arrest and DNA-damage-inducible, beta (GADD45B)
NM_006705.2	54.7	135.8	2.5	0.0017	Growth arrest and DNA-damage-inducible, gamma (GADD45G)
NM_005811.2	104.3	143.9	1.4	0.0054	Growth differentiation factor 11 (GDF11)
NM_005260.2	59.2	111.9	1.9	0.0026	Growth differentiation factor 9 (GDF9)
NM_005261.2	874.5	1515.8	1.7	0.0010	GTP binding protein overexpressed in skeletal muscle (GEM), transcript variant 1
NM_012202.1	334.3	519.5	1.6	0.0088	Guanine nucleotide binding protein (G protein), gamma 3 (GNG3)
NM_004120.3	93.9	186.4	2.0	0.0006	Guanylate binding protein 2, interferon-inducible (GBP2)
NM_016315.1	819.3	1348.1	1.6	0.0079	GULP, engulfment adaptor PTB domain containing 1 (GULP1)
NM_014413.2	3985.6	6055.4	1.5	0.0095	Heme-regulated initiation factor 2-alpha kinase (HRI)
NM_006674.2	252.3	660.2	2.6	0.0027	HLA complex P5 (HCP5)
NM_002127.3	5114.9	12125.2	2.4	0.0000	HLA-G histocompatibility antigen, class I, G (HLA-G)
NM_002127.3	329.9	1165.4	3.5	0.0005	HLA-G histocompatibility antigen, class I, G (HLA-G)
NM_015336.1	402.8	613.8	1.5	0.0049	Huntingtin interacting protein 14 (HIP14)
NM_012484.1	2323.2	746.1	-3.1	0.0032	Hyaluronan-mediated motility receptor (RHAMM) (HMMR), transcript variant 1
NM_030796.2	311.7	644.5	2.1	0.0048	Hypothetical protein dkfzp564k0822 (DKFZP564K0822)
NM_018289.2	149.8	260.6	1.7	0.0000	Hypothetical protein FLJ10979 (FLJ10979)
NM_032376.2	836.4	1732.0	2.1	0.0044	Hypothetical protein MGC4251 (MGC4251)
NM_006389.2	334.8	661.7	2.0	0.0018	Hypoxia up-regulated 1 (HYOU1)
NM_013332.1	1361.3	788.3	-1.7	0.0068	Hypoxia-inducible protein 2 (HIG2)

Table 5.3. Contd.

NCBI Accession	Control Average	Indole Average	Fold Change (ind/cont)	*p*-value	Description
NM_014002.1	196.1	378.2	1.9	0.0042	Inhibitor of kappa light polypeptide gene enhancer in B-cells, kinase epsilon (IKBKE), mrna
NM_002211.2	4541.4	6901.7	1.5	0.0072	Integrin, beta 1 (fibronectin receptor, beta polypeptide, antigen CD29 includes MDF2, MSK12) (ITGB1), transcript variant 1A
NM_022873.1	326.7	612.7	1.9	0.0032	Interferon, alpha-inducible protein (clone IFI-6-16) (G1P3), transcript variant 3
NM_005533.2	130.7	310.3	2.4	0.0002	Interferon-induced protein 35 (IFI35)
NM_001549.2	99.2	164.1	1.7	0.0011	Interferon-induced protein with tetratricopeptide repeats 4 (IFIT4)
NM_012420.1	128.9	253.1	2.0	0.0010	Interferon-induced protein with tetratricopeptide repeats 5 (IFIT5)
NM_006084.3	259.5	1055.6	4.1	0.0003	Interferon-stimulated transcription factor 3, gamma 48kda (ISGF3G)
NM_012275.2	21.2	34.5	1.6	0.0026	Interleukin 1 family, member 5 (delta) (IL1F5), transcript variant 1
NM_014271.2	147.7	283.2	1.9	0.0024	Interleukin 1 receptor accessory protein-like 1 (IL1RAPL1)
NM_006858.2	1079.2	1890.1	1.8	0.0093	Interleukin 1 receptor-like 1 ligand (IL1RL1LG)
NM_003854.2	68.1	116.2	1.7	0.0013	Interleukin 1 receptor-like 2 (IL1RL2)
NM_000628.3	265.9	585.1	2.2	0.0002	Interleukin 10 receptor, beta (IL10RB)
NM_004512.3	111.5	223.7	2.0	0.0004	Interleukin 11 receptor, alpha (IL11RA), transcript variant 1
NM_000882.2	242.1	140.9	-1.7	0.0029	Interleukin 12A (natural killer cell stimulatory factor 1, cytotoxic lymphocyte maturation factor 1, p35) (IL12A)
NM_138284.1	349.0	215.7	-1.6	0.0071	Interleukin 17D (IL17D)
NM_005699.2	70.6	105.5	1.5	0.0040	Interleukin 18 binding protein (IL18BP), transcript variant C
NM_000878.2	53.3	78.1	1.5	0.0040	Interleukin 2 receptor, beta (IL2RB)
NM_181339.1	265.6	424.7	1.6	0.0062	Interleukin 24 (IL24), transcript variant 2
NM_173065.1	521.7	781.7	1.5	0.0004	Interleukin 28 receptor, alpha (interferon, lambda receptor) (IL28RA), transcript variant 3
NM_172138.1	69.4	111.2	1.6	0.0022	Interleukin 28A (interferon, lambda 2) (IL28A)
NM_000588.3	15.4	19.4	1.3	0.0079	Interleukin 3 (colony-stimulating factor, multiple) (IL3)
NM_000589.2	213.6	492.7	2.3	0.0009	Interleukin 4 (IL4), transcript variant 1

Table 5.3. Contd.

NCBI Accession	Control Average	Indole Average	Fold Change (ind/cont)	*p*-value	Description
NM_000584.2	1003.0	557.4	-1.8	0.0265	Interleukin 8 (IL8)
NM_002227.1	167.8	330.8	2.0	0.0018	Janus kinase 1 (a protein tyrosine kinase) (JAK1)
NM_004972.2	73.9	130.5	1.8	0.0059	Janus kinase 2 (a protein tyrosine kinase) (JAK2)
NM_000215.2	72.6	111.5	1.5	0.0002	Janus kinase 3 (a protein tyrosine kinase, leukocyte) (JAK3)
AB032991.1	632.5	1352.3	2.1	0.0019	KIAA1165 protein
NM_005810.3	42.7	80.8	1.9	0.0073	Killer cell lectin-like receptor subfamily G, member 1 (KLRG1)
NM_005567.2	3281.8	7208.0	2.2	0.0036	Lectin, galactoside-binding, soluble, 3 binding protein (LGALS3BP)
NM_006840.2	58.3	103.6	1.8	0.0023	Leukocyte immunoglobulin-like receptor, subfamily B (with TM and ITIM domains), member 5 (LILRB5)
NM_014387.2	50.8	90.0	1.8	0.0035	Linker for activation of T cells (LAT)
NM_005516.3	4500.2	8437.6	1.9	0.0100	Major histocompatibility complex, class I, E (HLA-E)
NM_018950.1	5745.2	9954.3	1.7	0.0054	Major histocompatibility complex, class I, F (HLA-F)
NM_006120.2	507.5	999.9	2.0	0.0032	Major histocompatibility complex, class II, DM alpha (HLA-DMA)
NM_002118.3	748.1	1603.3	2.1	0.0103	Major histocompatibility complex, class II, DM beta (HLA-DMB)
NM_002120.2	430.7	900.5	2.1	0.0017	Major histocompatibility complex, class II, DO beta (HLA-DOB)
NM_033554.2	26.0	57.0	2.2	0.0054	Major histocompatibility complex, class II, DP alpha 1 (HLA-DPA1)
NM_002125.3	88.7	142.8	1.6	0.0094	Major histocompatibility complex, class II, DR beta 5 (HLA-DRB5)
NM_014751.2	175.1	347.7	2.0	0.0033	Metastasis suppressor 1 (MTSS1)
NM_014268.1	444.7	872.9	2.0	0.0078	Microtubule-associated protein, RP/EB family, member 2 (MAPRE2)
NM_002751.5	442.6	726.7	1.6	0.0033	Mitogen-activated protein kinase 11 (MAPK11), transcript variant 1
NM_002750.2	167.0	288.4	1.7	0.0102	Mitogen-activated protein kinase 8 (MAPK8), transcript variant 2
NM_006301.2	127.0	265.3	2.1	0.0072	Mitogen-activated protein kinase kinase kinase 12 (MAP3K12)
NM_004721.3	61.5	128.9	2.1	0.0042	Mitogen-activated protein kinase kinase kinase 13 (MAP3K13)
NM_006609.2	271.6	521.9	1.9	0.0004	Mitogen-activated protein kinase kinase kinase 2 (MAP3K2)
NM_006116.2	87.8	208.7	2.4	0.0029	Mitogen-activated protein kinase kinase kinase 7 interacting protein 1 (MAP3K7IP1), transcript variant alpha

Table 5.3. Contd.

NCBI Accession	Control Average	Indole Average	Fold Change (ind/cont)	*p*-value	Description
NM_005204.2	230.6	387.6	1.7	0.0090	Mitogen-activated protein kinase kinase kinase 8 (MAP3K8)
NM_006575.3	460.7	751.9	1.6	0.0059	Mitogen-activated protein kinase kinase kinase kinase 5 (MAP4K5), transcript variant 1
NM_005439.1	3071.5	4872.6	1.6	0.0080	Myeloid leukemia factor 2 (MLF2)
NM_002463.1	80.7	127.6	1.6	0.0079	Myxovirus (influenza virus) resistance 2 (mouse) (MX2)
NM_002488.2	1416.3	2187.3	1.5	0.0009	NADH dehydrogenase (ubiquinone) 1 alpha subcomplex, 2, 8kda (NDUFA2)
NM_030571.2	917.9	1285.7	1.4	0.0007	Nedd4 family interacting protein 1 (NDFIP1)
NM_002499.1	74.0	183.1	2.5	0.0004	Neogenin homolog 1 (chicken) (NEO1)
NM_017595.4	306.8	630.2	2.1	0.0008	NFKB inhibitor interacting Ras-like 2 (NKIRAS2), transcript variant 2
NM_002548.1	367.0	666.1	1.8	0.0015	Olfactory receptor, family 1, subfamily D, member 2 (OR1D2)
NM_002859.1	347.5	549.1	1.6	0.0077	Paxillin (PXN)
NM_005026.2	56.9	124.1	2.2	0.0002	Phosphoinositide-3-kinase, catalytic, delta polypeptide (PIK3CD)
NM_003629.2	256.6	482.4	1.9	0.0024	Phosphoinositide-3-kinase, regulatory subunit, polypeptide 3 (p55, gamma) (PIK3R3)
NM_003629.2	139.0	66.5	-2.1	0.0054	Phosphoinositide-3-kinase, regulatory subunit, polypeptide 3 (p55, gamma) (PIK3R3)
NM_014308.1	281.9	530.9	1.9	0.0057	Phosphoinositide-3-kinase, regulatory subunit, polypeptide p101 (P101-PI3K)
BC028212.1	555.6	920.3	1.7	0.0002	Phosphoinositide-3-kinase, regulatory subunit, polypeptide p101, mrna (cdna clone MGC:39947 IMAGE:5215094)
NM_002784.2	122.1	191.1	1.6	0.0022	Pregnancy specific beta-1-glycoprotein 9 (PSG9)
NM_025239.2	68.8	135.3	2.0	0.0008	Programmed cell death 1 ligand 2 (PDCD1LG2)
NM_000958.2	174.0	289.9	1.7	0.0026	Prostaglandin E receptor 4 (subtype EP4) (PTGER4)
NM_006404.3	931.5	1586.9	1.7	0.0015	Protein C receptor, endothelial (EPCR) (PROCR)
NM_005608.1	24.4	76.4	3.1	0.0004	Protein tyrosine phosphatase, receptor type, C-associated protein (PTPRCAP)
NM_002564.2	120.3	248.3	2.1	0.0032	Purinergic receptor P2Y, G-protein coupled, 2 (P2RY2), transcript variant 2
NM_001002292.1	820.9	2079.1	2.5	0.0012	Putative nfkb activating protein 373 (FLJ23091), transcript variant 2, mrna

Table 5.3. Contd.

NCBI Accession	Control Average	Indole Average	Fold Change (ind/cont)	*p*-value	Description
X58529.1	153.2	512.8	3.3	0.0016	Rearranged immunoglobulin mrna for mu heavy chain enhancer and constant region
NM_133631.1	51.9	91.0	1.8	0.0051	Roundabout, axon guidance receptor, homolog 1 (Drosophila) (ROBO1), transcript variant 2
NM_016479.3	206.2	603.7	2.9	0.0052	Scotin (SCOTIN)
NM_003004.1	82.0	125.6	1.5	0.0075	Secreted and transmembrane 1 (SECTM1)
NM_000655.2	125.0	60.7	-2.1	0.0038	Selectin L (lymphocyte adhesion molecule 1) (SELL)
NM_006379.2	34.2	110.8	3.2	0.0005	Sema domain, immunoglobulin domain (Ig), short basic domain, secreted, (semaphorin) 3C (SEMA3C)
NM_173050.1	5.4	17.0	3.1	0.0017	Signal peptide, CUB domain, EGF-like 1 (SCUBE1)
NM_007315.2	825.9	1097.5	1.3	0.0008	Signal transducer and activator of transcription 1, 91kda (STAT1), transcript variant alpha
NM_005419.2	131.7	340.4	2.6	0.0063	Signal transducer and activator of transcription 2, 113kda (STAT2)
NM_003150.3	339.0	739.8	2.2	0.0078	Signal transducer and activator of transcription 3 (acute-phase response factor) (STAT3), transcript variant 2
NM_003152.2	55.0	88.7	1.6	0.0077	Signal transducer and activator of transcription 5A (STAT5A)
NM_012448.3	172.6	303.7	1.8	0.0037	Signal transducer and activator of transcription 5B (STAT5B)
NM_003153.3	175.0	344.6	2.0	0.0021	Signal transducer and activator of transcription 6, interleukin-4 induced (STAT6)
NM_015915.2	39.7	119.9	3.0	0.0013	Spastic paraplegia 3A (autosomal dominant) (SPG3A)
NM_003726.2	333.6	679.9	2.0	0.0012	Src family associated phosphoprotein 1 (SCAP1)
NM_006463.3	383.1	608.6	1.6	0.0065	STAM binding protein (STAMBP), transcript variant 1
NM_003498.3	203.1	730.0	3.6	0.0073	Stannin (SNN)
NM_003932.3	3255.6	5274.5	1.6	0.0018	Suppression of tumorigenicity 13 (colon carcinoma) (Hsp70 interacting protein) (ST13)
NM_003932.3	2631.4	3794.9	1.4	0.0026	Suppression of tumorigenicity 13 (colon carcinoma) (Hsp70 interacting protein) (ST13)
NM_198327.1	258.7	452.0	1.7	0.0099	Suppression of tumorigenicity 7 like (ST7L), transcript variant 5

Table 5.3. Contd.

NCBI Accession	Control Average	Indole Average	Fold Change (ind/cont)	*p*-value	Description
NM_198327.1	111.0	177.0	1.6	0.0057	Suppression of tumorigenicity 7 like (ST7L), transcript variant 5
NM_006289.2	64.4	97.9	1.5	0.0051	Talin 1 (TLN1)
NM_006053.2	137.3	428.7	3.1	0.0002	T-cell, immune regulator 1, atpase, H+ transporting, lysosomal V0 protein a isoform 3 (TCIRG1), transcript variant 2
NM_016151.2	300.8	569.9	1.9	0.0087	Thousand and one amino acid protein kinase (TAO1)
NM_004783.2	260.7	448.8	1.7	0.0010	Thousand and one amino acid protein kinase (TAO1)
NM_199356.1	75.2	167.7	2.2	0.0019	Thrombopoietin (myeloproliferative leukemia virus oncogene ligand, megakaryocyte growth and development factor) (THPO), transcript variant 3
NM_004620.2	453.8	790.1	1.7	0.0020	TNF receptor-associated factor 6 (TRAF6), transcript variant 2
NM_019009.2	1157.0	1840.9	1.6	0.0044	Toll interacting protein (TOLLIP)
NM_003265.2	121.3	227.5	1.9	0.0021	Toll-like receptor 3 (TLR3)
NM_017442.2	298.1	631.4	2.1	0.0036	Toll-like receptor 9 (TLR9), transcript variant A
NM_021649.3	95.8	195.7	2.0	0.0016	Toll-like receptor adaptor molecule 2 (TICAM2), mrna
NM_007233.1	311.5	591.4	1.9	0.0016	TP53 activated protein 1 (TP53AP1)
NM_005423.3	948.6	1587.7	1.7	0.0087	Trefoil factor 2 (spasmolytic protein 1) (TFF2), mrna
NM_006670.3	358.5	1010.0	2.8	0.0002	Trophoblast glycoprotein (TPBG)
NM_003809.2	203.6	350.0	1.7	0.0085	Tumor necrosis factor (ligand) superfamily, member 12 (TNFSF12), transcript variant 1, mrna
NM_003808.2	63.0	108.9	1.7	0.0013	Tumor necrosis factor (ligand) superfamily, member 13 (TNFSF13), transcript variant alpha
NM_003326.2	116.6	243.1	2.1	0.0057	Tumor necrosis factor (ligand) superfamily, member 4 (tax-transcriptionally activated glycoprotein 1, 34kda) (TNFSF4)
NM_000594.2	268.9	509.6	1.9	0.0073	Tumor necrosis factor (TNF superfamily, member 2) (TNF)
NM_001243.2	264.9	510.4	1.9	0.0025	Tumor necrosis factor receptor superfamily, member 8 (TNFRSF8), transcript variant 1
NM_021137.3	555.0	1302.7	2.3	0.0003	Tumor necrosis factor, alpha-induced protein 1 (endothelial) (TNFAIP1)

Table 5.3. Contd.

NCBI Accession	Control Average	Indole Average	Fold Change (ind/cont)	*p*-value	Description
NM_025218.1	1021.7	2060.3	2.0	0.0025	UL16 binding protein 1 (ULBP1)
NM_003361.1	31.1	60.7	2.0	0.0008	Uromodulin (uromucoid, Tamm-Horsfall glycoprotein) (UMOD)
Cell structure/shape (136)					
NM_032432.2	85.8	203.0	2.4	0.0022	Actin binding LIM protein family, member 2 (ABLIM2)
NM_001103.1	21.6	51.0	2.4	0.0104	Actinin, alpha 2 (ACTN2)
NM_020445.1	2803.1	1921.5	-1.5	0.0017	Actin-related protein 3-beta (ARP3BETA)
NM_001627.1	227.9	406.8	1.8	0.0030	Activated leukocyte cell adhesion molecule (ALCAM)
NM_001119.3	1416.4	2459.8	1.7	0.0079	Adducin 1 (alpha) (ADD1), transcript variant 1
NM_004319.1	61.5	149.5	2.4	0.0011	Astrotactin (ASTN), transcript variant 1
NM_031885.2	176.1	416.9	2.4	0.0053	Bardet-Biedl syndrome 2 (BBS2)
NM_199173.2	164.6	303.7	1.8	0.0047	Bone gamma-carboxyglutamate (gla) protein (osteocalcin) (BGLAP)
NM_014567.2	227.6	457.9	2.0	0.0033	Breast cancer anti-estrogen resistance 1 (BCAR1)
NM_004360.2	5445.5	9723.2	1.8	0.0008	Cadherin 1, type 1, E-cadherin (epithelial) (CDH1)
NM_004933.2	277.6	511.8	1.8	0.0025	Cadherin 15, M-cadherin (myotubule) (CDH15)
NM_004934.2	97.9	157.9	1.6	0.0020	Cadherin 18, type 2 (CDH18)
NM_144985.2	50.8	117.0	2.3	0.0004	Cadherin-like 24 (CDH24)
NM_033139.2	187.6	290.0	1.5	0.0081	Caldesmon 1 (CALD1), transcript variant 4
NM_024734.2	192.5	461.9	2.4	0.0002	Calmin (calponin-like, transmembrane) (CLMN)
NM_001746.2	2476.7	5527.0	2.2	0.0012	Calnexin (CANX)
NM_001331.1	430.7	723.5	1.7	0.0040	Catenin (cadherin-associated protein), delta 1 (CTNND1)
NM_001332.2	131.6	295.0	2.2	0.0077	Catenin (cadherin-associated protein), delta 2 (neural plakophilin-related arm-repeat protein) (CTNND2)
NM_001771.1	92.7	153.2	1.7	0.0045	CD22 antigen (CD22)
NM_001001389.1	219.9	369.2	1.7	0.0001	CD44 antigen (homing function and Indian blood group system) (CD44), transcript variant 2

Table 5.3. Contd.

NCBI Accession	Control Average	Indole Average	Fold Change (ind/cont)	*p*-value	Description
NM_001001389.1	151.8	370.5	2.4	0.0005	CD44 antigen (homing function and Indian blood group system) (CD44), transcript variant 2
NM_001777.2	125.8	267.9	2.1	0.0083	CD47 antigen (Rh-related antigen, integrin-associated signal transducer) (CD47), transcript variant 1
NM_004848.1	301.2	1359.7	4.5	0.0002	Chromosome 1 open reading frame 38 (c1orf38)
NM_020770.1	183.9	477.0	2.6	0.0003	Cingulin (CGN)
NM_021101.3	89.4	172.4	1.9	0.0030	Claudin 1 (CLDN1)
NM_005602.4	106.2	28.9	-3.7	0.0023	Claudin 11 (oligodendrocyte transmembrane protein) (CLDN11)
NM_012129.2	447.7	829.1	1.9	0.0017	Claudin 12 (CLDN12)
NM_020384.2	232.1	105.6	-2.2	0.0039	Claudin 2 (CLDN2)
NM_194284.1	720.0	1425.8	2.0	0.0010	Claudin 23 (CLDN23)
NM_001306.2	651.1	2295.6	3.5	0.0009	Claudin 3 (CLDN3)
NM_001305.3	4658.2	12252.5	2.6	0.0007	Claudin 4 (CLDN4)
NM_021195.3	43.8	73.9	1.7	0.0099	Claudin 6 (CLDN6)
NM_001307.3	1176.0	3477.4	3.0	0.0028	Claudin 7 (CLDN7)
NM_000089.3	44.7	19.6	-2.3	0.0058	Collagen, type I, alpha 2 (COL1A2)
NM_020441.1	664.7	1878.2	2.8	0.0021	Coronin, actin binding protein, 1B (CORO1B)
NM_012076.2	341.0	745.6	2.2	0.0056	Crumbs homolog 1 (Drosophila) (CRB1), transcript variant 1
NM_194447.1	76.0	139.0	1.8	0.0049	C-type (calcium dependent, carbohydrate-recognition domain) lectin, superfamily member 6 (CLECSF6), transcript variant 3
NM_024422.2	243.5	483.7	2.0	0.0075	Desmocollin 2 (DSC2), transcript variant Dsc2a
NM_001943.1	1625.1	3702.8	2.3	0.0002	Desmoglein 2 (DSG2)
NM_173674.1	30.1	44.9	1.5	0.0027	Discoidin, CUB and LCCL domain containing 1 (DCBLD1)
NM_014992.1	225.3	488.1	2.2	0.0000	Dishevelled associated activator of morphogenesis 1 (DAAM1)
NM_004395.2	1287.5	2345.4	1.8	0.0013	Drebrin 1 (DBN1), transcript variant 1
NM_004010.1	154.6	456.7	3.0	0.0002	Dystrophin (muscular dystrophy, Duchenne and Becker types) (DMD), transcript variant Dp427p2
NM_003633.1	2528.5	4064.2	1.6	0.0010	Ectodermal-neural cortex (with BTB-like domain) (ENC1)
NM_032048.1	358.0	259.2	-1.4	0.0016	Elastin microfibril interfacer 2 (EMILIN2)

Table 5.3. Contd.

NCBI Accession	Control Average	Indole Average	Fold Change (ind/cont)	*p*-value	Description
NM_000118.1	9.4	24.8	2.6	0.0066	Endoglin (Osler-Rendu-Weber syndrome 1) (ENG)
NM_004429.3	161.9	282.0	1.7	0.0035	Ephrin-B1 (EFNB1)
NM_005797.2	945.0	1591.6	1.7	0.0018	Epithelial V-like antigen 1 (EVA1), transcript variant 1
NM_177996.1	142.1	312.8	2.2	0.0039	Erythrocyte membrane protein band 41-like 1 (EPB41L1), transcript variant 2
NM_001978.1	261.6	606.5	2.3	0.0068	Erythrocyte membrane protein band 49 (dematin) (EPB49)
NM_006691.2	30.8	59.1	1.9	0.0010	Extracellular link domain containing 1 (XLKD1)
NM_022549.2	175.2	287.0	1.6	0.0056	Fasciculation and elongation protein zeta 1 (zygin I) (FEZ1), transcript variant 2
NM_013281.2	76.7	178.3	2.3	0.0011	Fibronectin leucine rich transmembrane protein 3 (FLRT3), transcript variant 1
NM_001458.1	540.0	1056.0	2.0	0.0007	Filamin C, gamma (actin binding protein 280) (FLNC)
AK074096.1	527.0	797.1	1.5	0.0036	FLJ00167 protein
AK074177.1	13.1	49.1	3.7	0.0092	FLJ00250 protein
NM_005267.2	109.0	214.3	2.0	0.0088	Gap junction protein, alpha 8, 50kda (connexin 50) (GJA8)
NM_024009.1	29.1	71.6	2.5	0.0062	Gap junction protein, beta 3, 31kda (connexin 31) (GJB3)
NM_153212.1	49.3	84.2	1.7	0.0029	Gap junction protein, beta 4 (connexin 303) (GJB4)
NM_181538.1	14.2	44.2	3.1	0.0059	Gap junction protein, epsilon 1, 29kda (GJE1)
NM_000177.3	2045.1	4513.1	2.2	0.0046	Gelsolin (amyloidosis, Finnish type) (GSN), transcript variant 1
NM_002149.2	145.8	342.6	2.3	0.0023	Hippocalcin-like 1 (HPCAL1), transcript variant 1
NM_003959.1	34.5	64.1	1.9	0.0029	Huntingtin interacting protein-1-related (HIP1R)
NM_003637.3	73.1	146.7	2.0	0.0104	Integrin, alpha 10 (ITGA10)
NM_012211.2	765.7	1125.2	1.5	0.0102	Integrin, alpha 11 (ITGA11)
NM_005501.1	3602.9	5966.2	1.7	0.0070	Integrin, alpha 3 (antigen CD49C, alpha 3 subunit of VLA-3 receptor) (ITGA3), transcript variant b
NM_000210.1	3308.6	6463.9	2.0	0.0053	Integrin, alpha 6 (ITGA6)
NM_000213.2	539.0	1237.0	2.3	0.0070	Integrin, beta 4 (ITGB4)
NM_000888.3	42.8	169.7	4.0	0.0015	Integrin, beta 6 (ITGB6)

Table 5.3. Contd.

NCBI Accession	Control Average	Indole Average	Fold Change (ind/cont)	*p*-value	Description
NM_002214.1	51.0	80.6	1.6	0.0024	Integrin, beta 8 (ITGB8)
NM_080878.2	137.6	270.0	2.0	0.0065	Intelectin 2 (ITLN2)
NM_000873.2	503.2	773.9	1.5	0.0027	Intercellular adhesion molecule 2 (ICAM2)
NM_017415.1	58.9	132.8	2.3	0.0020	Kelch-like 3 (Drosophila) (KLHL3)
NM_014718.1	120.5	293.3	2.4	0.0030	KIAA0726 protein, complete cds
AB028952.1	1224.6	2813.1	2.3	0.0010	KIAA1029 protein
NM_024003.1	99.4	339.4	3.4	0.0019	L1 cell adhesion molecule (hydrocephalus, stenosis of aqueduct of Sylvius 1, MASA (mental retardation, aphasia, shuffling gait and adducted thumbs) syndrome, spastic paraplegia 1) (L1CAM), transcript variant 2
NM_000227.2	712.8	1310.4	1.8	0.0014	Laminin, alpha 3 (LAMA3), transcript variant 2
NM_002292.2	233.8	457.3	2.0	0.0014	Laminin, beta 2 (laminin S) (LAMB2)
NM_002345.2	20.1	49.3	2.5	0.0055	Lumican (LUM)
NM_005581.2	114.5	379.8	3.3	0.0022	Lutheran blood group (Auberger b antigen included) (LU)
NM_002348.1	32.4	50.3	1.6	0.0099	Lymphocyte antigen 9 (LY9)
NM_002298.2	444.9	734.5	1.7	0.0073	Lymphocyte cytosolic protein 1 (L-plastin) (LCP1)
NM_013404.1	438.1	1402.4	3.2	0.0080	Mesothelin (MSLN), transcript variant 2
NM_005928.1	137.1	336.5	2.5	0.0006	Milk fat globule-EGF factor 8 protein (MFGE8)
AB038784.1	940.6	2441.9	2.6	0.0019	MUC3A mrna for intestinal mucin
NM_182741.1	202.3	378.1	1.9	0.0073	Mucin 1, transmembrane (MUC1)
NM_033049.1	342.0	1516.5	4.4	0.0013	Mucin 13, epithelial transmembrane (MUC13)
NM_152673.1	558.4	2013.4	3.6	0.0002	Mucin 20 (MUC20)
NM_031265.1	44.5	110.7	2.5	0.0064	Mucin and cadherin-like (MUCDHL), transcript variant 4
NM_005936.1	15.7	52.1	3.3	0.0000	Myeloid/lymphoid or mixed-lineage leukemia (trithorax homolog, Drosophila); translocated to, 4 (MLLT4)
NM_004998.1	259.8	585.4	2.3	0.0034	Myosin IE (MYO1E)
NM_006393.1	554.4	1262.2	2.3	0.0006	Nebulette (NEBL), transcript variant 1
NM_015080.2	360.5	1001.8	2.8	0.0006	Neurexin 2 (NRXN2), transcript variant alpha-1
NM_018977.1	15.7	41.0	2.6	0.0052	Neuroligin 3 (NLGN3)

Table 5.3. Contd.

NCBI Accession	Control Average	Indole Average	Fold Change (ind/cont)	*p*-value	Description
U83115.1	171.3	418.6	2.4	0.0055	Non-lens beta gamma-crystallin like protein (AIM1) mrna
NM_022141.3	493.9	957.3	1.9	0.0058	Parvin, gamma (PARVG)
NM_005032.3	765.5	1281.9	1.7	0.0093	Plastin 3 (T isoform) (PLS3)
NM_005761.1	95.4	207.4	2.2	0.0035	Plexin C1 (PLXNC1)
NM_000296.2	82.1	146.3	1.8	0.0005	Polycystic kidney disease 1 (autosomal dominant) (PKD1)
NM_000313.1	232.0	565.7	2.4	0.0003	Protein S (alpha) (PROS1)
NM_080792.1	162.1	240.5	1.5	0.0037	Protein tyrosine phosphatase, non-receptor type substrate 1 (PTPNS1)
NM_080792.1	47.2	82.9	1.8	0.0043	Protein tyrosine phosphatase, non-receptor type substrate 1 (PTPNS1)
NM_032973.1	164.9	320.6	1.9	0.0076	Protocadherin 11 Y-linked (PCDH11Y), transcript variant c
NM_033056.2	1557.0	2887.7	1.9	0.0099	Protocadherin 15 (PCDH15)
NM_033100.1	36.9	77.0	2.1	0.0007	Protocadherin 21 (PCDH21)
NM_031852.1	114.4	259.8	2.3	0.0072	Protocadherin alpha 7 (PCDHA7), transcript variant 2
NM_013340.2	109.4	157.0	1.4	0.0001	Protocadherin beta 1 (PCDHB1)
NM_018939.2	82.6	140.9	1.7	0.0008	Protocadherin beta 6 (PCDHB6)
NM_019119.3	49.0	80.1	1.6	0.0076	Protocadherin beta 9 (PCDHB9)
NM_018917.2	260.7	422.4	1.6	0.0021	Protocadherin gamma subfamily A, 4 (PCDHGA4), transcript variant 1
NM_032054.1	226.1	442.6	2.0	0.0027	Protocadherin gamma subfamily A, 5 (PCDHGA5), transcript variant 2
NM_002906.2	1027.9	553.3	-1.9	0.0033	Radixin (RDX)
NM_014470.2	160.0	304.4	1.9	0.0066	Rho family gtpase 1 (RND1)
NM_005506.2	3373.6	8365.3	2.5	0.0026	Scavenger receptor class B, member 2 (SCARB2)
NM_003005.2	140.1	220.0	1.6	0.0100	Selectin P (granule membrane protein 140kda, antigen CD62) (SELP)
NM_003966.1	76.5	175.8	2.3	0.0012	Sema domain, seven thrombospondin repeats (type 1 and type 1-like), transmembrane domain (TM) and short cytoplasmic domain, (semaphorin) 5A (SEMA5A)
NM_016543.1	273.2	435.8	1.6	0.0046	Sialic acid binding Ig-like lectin 7 (SIGLEC7)
NM_015385.1	89.1	166.8	1.9	0.0009	Sorbin and SH3 domain containing 1 (SORBS1)
NM_003127.1	1321.2	2456.5	1.9	0.0072	Spectrin, alpha, non-erythrocytic 1 (alpha-fodrin) (SPTAN1)

Table 5.3. Contd.

NCBI Accession	Control Average	Indole Average	Fold Change (ind/cont)	*p*-value	Description
NM_178313.1	884.1	1878.7	2.1	0.0002	Spectrin, beta, non-erythrocytic 1 (SPTBN1), transcript variant 2
NM_006307.2	123.4	183.6	1.5	0.0020	Sushi-repeat-containing protein, X-linked (SRPX)
Y11072.1	615.9	1047.6	1.7	0.0029	Synaptopodin
NM_003098.2	148.1	365.8	2.5	0.0051	Syntrophin, alpha 1 (dystrophin-associated protein A1, 59kda, acidic component) (SNTA1)
NM_003285.1	298.0	579.2	1.9	0.0010	Tenascin R (restrictin, janusin) (TNR)
NM_003247.2	213.2	404.7	1.9	0.0034	Thrombospondin 2 (THBS2)
NM_003257.2	1192.5	1667.4	1.4	0.0037	Tight junction protein 1 (zona occludens 1) (TJP1), transcript variant 1
NM_014428.1	46.7	266.0	5.7	0.0080	Tight junction protein 3 (zona occludens 3) (TJP3)
NM_080604.1	343.8	655.1	1.9	0.0037	Tight junction protein 4 (peripheral) (TJP4)
NM_000358.1	101.7	295.6	2.9	0.0022	Transforming growth factor, beta-induced, 68kda (TGFBI)
NM_014548.2	16.9	43.7	2.6	0.0037	Tropomodulin 2 (neuronal) (TMOD2)
NM_000368.2	642.4	1239.9	1.9	0.0065	Tuberous sclerosis 1 (TSC1)
NM_017549.1	2465.2	3912.4	1.6	0.0090	Upregulated in colorectal cancer gene 1 (UCC1)
NM_007124.1	30.1	78.4	2.6	0.0076	Utrophin (homologous to dystrophin) (UTRN)
NM_001078.2	79.7	101.0	1.3	0.0069	Vascular cell adhesion molecule 1 (VCAM1), transcript variant 1
NM_015873.1	153.4	344.6	2.2	0.0005	Villin-like (VILL)
NM_014000.1	853.4	1308.2	1.5	0.0008	Vinculin (VCL), transcript variant meta-VCL
Apoptosis (35)					
NM_014977.1	87.4	289.1	3.3	0.0002	Apoptotic chromatin condensation inducer 1 (ACIN1)
NM_033027.2	1016.7	1747.7	1.7	0.0041	AXIN1 up-regulated 1 (AXUD1)
NM_001166.3	438.1	685.0	1.6	0.0101	Baculoviral IAP repeat-containing 2 (BIRC2)
NM_001165.3	121.2	195.7	1.6	0.0006	Baculoviral IAP repeat-containing 3 (BIRC3), transcript variant 1
NM_016077.1	5901.6	3361.9	-1.8	0.0066	Bcl-2 inhibitor of transcription (Bit1)
NM_004330.1	1475.1	1202.1	-1.2	0.0083	BCL2/adenovirus E1B 19kda interacting protein 2 (BNIP2)

Table 5.3. Contd.

NCBI Accession	Control Average	Indole Average	Fold Change (ind/cont)	*p*-value	Description
NM_004331.2	656.3	1384.1	2.1	0.0033	BCL2/adenovirus E1B 19kda interacting protein 3-like (BNIP3L)
NM_004324.3	1352.9	1898.3	1.4	0.0050	BCL2-associated X protein (BAX), transcript variant beta
NM_138639.1	87.4	175.8	2.0	0.0084	BCL2-like 12 (proline rich) (BCL2L12), transcript variant 1
NM_015367.2	495.4	951.9	1.9	0.0099	BCL2-like 13 (apoptosis facilitator) (BCL2L13), nuclear gene encoding mitochondrial protein
NM_030766.1	570.8	1042.7	1.8	0.0019	BCL2-like 14 (apoptosis facilitator) (BCL2L14), transcript variant 2
NM_014959.1	42.4	96.5	2.3	0.0029	Caspase recruitment domain family, member 8 (CARD8)
NM_014430.1	106.9	289.7	2.7	0.0002	Cell death-inducing DFFA-like effector b (CIDEB)
NM_022336.1	98.7	220.8	2.2	0.0015	Ectodysplasin 1, anhidrotic receptor (EDAR)
NM_032346.1	1247.5	714.0	-1.7	0.0077	Hypothetical protein MGC13096 (MGC13096)
NM_022151.3	135.3	289.9	2.1	0.0080	Modulator of apoptosis 1 (MOAP1)
NM_002462.2	448.5	695.2	1.5	0.0023	Myxovirus (influenza virus) resistance 1, interferon-inducible protein p78 (mouse) (MX1)
BC028066.1	38.1	91.1	2.4	0.0078	NACHT, leucine rich repeat and PYD containing 1, mrna (cdna clone IMAGE:5212243)
NM_013436.3	2241.2	4173.6	1.9	0.0009	NCK-associated protein 1 (NCKAP1), transcript variant 1
NM_014380.1	1884.4	2664.4	1.4	0.0016	Nerve growth factor receptor (TNFRSF16) associated protein 1 (NGFRAP1), transcript variant 3
NM_013982.1	37.6	66.5	1.8	0.0077	Neuregulin 2 (NRG2), transcript variant 3
NM_020529.1	770.4	1530.2	2.0	0.0026	Nuclear factor of kappa light polypeptide gene enhancer in B-cells inhibitor, alpha (NFKBIA)
NM_007318.1	1238.4	2422.2	2.0	0.0033	Presenilin 1 (Alzheimer disease 3) (PSEN1), transcript variant I-463
NM_003015.2	265.9	620.7	2.3	0.0016	Secreted frizzled-related protein 5 (SFRP5)
NM_020796.2	40.6	87.9	2.2	0.0049	Sema domain, transmembrane domain (TM), and cytoplasmic domain, (semaphorin) 6A (SEMA6A)
NM_018957.2	95.4	144.7	1.5	0.0055	SH3-domain binding protein 1 (SH3BP1)

Table 5.3. Contd.

NCBI Accession	Control Average	Indole Average	Fold Change (ind/cont)	*p*-value	Description
NM_006747.2	329.1	674.6	2.0	0.0011	Signal-induced proliferation-associated gene 1 (SIPA1), transcript variant 2
NM_004295.2	1440.4	2616.3	1.8	0.0027	TNF receptor-associated factor 4 (TRAF4), transcript variant 1
NM_001252.2	29.7	97.9	3.3	0.0013	Tumor necrosis factor (ligand) superfamily, member 7 (TNFSF7)
NM_003811.2	109.2	67.4	-1.6	0.0001	Tumor necrosis factor (ligand) superfamily, member 9 (TNFSF9)
NM_003820.2	72.2	227.7	3.2	0.0001	Tumor necrosis factor receptor superfamily, member 14 (herpesvirus entry mediator) (TNFRSF14)
NM_001065.2	335.7	839.2	2.5	0.0057	Tumor necrosis factor receptor superfamily, member 1A (TNFRSF1A)
NM_014452.3	9366.6	7032.8	-1.3	0.0065	Tumor necrosis factor receptor superfamily, member 21 (TNFRSF21)
NM_004881.2	600.3	1163.4	1.9	0.0004	Tumor protein p53 inducible protein 3 (TP53I3), transcript variant 1
NM_006377.2	1291.4	2133.5	1.7	0.0081	Unc-13 homolog B (C elegans) (UNC13B)

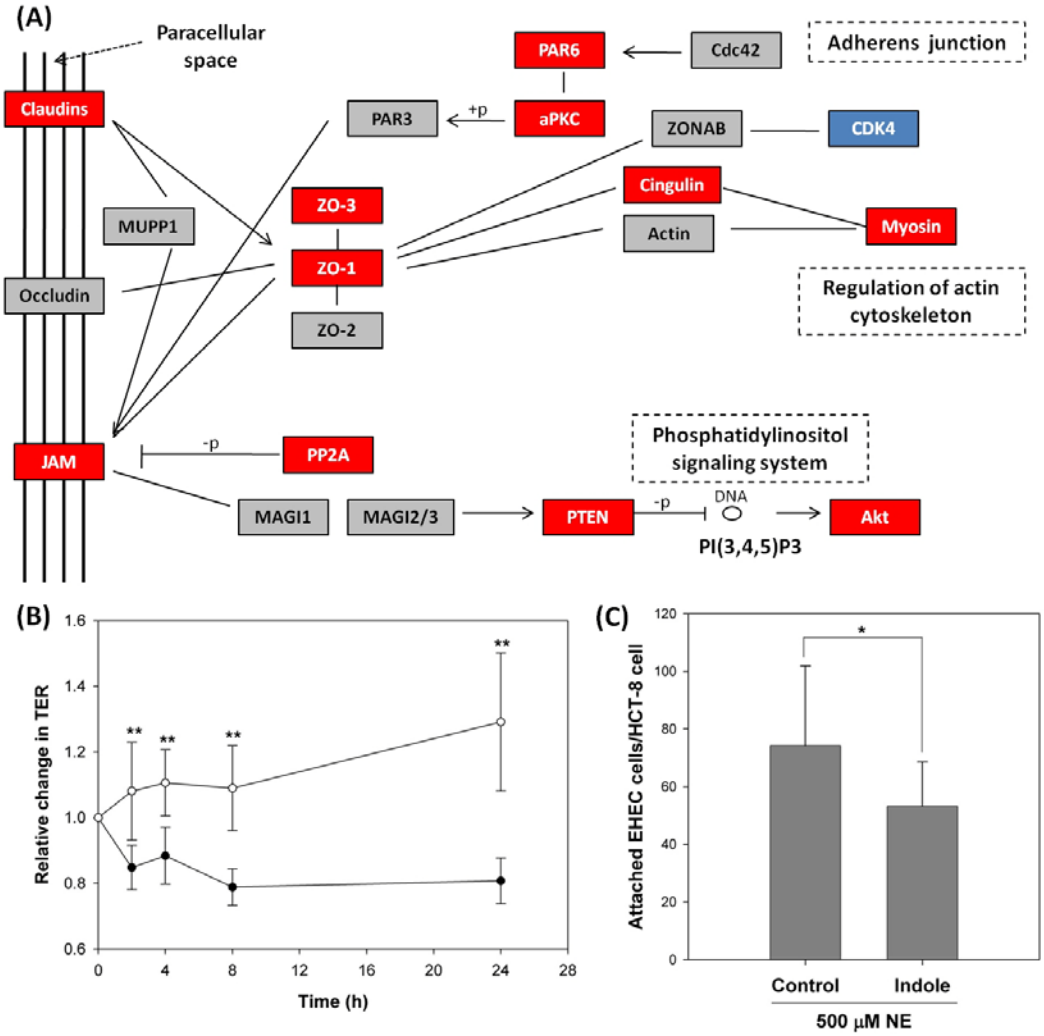

Fig. 5.2. Changes in tight junction proteins and trans-epithelial resistance. (A) Pathways containing differentially-expressed genes involved in tight junction formation were adapted from Pathway Express using KEGG classifications. Red: up-regulation; blue: down-regulation, and gray: no change in expression; arrow: molecular interaction leading to activation; blunt line without an arrowhead: molecular interaction leading to inhibition. The pathway scheme shown is based on microarray data and does not include post-transcriptional regulation. (B) Changes in the TER of polarized HCT-8 cells exposed to either solvent (●) or indole (○) for 24 h. Data represent mean ± standard deviation from seven measurements at each time-point and two independent experiments. (C) Effect of indole pretreatment on adherence of EHEC to HCT-8 cells in the presence of 500 μM NE. Data represent mean ± standard deviation from three wells per experiment and three independent experiments. * denotes statistical significance using the Student's T-test test at $p < 0.05$ and ** denotes significance at $p < 0.005$.

The trans-epithelial resistance (TER) of epithelial cells after indole exposure was measured to investigate the effect of indole on tight junction integrity and cell permeability. Fig. 5.2B shows that indole increased the TER of HCT-8 cells within 4 h of exposure and by 1.6-fold after 24 h. Since increase in mucin production has been previously shown to attenuate pathogen colonization (154), we also investigated the effect of indole exposure on the colonization of HCT-8 cells by EHEC. Pretreatment of HCT-8 cells with 1 mM indole for 24 h decreased the NE-mediated EHEC colonization (26) by 1.4-fold (Fig. 5.2C). These phenotypic results are consistent with changes in gene expression and suggest that exposure to physiologically-relevant concentrations of indole strengthens intestinal epithelial cell barrier properties and increases resistance to pathogen colonization.

5.4.3 Changes in Toll-like Receptor Signaling

Exposure to 1 mM indole led to an increase in the expression of two TLR genes – TLR-3 and TLR-9. TLRs respond to bacterial ligands and activate the host immune system; however, TLR-2, TLR-3, and TLR-9 have been reported to modulate intestinal inflammation and maintain homeostasis (91). More importantly, TLRs that play a significant role in responding to pathogens (e.g., TLR2, TLR4) were not altered in expression. Additionally, genes involved in the modulation of TLR signaling – TOLLIP, SIGIRR, and SOCS5 – were also induced by indole. Similarly, genes involved in the phosphoinositide-3-kinase (PI3K) pathway, that modulates TLR signaling (Fig. 5.3A) and leads to anti-inflammatory cytokine IL-10 induction (142), were also induced by indole. Three genes involved in PI3K signaling (PIK3CA, PIK3CB, and PIK3CD) were induced, as was the transcription factor AKT1 that is activated by signaling through the PI3K pathway. Downstream target genes of AKT1, including the cAMP response element-binding protein (CREB) and IL-10, were also induced upon addition of indole. Thus, our data

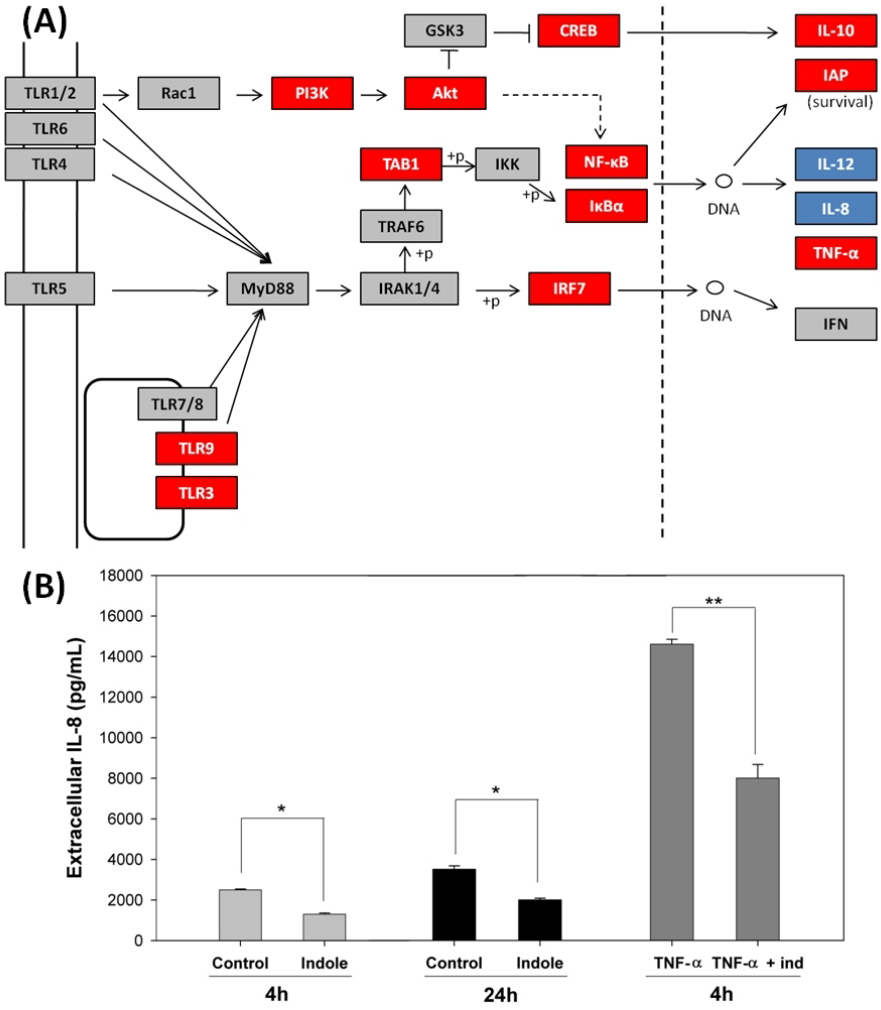

Fig. 5.3. Changes in Toll-like receptor, IL-8 and IL-10 signaling. (A) Pathways containing differentially-expressed genes involved in tight junction formation were adapted from Pathway Express using KEGG classifications. Red: up-regulation; blue: down-regulation, and gray: no change in expression; arrow: molecular interaction leading to activation; blunt line without an arrowhead: molecular interaction leading to inhibition. The pathway scheme shown is based on microarray data and does not include post-transcriptional regulation. (B) Secretion of IL-8 in HCT-8 cells exposed to indole for 4 h or 24 h, in the presence or absence of 40 ng/mL TNF-α. Data represent mean ± standard deviation from three independent experiments. (C) Intracellular staining and flow cytometry of IL-10 in HCT-8 cells exposed to indole for 24 h. Two-color dot plots of number of PE-stained cells and forward scatter for solvent control, indole-treated and unstained cells are shown. Percentages in the boxed region indicate the proportion of HCT-8 cells producing IL-10 in one representative experiment. (D) Average increase in IL-10 expression data from three independent experiments. * denotes statistical significance using the Student's T-test test at $p < 0.05$ and ** denotes significance at $p < 0.005$.

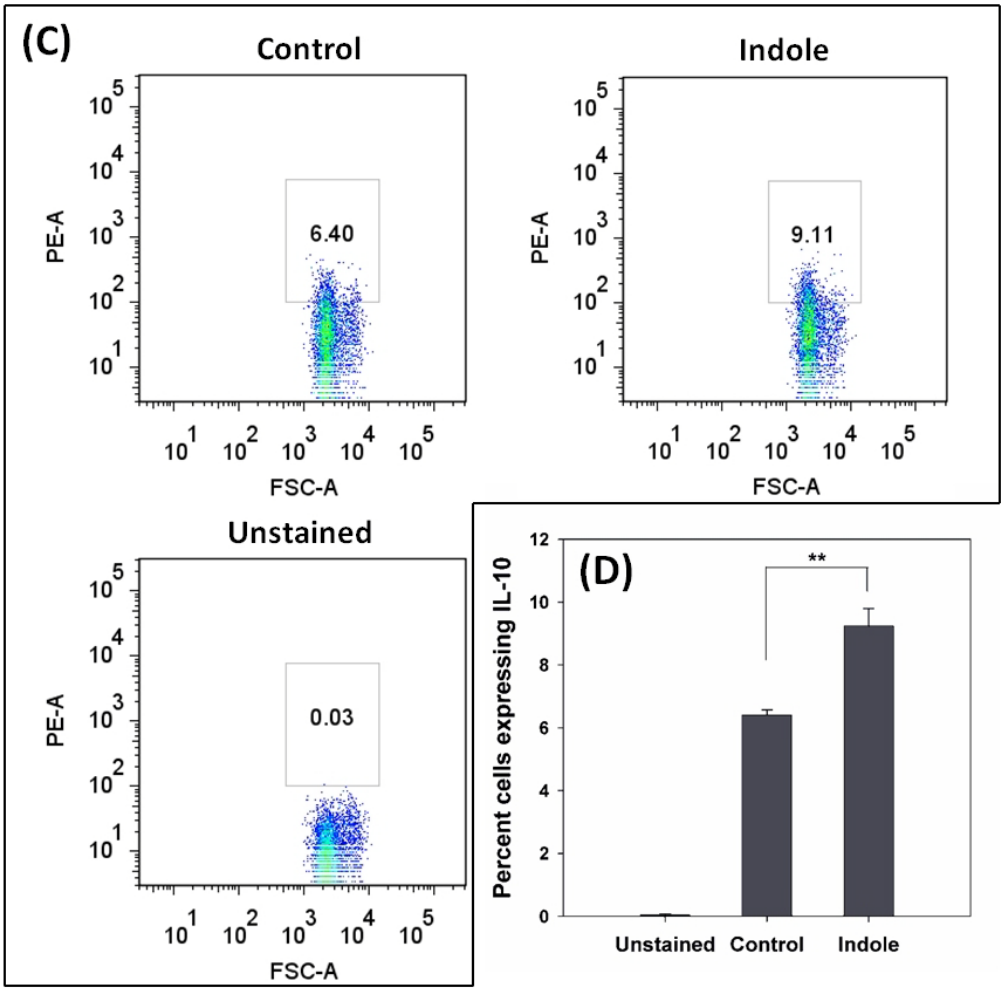
(C)
Control
Indole
Unstained
PE-A
FSC-A
6.40
9.11
0.03
(D)
Percent cells expressing IL-10
**
Unstained
Control
Indole

Fig. 5.3. Contd.

strongly suggest that indole modulates TLR signaling in HCT-8 intestinal epithelial cells, both through up-regulation of anti-inflammatory TLR, and through the PI3K-mediated down-regulation of inflammatory TLR signaling.

Since TLR3 and TLR9 are not present on the cell membrane but are internal (i.e., on the endosomal membrane), we determined if indole was internalized by HCT-8 cells. Measurement of extracellular indole (25) showed that indole was not significantly internalized by HCT-8 cells, as ~90% of the indole added (1 mM) was still detected in the culture medium after 24 h.

5.4.4 Changes in inflammatory cytokine and chemokine gene expression

Exposure to indole for 24 h coordinately altered the expression of several cytokines in HCT-8 intestinal epithelial cells. Genes that were increased in expression upon exposure to 1 mM indole included the precursor to the pro-inflammatory cytokine IL-1 (pre-IL-1). In addition, the receptor for the pro-inflammatory cytokine IL-2, IL-4, IL-18 binding protein, IL-24, and IL-28 were all induced; suggesting indole exposure leads to an increase in cytokine expression and signaling in HCT-8 intestinal epithelial cells. In addition to altering the expression of cytokines, indole also induced the expression of several chemokines (CCL25, CCL4, CCL16, CXCL3, XCL1 and CX3CL1) in HCT-8 cells.

However, not all changes in expression were pro-inflammatory as the expression of receptors for anti-inflammatory cytokines (IL-10, IL-11) was also induced by indole. In addition, the expression of several other pro-inflammatory cytokines was decreased in HCT-8 cells upon exposure to indole. IL-8, an alarm cytokine that induces migration of neutrophils across the endothelium, basophil chemotaxis to the infection site, and enhances removal of microbes through neutrophil recruitment (74), was repressed (Fig. 5.3A) upon exposure to indole. CXCL5 (or ENA-78), a chemokine that is structurally and functionally similar to IL-8 (155) and is highly

expressed in intestinal epithelial cells during chronic inflammation (155), was also repressed. IL-12, which is one of the first cytokines to be released in response to detection of a pathogen through TLR signaling and is important in the initiation of the inflammatory response (84), was repressed. These changes in expression suggest that exposure to indole leads to coordinated changes in the expression of pro- and anti-inflammatory cytokines and chemokines.

Changes in IL-8 expression upon 1 mM indole exposure were monitored using ELISA to corroborate changes observed with microarrays (Fig. 5.3B). Indole decreased basal IL-8 production in HCT-8 cells at 4 h and 24 h by -1.9-fold and -1.8-fold respectively. Additionally, indole also decreased TNF-α-induced IL-8 production by -1.8-fold, which is consistent with microarray data on the down-regulation of IL-8 mRNA. Intracellular staining and flow cytometry was used to also monitor expression of the anti-inflammatory cytokine IL-10. Figures 5.3C and 5.3D show that indole increased IL-10 expression by 1.5-fold, which together with the increase in IL-10 receptor mRNA expression further suggests that indole increases anti-inflammatory signaling as well.

Downstream mediators of cytokine signaling (i.e., signaling kinases) such as the mitogen-activated protein kinase (MAPK) pathway, which is central to the inflammatory signaling, were differentially expressed. Specifically, the expression of dual specificity phosphatases (DUSPs) – Dusp1, Dusp3, Dusp10, Dusp16, Dusp18 and Dusp22 that function as inhibitors of MAPK signaling (156) – was increased in expression upon indole exposure. However, since several MAPK genes were also up-regulated, further analysis of the phosphorylation state of different pathway components is required to fully understand the changes in MAPK signaling upon indole exposure. Indole also induced the expression of genes in the Jak/STAT signaling pathway, which is activated by pro-inflammatory molecules such as IFN-γ leading to increased microbial killing and cytokine production (157). Jak-1, -2 and -3 were

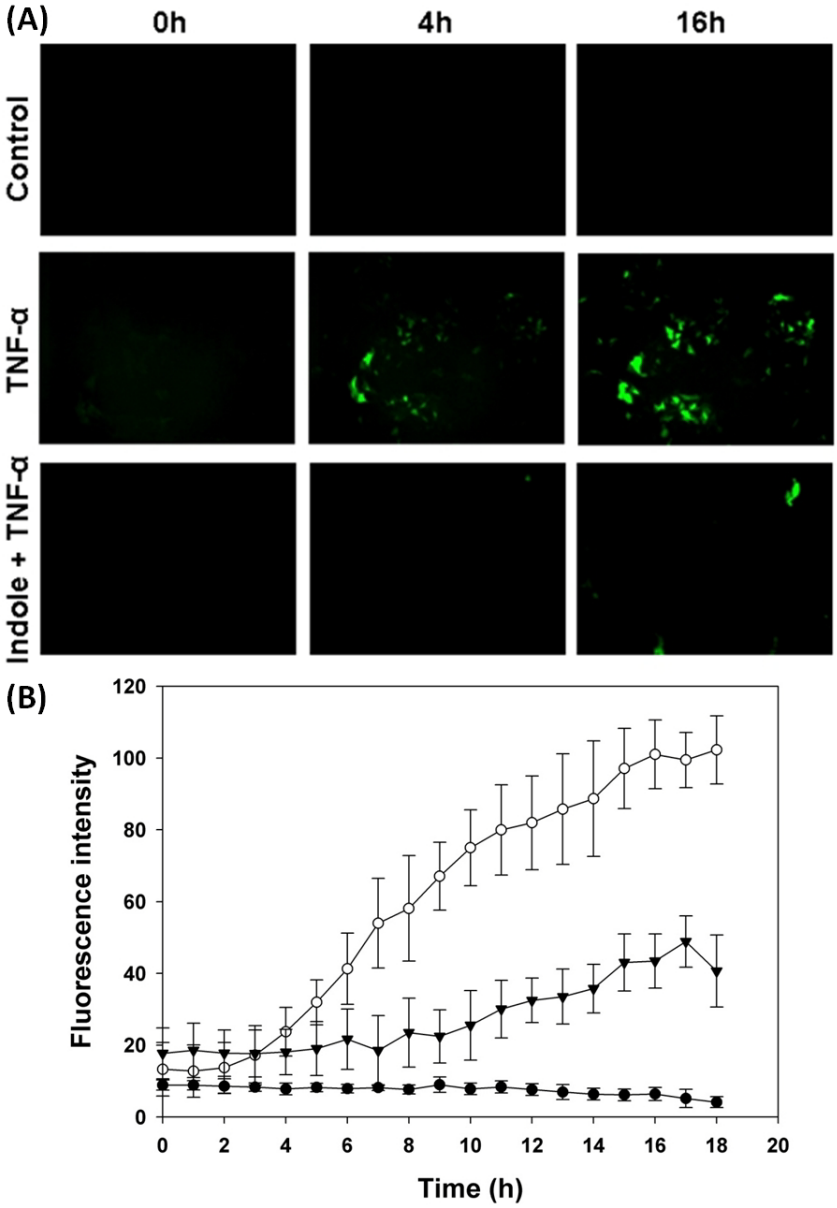

Fig. 5.4. Modulation of NF-κB expression by indole. (A) Effect of indole on NF-κB activation by TNF-α in HCT-8 cells and the resultant GFP expression. (B) Quantification of NF-κB activity in (●) control cells, (○) cells treated with TNF-α to induce NF-κB expression, and (▼) cells treated with indole and TNF-α. Data shown are mean ± standard deviation from images obtained at four locations in three independent experiments.

induced along with STAT-1, -2, -3, -5 and -6 (Table 5.3). The interferon-stimulated transcription factor 3γ (ISGF3G), which is activated by STAT1 to regulate IFN-γ stimulated genes, was also induced in expression upon exposure to indole, along with SOCS, a repressor of Jak-STAT signaling. Therefore, in addition to inducing changes in pro- and anti-inflammatory mediators, exposure to indole also induced coordinated changes in the downstream signaling pathways utilized by these cytokines and chemokines.

We also monitored activation of the prototypical pro-inflammatory transcription factor NF-κB, that has been shown to mediate the inflammatory response both *in vitro* and *in vivo* (158-159), using a HCT-8 GFP reporter cell line for NF-κB (148). Our data show that indole reduced the TNF-α-mediated increase in NF-κB activation in HCT-8 intestinal epithelial cells by 3-fold over 18 h (Figs. 5.4A & 5.4B) and clearly indicate the ability of indole to attenuate TNF-α-mediated inflammation in HCT-8 cells.

5.4.5 Specificity of indole in attenuating NF-κB activation and promoting epithelial cell barrier properties

We investigated the effect of five indole-like molecules (Fig. 5.5) – 1H-indole-2,3-dione (isatin), 7-hydroxyindole (7-HI), 5-hydroxyindole (5-HI), 2-hydroxyindole (2-HI), and indole-3-acetic acid (I3AA) – for establishing the specificity of indole in attenuating NF-κB activation and promoting TER. Fig. 5.6A shows that only 5-HI significantly repressed NF-κB activity in a manner similar to that observed with indole (Fig. 5.4), while the effectiveness of the other molecules varied from having no effect or marginal (7-HI, I3AA, and 2-HI) to actually increasing NF-κB activation (isatin). However, 5-HI did not cause a significant change in the TER of HCT-8 cells after 24 h (Fig. 5.6B), and among the molecules tested, only 7-HI increased the TER to levels comparable with indole (Fig. 5.2B). Thus, although indole-like molecules were

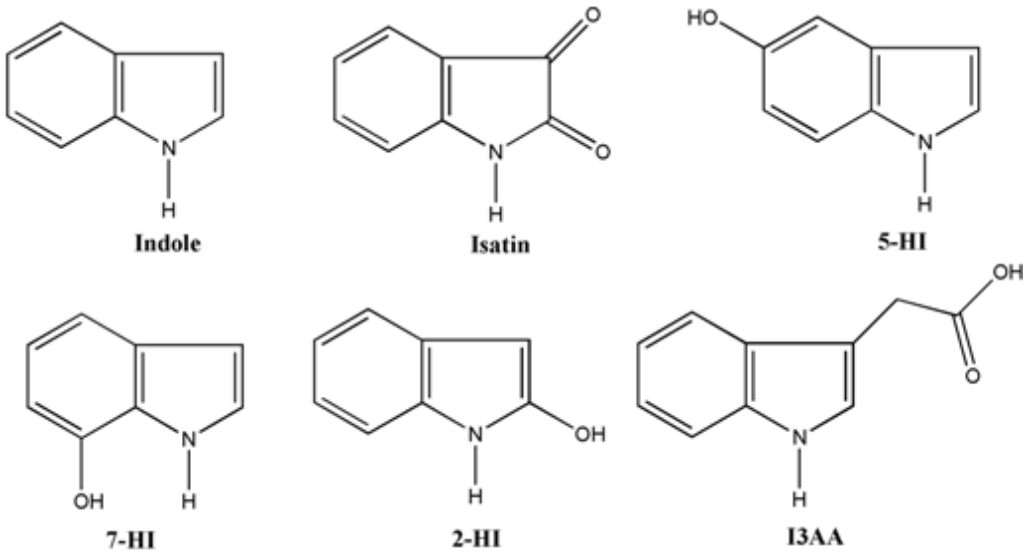

Fig. 5.5. Chemical structure of indole-like compounds used in the study. Indole, isatin, 7-hydroxyindole (7-HI), 5-hydroxyindole (5-HI), 2-hydroxyindole (2-HI), and indole-3-acetic acid (I3AA).

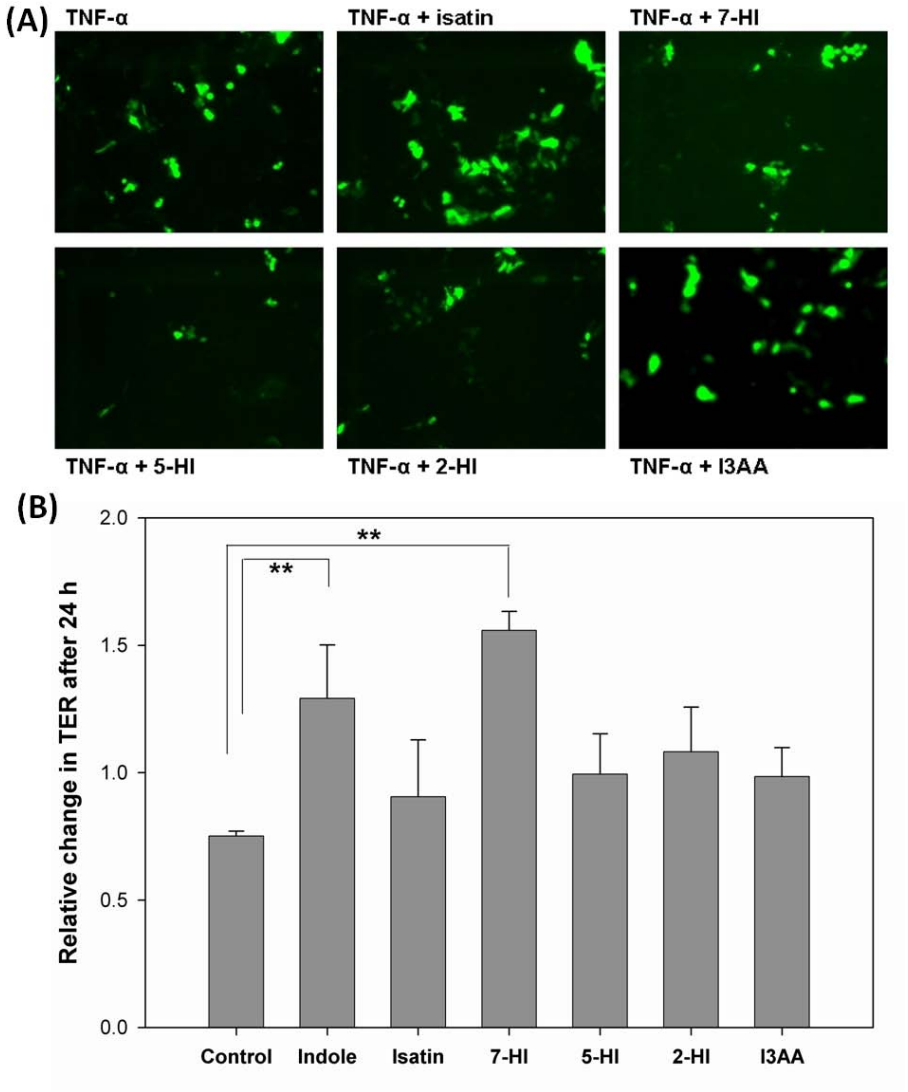

Fig. 5.6. Changes in HCT-8 cell phenotypes with aromatic bicyclic molecules. (A) NF-κB expression in HCT-8 cells and the resultant GFP expression. Images shown are after 16 h of exposure to TNF-α and are representative of data from three independent experiments. (B) Changes in trans-epithelial resistance after exposure to indole-like molecules for 24 h. Data represent mean ± standard deviation from three independent experiments. ** denotes statistical significance using the Student's T-test test at $p < 0.005$.

able to either attenuate NF-κB activation or increase TER at the concentrations tested, changes in both phenotypes were observed only with indole.

In order to further establish that the beneficial effects of indole were not due to an increase in HCT-8 cell number or viability, we determined the change in HCT-8 cell density after exposure to indole for 24 h. Cells exposed to indole showed > 99% viability after 24 h (live cell density in control and indole treated cells was $3.1 \times 10^6 \pm 0.6 \times 10^6$ and $3.0 \times 10^6 \pm 0.7 \times 10^6$ cells/ml, respectively), with a similar increase in the % of live cells as the solvent control. These data suggest that the beneficial effects of indole are not metabolic (i.e., due to an increase in cell numbers).

The whole-transcriptome data were substantiated with qRT-PCR where genes from inflammatory cytokines and signaling, and epithelial barrier function were profiled. ISGF3G was induced 4.1-fold in the microarrays and 5.1 ± 0.1 in qRT-PCR. Similar results were seen for CXCL5 (-5.2-fold in the arrays, -13.6 ± 0.6-fold in qRT-PCR), pre-IL-1 (5.6-fold in the arrays, 5.9 ± 0.2-fold in qRT-PCR), IL-8 (-1.8-fold in the arrays, -1.4 ± 0.1-fold in qRT-PCR), cldn3 (3.5-fold in the arrays, 4.9 ± 0.2-fold in qRT-PCR), TJP3 (5.7-fold in the arrays, 5.5 ± 0.2-fold in RT-PCR), and muc13 (4.4-fold in the arrays, 2.3 ± 0.2-fold in qRT-PCR). Thus, the expression results from whole-transcriptome analysis were in good agreement with the qRT-PCR results.

5.5 DISCUSSION

The recognition of host cell signaling molecules by pathogens through inter-kingdom communication and its role in pathogenesis has been recently documented (16, 26). However, little is known about recognition of bacterial signals by host cells. To-date, specific prokaryotic signals such as the *P. aeruginosa* quorum sensing molecules (AHLs) have been shown to be deleterious to host cells as they help pathogen infections. Here, we show for the first time that

the bacterial stationary phase signal indole is recognized by intestinal epithelial cells, and used to strengthen host cell-barrier properties and maintain controlled inflammation. This is supported by multiple lines of evidence showing that indole (i) increases the expression of genes involved in formation of tight junctions and actin cytoskeleton, as well as increases the trans-epithelial resistance of polarized HCT-8 intestinal epithelial cells, (ii) attenuates IL-8 secretion and TNF-α-mediated NF-κB activation in HCT-8 cells, while increasing IL-10 secretion, (iii) increases resistance of HCT-8 cells to NE-mediated increase in EHEC colonization, and (iv) reduces expression of pro-inflammatory cytokines and chemokines while inducing expression of anti-inflammatory cytokines. Therefore, we propose that indole can be a beneficial inter-kingdom signal that helps improve intestinal epithelial cell function, maintain controlled inflammation, and increase resistance to pathogen colonization.

Several studies have shown that cell-free supernatants of probiotic bacterial cultures increase host epithelial cell barrier properties and resistance to pathogen colonization. However, the identity of specific molecule(s) that contribute to this protective effect and the mechanisms involved are not known, as culture supernatants are complex mixtures comprising of media components, metabolites, and signals secreted by different bacterial species. The data presented here show that indole elicits a response similar to probiotic strains by strengthening host cell barrier properties. Since indole is produced by several commensal bacteria (e.g., *E. coli*, *Bacteroides ovatus*, *Clostridium bifermentans*) that colonize the human GI tract (160), it is intriguing to speculate that the beneficial effects of some probiotic strains are mediated, in part, through indole.

While 4,102 genes (or 8% of the transcriptome) were differentially regulated by indole, it is worth noting that only 83 genes were regulated by 4.0-fold or higher. A moderate response to indole is to be expected since especially indole is abundant in the human GI tract (~ 100 μM

in human feces) (44), and is less likely to perturb the epithelial cell transcriptome like a pathogen. In this regard, our data is similar to that reported by Hasegawa et al. (156) who showed that two different species of commensal bacteria, *Streptococcus gordonii* and *Fusobacterium nucleatum*, perturbed the gingival epithelial cell transcriptome to a lesser extent than the pathogens *Poryphyromonas gingivalis* and *Aggregatibacter actinomycetemcomitans*, which elicited more widespread organism-specific changes in the transcriptome. Striking similarities are also evident between our data and changes in gene expression elicited by *S. gordonii* and *F. nucleatum* in gingival epithelial cells. For example, gene families that were differentially expressed in intestinal epithelial cells upon exposure to indole – tight junction proteins, actin cytoskeleton, cell cycle regulators, phosphatidylinositol signaling, MAP kinase signaling, TLR signaling, and Wnt signaling – were all altered in gingival epithelial cells as well when exposed to commensal bacteria.

In addition to the similarities with commensal response in gingival epithelial cells, significant differences are also observed between the indole response in intestinal epithelial cells and pathogen-mediated changes in expression in gingival epithelial cells. One such example is the activation of caspase-1 by pathogenic bacteria (e.g. lipopolysaccharide, *Salmonella typhimurium* type III secretion), which leads to increased secretion of pro-inflammatory cytokines such as IL-1β and the induction of apoptosis. Hasegawa et al. (156) reported that commensal bacteria did not activate caspase-1 thus indicating physiologic balance between the host and the organism. Similarly, no caspase-1 gene expression was observed in HCT-8 intestinal epithelial cells exposed to indole, which also suggests favorable recognition of indole by intestinal epithelial cells. Furthermore, the lack of activation of TLR signaling by indole, similar to that seen with oral commensal bacteria (156) and opposite to that of oral pathogens

(159), also strongly suggests indole is recognized as a beneficial signal and not detected as a pathogenic signal by intestinal epithelial cells.

The attenuation of basal IL-8 secretion as well as the decrease in TNF-α-mediated increase in IL-8 secretion indicates that indole also exerts anti-inflammatory effects in intestinal epithelial cells. IL-8 is an alarm chemokine that is highly induced by pathogens in a wide variety of cells including human human colon adenocarcinoma cells. For example, a 4- to 30-fold increase in IL-8 and ENA-78 (CXCL5) has been observed in HT-29 and Caco-2 intestinal epithelial cells upon exposure to *Salmonella dublin* (161). However in our study, exposure to indole decreased the expression of ENA-78 and IL-8, which suggests that indole is not recognized as a pathogen signal by intestinal epithelial cells, and strongly proposes an anti-inflammatory role for indole in GI tract inflammation.

It has been proposed that bacteria (or molecules secreted by them) induce the expression of pro- and anti-inflammatory cytokines (162), which function coordinately (i.e., as a network) to regulate the host response to commensal bacteria (162). Disruption of this regulated cytokine response leads to sustained inflammation, as has been shown with IL-10 KO mice developing chronic enterocolitis even in the absence of pathogen colonization (82). In addition, this heightened level of alertness also enables host cells to respond rapidly to the presence of pathogens. Our data showing that indole upregulates the expression of both pro- and anti-inflammatory cytokines is in good agreement with this hypothesis, and suggests that indole-mediated communication between commensal bacteria and host cells controls the balance between pro- and inflammatory cytokine signaling in intestinal epithelial cells.

The intestinal epithelial cell inflammatory response to pathogens is orchestrated, in part, through activation of NF-κB (158-159), which is well established. Our data showing that indole reduced TNF-α-mediated NF-κB activation in intestinal epithelial cells supports the anti-

inflammatory role for indole. Since commensal bacteria reduce the *S. typhimurium*-induced NF-κB activity (158) and inflammation in mice, it is intriguing to speculate that indole could be a signal through which probiotics reduce intestinal inflammation.

The effect of indole on HCT-8 cells also extends beyond alterations in gene expression to changes in prototypical intestinal epithelial cell functions such as barrier integrity. First, the increase in tight junction protein expression and TER is significant, as an increase in tight junction resistance leads to decreased paracellular permeability and reduces the ability of pathogens to cross the epithelial cell barrier. Second, the induction of 50 cytoskeleton genes suggests increased resistance to pathogen colonization since pathogens like *P. aeruginosa*, *Shigella flexneri, Listeria monocytogenes* and enteropathogenic *E. coli* disrupt epithelial cell morphology during infection by interfering with the actin cytoskeleton (163-165). Third, the increase in the expression of several mucin genes is also likely to decrease pathogen colonization, as Kim et al. (154) recently reported that lactobacilli increased the production of mucin 2 (muc2) to inhibit EHEC attachment to epithelial cells *in vitro*. These three lines of evidence strongly support the hypothesis that indole elicits beneficial changes in intestinal epithelial cells.

The alteration of TER and the regulation of inflammation by indole has significant implications in the treatment of chronic intestinal inflammatory diseases such as Crohn's disease, which is an auto-immune disease characterized by sustained inflammation and deterioration of epithelial cell barrier function. Currently no drug-based or surgical cure for this disease exists. Based on the data showing indole elicits anti-inflammatory changes in expression and increases epithelial cell barrier properties, we propose that indole could represent a novel, yet safe (as it is naturally present in the human GI tract), modality for regulating intestinal inflammation and promoting epithelial cell function.

In summary, our *in vitro* studies indicate the importance of indole in favorable inter-kingdom signaling interactions between the intestinal epithelial cells and commensal bacteria. Our results show coordinated control of inflammation in the presence of indole through the repression of several inflammatory cytokines and coordinated regulation of signaling pathways, along with fortification of cell structure through up-regulation of actin cytoskeleton and tight junction proteins. The recognition of indole as an inter-kingdom signal by human cells is also consistent with the recognition of the bacterial product indole-3-acetic acid, and provides an initial basis for understanding symbiotic inter-kingdom interactions at the molecular level, as well as insights into some GI-tract diseases and pathogenic infections.

CHAPTER VI

A SECRETED FACTOR FROM HUMAN INTESTINAL EPITHELIAL CELLS INCREASES ENTEROHEMORRHAGIC *ESCHERICHIA COLI* VIRULENCE

6.1 OVERVIEW

EHEC is a food-borne pathogen that colonizes human GI tract and leads to infection. To understand the process of colonization and to decipher if any factors secreted by intestinal epithelial cells help EHEC during the infection process, we studied expression of EHEC virulence gene expression when exposed to intestinal epithelial cell conditioned medium. In our study, we observed that exposure to epithelial cell conditioned medium for 1 h and 3 h increases expression of 32 out of 41 EHEC LEE virulence genes. In addition, expression of the shiga toxin 1 (Stx1) gene is up-regulated at 1 h of exposure. Also, 17 genes encoded by prophage 933W, including those for Stx2, are also upregulated at both time-points. The increase in 933W prophage expression is mirrored by a 2.7-fold increase in intracellular Stx2 phage titers. Consistent with the increase in virulence gene expression, we observed a 5-fold increase in EHEC attachment to epithelial cells when exposed to conditioned medium, suggesting that EHEC utilizes host cell molecules to increase virulence and infectivity. The molecule(s) responsible for increased EHEC virulence is heat-sensitive as heating the conditioned medium to 95^{o}C abolishes the increase in attachment to epithelial cells. A similar decrease was observed when the conditioned medium was treated with proteinase-K to degrade the proteins. The secreted molecule(s) was found to be larger than 3 kDa and strongly suggests that the HCT-8 secreted molecule that increases EHEC virulence and colonization is a protein-based molecule.

6.2 INTRODUCTION

The GI tract is colonized by approximately 10^{14} commensal bacteria consisting of hundreds of bacterial species, including the genus *Escherichia* (28). The introduction of pathogenic bacteria such as EHEC into the human GI tract results in colonization of host cells and leads to the onset of bloody diarrhea and hemolytic uremic syndrome. EHEC infections progress through a three-step mechanism, the first of which involves adhesion of bacteria to host cells and the formation of micro-colonies (12). EHEC infections pose a serious clinical problem as they are often associated with complications and permanent disabilities, including neurological defects, hypertension, and renal insufficiency (166). Understanding the mechanisms underlying EHEC pathogenicity could lead to better approaches for attenuating the deleterious consequences associated with GI tract infections.

EHEC virulence is significantly affected by host molecules present in the GI tract microenvironment. Sperandio et al. (16) initially demonstrated that the eukaryotic hormone epinephrine restores the T3SS of EHEC in a EHEC *luxS* mutant, and suggested that some signaling occurs between epithelial cells and EHEC. Prior work from our lab has shown that phenotypes that affect EHEC infection – motility, chemotaxis, biofilm formation, gene expression, and attachment to epithelial cells – are increased in EHEC exposed to epi and NE (26). Similar observations have been made by Vlisidou et al. (98) who showed that NE increases adhesion of EHEC to cecal mucosa, colonic mucosa, and the ileum. These studies suggest that EHEC virulence and infectivity are enhanced by neuroendocrine hormones.

Several reports discuss effects of host factors like TNF-α on virulence of other pathogens. Cho et al. (167) studied the effects of recombinant guinea pig TNF-α (rgpTNF-α) on alveolar and peritoneal guinea pig macrophages infected with *Mycobacterium tuberculosis*. They established that TNF-α plays a protective role in host resistance against *M. tuberculosis*

infection. However, Scheidegger et al. (168) report a contradicting observation. They observed that *Toxoplasma gondii* tachyzoites infected and proliferated in rat brain slices; and addition of TNF-α significantly increases proliferation of the parasite, while addition of IFN-γ is detrimental to growth of both the parasite and the host tissue.

Several studies have suggested that presence of host cells enhance pathogen gene expression and virulence. Jandu et al. (169) investigated changes in the EHEC transcriptome when grown in presence of HEp-2 cells. They reported that, of the LEE virulence genes, only *escRSTU* are up-regulated in the presence of host epithelial cells. The authors also identified a new EHEC virulence factor, gene Z1787 in their study. However, since HEp-2 cells are not of intestinal origin and EHEC colonizes only the large intestine in humans, we hypothesized that epithelial cells of intestinal origin will be physiologically more relevant, and studied EHEC virulence and infection of HCT-8 cells, which are derived from enterocytes at the junction of the large and small bowel.

McCormick and co-workers (170) identified a host factor, hepoxilin A_3 (HXA_3), which recruits polymorphonuclear leukocytes to the site of infection. They discovered that a T3SS protein, SipA, of *S. typhimurium* promotes a lipid signal transduction cascade that leads to production of HXA_3 (171), and that lung epithelial cells produce HXA_3 in response to *P. aeruginosa* infection. Similarly, Ju et al. (172) discovered a novel 40-kDa protein, named LPS recognition protein (LRP), purified from the plasma of larvae of the large beetle, *Holotrichia diomphalia*. They established that this protein helps in the clearance of *E. coli in vivo* but not *S. aureus* or *Candida albicans*. Sequence analysis revealed that LRP contains six repeats of an EGF-like domain that causes selective agglutination of *E. coli*.

In this study, our goal was to establish whether cell secreted factors (e.g. proteins, metabolites, etc.) can act as an inter-kingdom signaling molecules and activate the virulence

machinery of EHEC in a manner similar to NE (since monolayers of HCT-8 cells were grown *in vitro* in Petri-dishes, we did not expect NE to be secreted in the conditioned medium). We hypothesized that EHEC infection is influenced by different eukaryotic molecules secreted by intestinal epithelial cells during growth and maintenance in the GI tract. The molecular basis of the alterations in EHEC physiology upon exposure to conditioned medium was investigated using DNA microarrays. EHEC colonization on exposure to fresh and conditioned media was also studied, along with changes in Stx2 production. Our results suggest an increase in EHEC virulence and colonization triggered by eukaryotic protein-based secretion molecules. Our future work includes identification of this secreted eukaryotic molecule(s) that increases EHEC pathogenesis, which can lead to novel strategies to counter EHEC infections.

6.3 MATERIALS AND METHODS

6.3.1 Growth and maintenance of eukaryotic cells and bacteria

The human colon-cancer cell line HCT-8 (ATCC, Manassas, VA), derived from enterocytes at the junction of the large and small bowel, was maintained in RPMI (Roswell Park Memorial Institute) 1640 medium with 10% horse serum, 1 mM sodium pyruvate, 10 mM HEPES, 100 U/ml penicillin and 100 µg/ml streptomycin, at 37°C in 5% CO_2, according to standard ATCC protocols (henceforth referred to as RPMI medium).

Escherichia coli O157:H7 EDL933 (EHEC, ATCC 43895) was purchased from ATCC (Manassas, VA) and unless stated, was grown and maintained in LB medium at 37^{o}C.

6.3.2 Collection of fresh and conditioned medium

RPMI medium without antibiotics and with heat-inactivated (65^{o}C, 1 h) horse serum was

used to prepare fresh and conditioned medium. Low-passage-number HCT-8 cells were cultured in 10 cm diameter Petri-dishes until ~ 80% confluence in normal RPMI medium. The cells were then washed twice with sterile PBS (9 g/l sodium chloride, 0.795 g/l sodium phosphate dibasic, and 0.144 g/l potassium phosphate monobasic) to remove traces of antibiotic containing medium and antibiotic-free RPMI medium with heat inactivated horse serum was added to the Petri-dish. An empty Petri-dish was similarly washed twice with PBS and antibiotic-free RPMI was added to it. The Petri-dishes were then incubated at 37°C in 5% CO_2 for 24 h. Conditioned medium was thus collected from the HCT-8 cells in Petri-dishes and stored at 4°C until further use. Similarly, fresh medium was collected from Petri-dishes without HCT-8 cells and stored.

6.3.3 Proteinase and heat inactivation of proteins

To degrade proteins present in fresh and conditioned media, 200 µg/ml proteinase K (Sigma-Aldrich, St. Louis, MO), a broad-spectrum serine protease, was added and the media were incubated for 1 h at 37°C. Proteinase K activity was then neutralized by adding 100 µg/ml Pefabloc (Sigma-Aldrich), which is a serine protease inhibitor, and incubating further at 37°C for 16 h. The treated media were stored at 4°C, until use.

Proteins from fresh and conditioned media were also heat inactivated by incubating at 95°C for 15 minutes. The heat denatured media were then cooled to room temperature and stored at 4°C, until use.

6.3.4 Fractionation of media through centrifugal filters

Fractionation of fresh and conditioned media was achieved using Amicon Ultra-4 centrifugal filter devices (Millipore, Billerica, MA) with a molecular weight cut-off of 3 kDa. Four ml fresh and conditioned media were loaded onto the top chamber of the devices and the

assembly was centrifuged at 4000 g for 30 minutes at 25^{o}C. Fractions containing small molecules (< 3 kDa) were collected at the bottom. Serum-free RPMI was added to the resulting top fraction to make a final volume of 3 ml. The media were stored at 4^{o}C until use.

6.3.5 Fractionation of media using ammonium sulfate precipitation

Precipitation of proteins from the media was achieved through sequential addition of saturated ammonium sulfate solution (77% in water). To 1 ml fresh and conditioned media, ammonium sulfate was added to a final concentration of 25% and the solutions were shaken at room temperature for 1 h. The solutions were then centrifuged at 4000 g for 10 minutes to collect the precipitated proteins in a pellet. The supernatants were transferred to new tubes and additional ammonium sulfate was added to increase the final concentration to 30% and the above procedure was repeated. The precipitated proteins were resuspended in serum-free RPMI and were desalted using Amicon Ultra-4 centrifugal filters. Four protein fractions were collected using 25%, 30%, 40%, and 67% ammonium sulfate.

6.3.6 RNA isolation and DNA microarrays

Overnight cultures of EHEC were diluted in LB medium to a turbidity of 0.1 at 600 nm. The cells were allowed to grow to a turbidity of 1.0 at 600 nm at 37°C and the EHEC cells were then resuspended in either fresh or conditioned medium. The cultures were then allowed to grow for 1 h or 3 h before cell pellets were collected by centrifugation and stored at -80°C.

Total RNA was isolated from the cell pellets (173) and RNA quality was assessed using gel electrophoresis. *Escherichia coli* Genome 2.0 arrays (Affymetrix, Santa Clara, CA, USA) containing 10,208 probe sets for all 20,366 genes present in four strains of *E. coli*, including EHEC, were used to profile changes in gene expression using RNA samples for each treatment.

Hybridization was performed for 16 h and the total cell intensity was scaled automatically in the software to an average value of 500. The data were inspected for quality and analyzed according to the procedures described by the manufacturer (Affymetrix Data Analysis Fundamentals), which include using premixed polyadenylated transcripts of the *Bacillus subtilis* genes (*lys*, *phe*, *thr*, and *dap*) at different concentrations. Genes were identified as differentially expressed if the expression ratio (between conditioned and fresh medium cells at different time-points) was greater than 1.5 (based on the standard deviation between values measuring relative changes in expression) and if the change in the *p*-value was less than 0.05. The differentially expressed genes were annotated using gene ontology definitions available in the Affymetrix NetAffx Analysis Center (http://www.affymetrix.com/analysis/index.affx). The expression data will be deposited in the National Center for Biotechnology Information Gene Expression Omnibus (GEO; http://www.ncbi.nlm.nih.gov/geo/).

A total of four microarrays were used in this study at the two time points for samples in fresh and conditioned media. The genes were sorted into various functional categories, and the role of conditioned medium in regulation of these genes was analyzed.

6.3.7 *In vitro* colonization assays

Adhesion of EHEC to HCT-8 cells was performed using a previously described protocol (26). Low-passage-number HCT-8 cells were cultured in standard 24-well tissue culture plates and grown at 37°C in 5% CO_2 until ~ 80% confluence. Next, HCT-8 monolayers were washed two times with PBS to remove traces of antibiotics, and different media to be tested were added to individual wells. Approximately 10^7 cells of a freshly-grown EHEC culture (OD of ~ 0.8 at 600 nm) were added to each well and incubated for 3 h at 37°C and 5% CO_2. Loosely attached cells were removed by washing the wells two times with PBS, and the HCT-8 cells were lysed in

the wells using 0.2% Triton X-100 in PBS. The cell suspension in each well was vigorously vortexed, and serial dilutions of the bacteria were spread on LB plates. Colonies were counted after 24 h incubation at 37°C.

6.3.8 Intracellular Stx2 plaque assay

Intracellular Stx2 plaque assay was adapted from a previously published study (174). Briefly, EHEC and *E. coli* DH5α were cultured overnight in LB medium. Next day, EHEC was re-inoculated in LB medium at starting turbidity of 0.1 at 600 nm and grown at 37^{o}C till it reached a turbidity of 1.0. The cells were then collected through centrifugation and were resuspended in fresh and conditioned media. The cultures were further incubated at 37^{o}C for additional 3 h. EHEC cells were again collected and were lysed using chloroform to collect the intracellular phage. At the same time, *E. coli* DH5α was freshly inoculated and grown till turbidity of 1.0. The EHEC phages were diluted 10-fold in 4-6 serial dilutions in 1 ml *E. coli* DH5α. One ml of the above dilutions was added to 5 ml of molten LB-top agar (8 g/l agar, 0.1% glucose, 5 mM $CaCl_2$) and poured over LB-bottom plates (10 g/l agar, 0.1% glucose, 5 mM $CaCl_2$). The plates were incubated at 37^{o}C for 24 h. The next day, the resulting Stx2 plaques were counted.

6.3.9 qRT-PCR

DNA microarray data was corroborated using qRT-PCR (26). The primers were designed using PrimerQuest online software (Table 6.1). qRT-PCR was performed using iScript one-step RT- PCR kit with SYBR green (Bio-Rad Laboratories, CA) on a MyiQ single-color real-time PCR detection system (Bio-Rad Laboratories). The threshold cycles, as calculated by

Table 6.1. Sequences of primers used for qRT-PCR

Gene	Forward Primer (5'-3')	Reverse Primer (5'-3')
escU	CAAGCTCTTGTCGTTGTTGCCT	TCCTTGGCTTCTCGTTTCACCT
eae	GCTGGCCCTTGGTTTGATCA	GCGGAGATGACTTCAGCACTT
fepE	CGCAATTGTCGCATTGAGCGAA	ACTCTTTCACCACCAACGCAGA
rrsG	TATTGCACAATGGGCGCAAG	ACTTAACAAACCGCCTGCGT

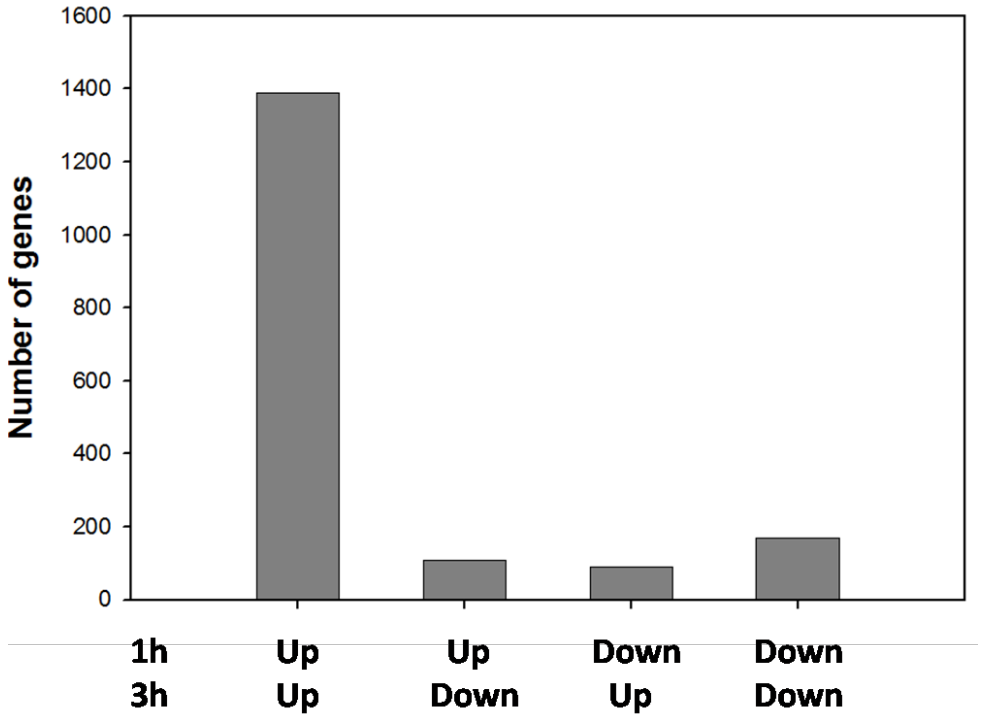

Fig. 6.1. Number of genes differentially regulated by conditioned medium. EHEC cells were exposed to fresh and conditioned media for either 1 h or 3 h and the RNA was isolated. The number of genes differentially regulated in presence of conditioned medium is shown by the bars.

the MyiQ optical system software (Bio-Rad Laboratories), were used to determine the relative changes between samples. The experiments were run in triplicate in 20 µl reactions and 50 ng of total RNA was used for each reaction, with the final forward and reverse primer concentrations at 0.15 µM each. After amplification, template specificity was ensured through melting curve analysis. *rrsG* was used as the housekeeping gene for normalizing the data.

6.4 RESULTS

6.4.1 Gene expression profiling in EHEC exposed to conditioned medium

Widespread changes in EHEC transcriptome were observed on exposure to conditioned medium, both at 1 h and 3 h. Approximately 1400 genes were up-regulated by conditioned medium at both 1 h and 3 h, while about 200 genes were down-regulated at both time-points. In addition, about 100 genes were up-regulated at 1 h and down-regulated at 3 h, or vice-versa (Fig. 6.1). We mainly focused on the 1400 genes that were up-regulated at both time-points in our discussion since most of the virulence related genes are in this category. Examples are LEE, flagella, prophage 933W, iron-related, and biofilm-related genes (Fig. 6.2). Table 6.2 lists some of the important genes found to be differentially regulated in our study.

The LEE Pathogenicity Island consists of 41 genes distributed in five operons (LEE1 through LEE5) and is a primary cause of EHEC virulence. In our study, 32 of these 41 genes (78%) were up-regulated by conditioned medium. The *eae* gene, which encodes the adhesin intimin (166), was up-regulated 1.7-fold at 3 h. *tir* encodes a receptor for intimin that is secreted into host cells (166), and was induced by 1.5-fold at 3 h. *espADF* genes encode proteins that are involved in the type III secretion system of EHEC, of which, EspF is encoded at the far end of LEE. All these proteins were up-regulated significantly at both time-points. The highest induced

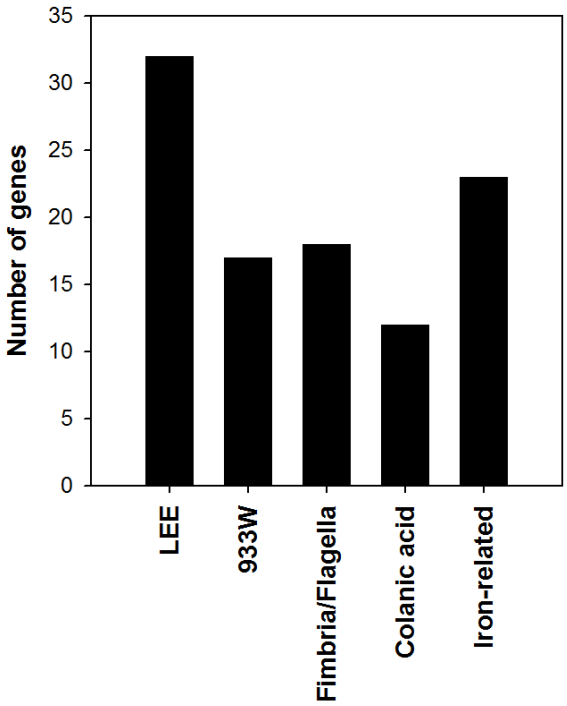

Fig. 6.2. Virulence-related genes regulated by conditioned medium. The bar graph represents important classes of virulence-related genes that were regulated by conditioned medium. Genes were classified based on molecular, cellular, or biological function. 78% of LEE genes, 67% of 933W genes, and 75% of colanic acid biosynthesis genes were differentially regulated.

Table 6.2. Important genes up-regulated in the presence of conditioned medium. *Statistically significant change in expression at *p*-value < 0.05

Probe Set ID	Gene Symbol	1h Fold Change	3h Fold Change	Description
Virulence/LEE Genes				
1759158_s_at	*stx1B*	2.1*	-1.1	Hemolysis
1768192_s_at	*stx1A*	1.7*	-1.1	Negative regulation of protein biosynthesis
1760207_s_at	*tir*	1.2	1.5*	Cell adhesion
1759472_s_at	*sepQ*	1.2	1.7*	
1764730_s_at	*sepL*	1.7*	1.7*	
1768968_s_at	*mviN*	1.3	1.5*	Pathogenesis
1761587_s_at	*espF*	1.5*	1.5*	
1761936_s_at	*espD*	1.5*	1.7*	Pathogenesis
1769270_s_at	*espA*	1.5*	1.7*	
1767609_s_at	*escU*	1.9*	2.8*	Transport
1764491_s_at	*escT*	2.3*	2.5*	Protein targeting
1763133_s_at	*escS*	2.1*	2.5*	Transport
1762528_s_at	*escR*	2.3*	2.3*	Type III protein (virulence-related) secretor activity
1761477_s_at	*escF*	1.7*	1.7*	Pathogenesis
1767897_s_at	*escD*	1.3	1.5*	
1767809_s_at	*escC*	1.4	1.5*	Transport
1760011_s_at	*eaeH*	1.6*	2.3*	Attaching and effacing protein
1764248_s_at	*eaeH*	1.3	1.7*	Cell adhesion
1766942_s_at	*eae*	1.3	1.7*	Cell adhesion
1763952_s_at	*ECs4480*	2.0*	1.4	Pathogenesis
1759147_at	*ECs3718*	1.3	1.7*	Pathogenesis
1765580_s_at	*Z4196*	1.6*	1.9*	Type III protein (virulence-related) secretor activity
1766891_s_at	*Z4190*	1.5*	2.1*	Type III protein (virulence-related) secretor activity
1763006_s_at	*Z4189*	1.5*	2.5*	Type III protein (virulence-related) secretor activity

Table 6.2. Contd.

Probe Set ID	Gene Symbol	1h Fold Change	3h Fold Change	Description
1769199_s_at	*Z4180*	1.0	1.5*	Type III protein (virulence-related) secretor activity
933W Prophage Genes				
1765575_s_at	*Z1459*	1.4	1.9*	Carbohydrate metabolism
1766027_s_at	*c1433*	1.3	1.9*	Lysis protein S homolog from lambdoid prophage DLP12
1763115_s_at	*c1555*	1.5*	1.1	Putative DNA N-6-adenine-methyltransferase of bacteriophage
1768861_s_at	*Z1458*	1.5*	1.9*	Regulation of transcription
1763468_s_at	*Z1495*	1.9*	1.1	
1759811_s_at	*Z1494*	1.7*	1.1	
1762616_s_at	*Z1493*	1.7*	1.3	
1760240_s_at	*Z1490*	1.6*	1.2	
1764484_s_at	*Z1487*	1.6*	1.4	
1760789_s_at	*Z1486*	1.6*	1.4	
1767326_s_at	*Z1482*	1.6*	1.3	
1767349_s_at	*Z1480*	1.6*	1.4	
1765250_s_at	*Z1478*	1.5*	1.1	
1762000_s_at	*Z1476*	1.5*	1.7*	
1760248_s_at	*Z1467*	1.5*	1.7*	
1761222_s_at	*Z1469*	1.4	1.9*	
1767360_s_at	*Z1468*	1.3	1.5*	
Fimbrial Genes				
1766324_s_at	*sfmH*	1.6*	1.6*	Fimbrial assembly protein
1763064_s_at	*sfmD*	1.7*	1.1	Putative outer membrane protein
1766811_s_at	*sfmC*	1.9*	1.2	Putative chaperone
1767430_s_at	*fliP*	1.5*	1.7*	Flagellar biosynthetic protein FliP precursor
1765241_s_at	*fliN*	1.6*	1.2	Flagellar motor switch protein FliN

Table 6.2. Contd.

Probe Set ID	Gene Symbol	1h Fold Change	3h Fold Change	Description
1763750_s_at	*fliF*	1.3	1.9*	Flagellar M-ring protein
1767873_s_at	*flhA*	1.5*	1.3	Flagellar biosynthesis protein FlhA
1761716_s_at	*fimZ*	1.7*	1.4	Fimbiral protein Z, putative transcriptional regulator of fimbrial expression (LuxR/UhpA family)
1762546_s_at	*fimC*	1.6*	1.3	Chaperone protein FimC precursor
1767098_s_at	*fimA*	1.1	1.7*	Major type 1 subunit fimbrin (pilin)
1767422_s_at	*ppdD*	1.6*	1.5*	Prepilin peptidase dependent protein D precursor
1763745_s_at	*ycbV*	1.5*	1.5*	Putative fimbrial-like protein
Multidrug Resistance				
1759593_s_at	*emrK*	1.7*	1.6*	Multidrug resistance protein K
1761644_s_at	*emrD*	1.3	1.6*	Multidrug resistance protein D
1762168_s_at	*emrB*	1.1	1.9*	Multidrug resistance; probably membrane translocase
Iron-related Genes				
1765511_s_at	*fixX*	1.4	1.9*	Ferredoxin-like protein
1762110_s_at	*fixC*	1.5*	1.7*	FixC protein
1760251_s_at	*fixB*	1.2	1.7*	Probable flavoprotein subunit, carnitine metabolism
1762922_s_at	*fhuD*	1.2	1.9*	Ferrichrome-binding periplasmic protein precursor
1761740_s_at	*fhuC*	1.1	1.6*	Ferrichrome transport ATP-binding protein fhuc
1766821_s_at	*fhuB*	1.2	1.9*	Ferrichrome transport system permease protein FhuB
1760499_s_at	*fepG*	1.1	1.6*	Ferric enterobactin transport protein

Table 6.2. Contd.

Probe Set ID	Gene Symbol	1h Fold Change	3h Fold Change	Description
1768501_s_at	*fepE*	1.9*	2.0*	Ferric enterobactin (enterochelin) transport
1768432_s_at	*fepB*	1.6*	1.1	Ferric enterobactin-binding periplasmic protein precursor
1769044_s_at	*chuY*	2.1*	1.2	
1765359_s_at	*chuW*	3.5*	1.7*	
1760730_s_at	*chuU*	2.6*	1.5*	Putative permease of iron compound ABC transport system
1768770_s_at	*chuT*	2.6*	1.2	
1763313_s_at	*chuS*	2.8*	1.9*	Putative heme/hemoglobin transport protein
1762260_s_at	*chuA*	2.1*	1.7*	
Colanic Acid Genes				
1761929_s_at	*wcaJ*	1.6	2.6	Putative colanic biosynthesis UDP-glucose lipid carrier transferase
1759709_s_at	*wcaI*	1.1	2.8	Putative colanic acid biosynthesis glycosyl transferase wcaI
1759993_s_at	*wcaH*	1.2	3.0	GDP-mannose mannosyl hydrolase
1765792_s_at	*wcaG*	1.7	2.8	GDP-4-keto-6-L-galactose reductase
1766922_s_at	*wcaF*	1.5	3.0	Putative colanic acid biosynthesis acetyltransferase wcaF
1759224_s_at	*wcaE*	1.1	2.3	Putative colanic acid biosynthesis glycosyl transferase wcaE
1763157_s_at	*wcaD*	1.4	1.5	Putative colanic acid polymerase
1763999_s_at	*wcaC*	1.0	2.0	Putative colanic acid biosynthesis glycosyl transferase wcaC
1768788_s_at	*wcaA*	1.1	1.5	Putative colanic acid biosynthesis glycosyl transferase wcaA

genes in LEE belonged to the *esc* operon, which also encodes type III secretion system in EHEC, and *escCDFRSTU* were all up-regulated at both time-points (Table 6.2).

Shiga toxin 1 (Stx1) of EHEC is responsible for cleavage of host ribosomal RNA, thus disrupting protein synthesis and killing infected cells (8). In our study, conditioned medium induced *stx1A* and *stx1B* gene expression at 1 h; suggesting an increase in EHEC pathogenicity.

EHEC also contains Stx2, which is encoded by the 933W prophage. While we did not see any change in *stx2A* and *stx2B* genes at any of the time-points, 17 out of 27 (63%) 933W prophage genes were up-regulated at both time-points (Table 6.2). Thus, conditioned medium also caused a direct or indirect increase in toxin production by EHEC.

Several genes associated with fimbriae and flagella were up-regulated by conditioned medium (Table 6.2), and induction of these genes is associated with increase in virulence (137). Colanic acid is a capsular exopolysaccharide that is involved in colonization (134), and we observed an increase in nine out of 12 genes (75%) of the *wca* operon (Table 6.2), which is involved in colanic acid biosynthesis, at both time-points. Increase in motility and biofilm formation of EHEC is directly related to increased virulence, and demonstrates the consistency in our data.

Iron has been reported to increase *E. coli* virulence through increased production of cytotoxins and leukotoxins (138), and in our study, several of these genes were up-regulated (Table 6.2). Together, the transcriptome data strongly suggest that EHEC is able to recognize some epithelial cell secreted factor in the conditioned medium, and up-regulate its virulence machinery.

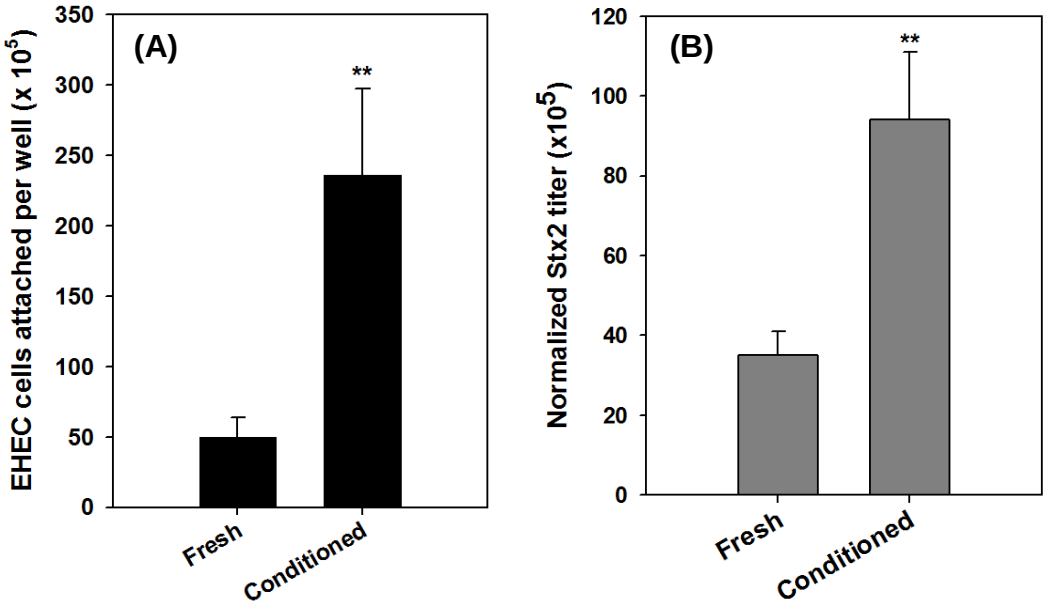

Fig. 6.3. EHEC virulence assays. (A) EHEC cells were colonized on HCT-8 cells in presence of fresh and conditioned media, and (B) formation of Stx2 plaques in fresh and conditioned media. Data represent mean ± standard deviation from three independent experiments. ** denotes statistical significance using the Student's T-test test at $p < 0.005$.

6.4.2 EHEC virulence assays

To determine the effect of epithelial cell secreted molecules on EHEC, colonization assay was performed with fresh and conditioned media. Conditioned medium increased EHEC attachment by 4.9-fold over fresh medium controls (Fig. 6.3A), suggesting recognition of some epithelial cell secreted product by EHEC through inter-kingdom signaling.

Since we observed an increase in expression of Stx2 genes through microarrays, we confirmed these observations with a phenotypic assay for Stx2 production. In the presence of conditioned medium, the intracellular titer of Stx2 phage increased by 2.7-fold (Fig. 6.3B), suggesting an increase in EHEC virulence. Thus, genotypic data were corroborated with phenotypic assays.

6.4.3 Identification of HCT-8 secreted molecule

The molecule(s) responsible for increased EHEC virulence are heat-sensitive as heating the conditioned medium to 95^{o}C abolished the increase in virulence (Fig. 6.4A). When the attachment assay was repeated with proteinase K-treated media, the ability of the conditioned medium to increase EHEC attachment to HCT-8 cells was lost (Fig. 6.4B). We concluded that a protein-based secreted molecule is responsible for the increase in EHEC colonization. In order to determine if a serum component contributes to the increase in colonization, the attachment experiment was repeated using conditioned medium from serum-free and 1% serum-containing media. However, exposure to these media did not lead to enhanced EHEC colonization (Figs. 6.4C and 6.4D), suggesting the importance of serum components in generation of the active molecule. The media were also fractionated using a commercially available centrifugal filter to further characterize the active protein-based molecule. The fraction that contained small molecules (< 3kDa) showed no increase in EHEC colonization (data not shown), while the

fraction containing large molecules (> 3 kDa) showed a 1.9-fold increase (Fig. 6.4E), suggesting that the active molecule is protein-based, and not an organic molecule or a small peptide. However, further fractionation using filters with different molecular weight cut-offs was not successful as high abundance proteins in horse serum (e.g., albumin which accounts for ~ 55% of serum (175)) clogged the membrane and prevented fractionation.

As an alternative to centrifugal filtration, we also used ammonium sulfate precipitation to fractionate the conditioned medium. However, none of the four fractions of conditioned medium increased EHEC colonization. We attributed this loss of activity to possible changes in protein structure during precipitation. Thus, we were unable to simplify the conditioned medium to help us identify the unknown active molecule(s).

6.4.4 qRT-PCR

The whole-transcriptome data were substantiated with qRT-PCR where genes from LEE Pathogenicity Island and iron uptake were profiled. *escU* was induced 2.8-fold in the microarrays and 3.2 ± 0.1 in qRT-PCR. Similar results were seen for *eae* (1.7-fold in the arrays, 3.7 ± 0.1-fold in qRT-PCR), and *fepE* (2-fold in the arrays, 2.5 ± 0.1-fold in qRT-PCR). Thus, the expression results from whole-transcriptome analysis were in good agreement with the qRT-PCR results.

6.5 DISCUSSION

It is becoming increasingly evident that cell-cell signaling inside the GI tract plays a key role in commensal survival, pathogen colonization, and host defense. Inter-kingdom signaling includes recognition of eukaryotic signaling molecules by commensal bacteria and pathogens, as well as prokaryotic signaling molecule recognition by host cells. Our lab has previously

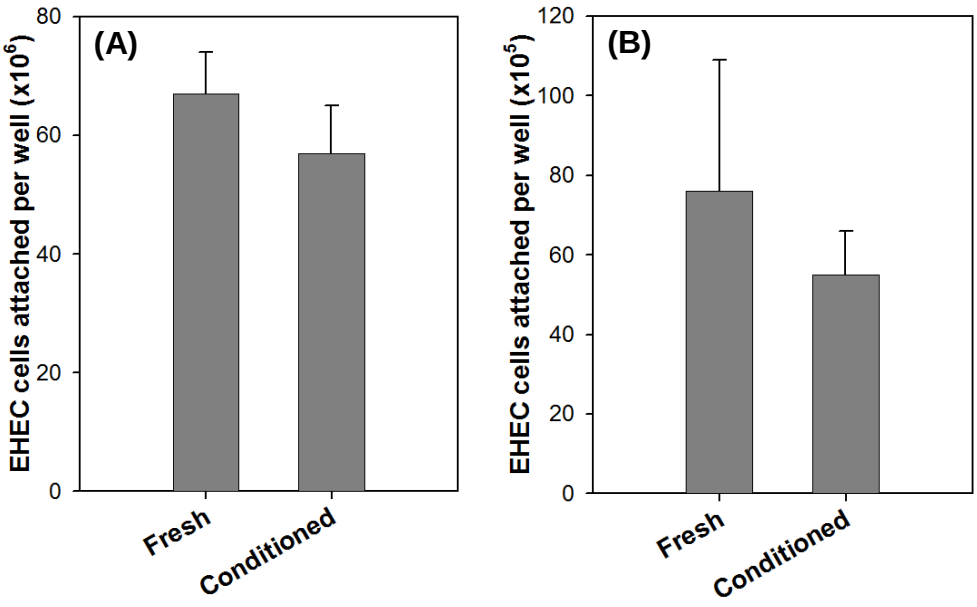

Fig. 6.4. EHEC colonization assay. EHEC cells were colonized on HCT-8 cells in presence of fresh and conditioned media that were (A) heat-denatured, (B) Proteinase K-degraded, (C) serum-free, (D) containing 1% serum, and (E) fractionated and contained molecules greater than 3 kDa. Data represent mean ± standard deviation from three independent experimental wells. ** denotes statistical significance using the Student's T-test test at $p < 0.005$.

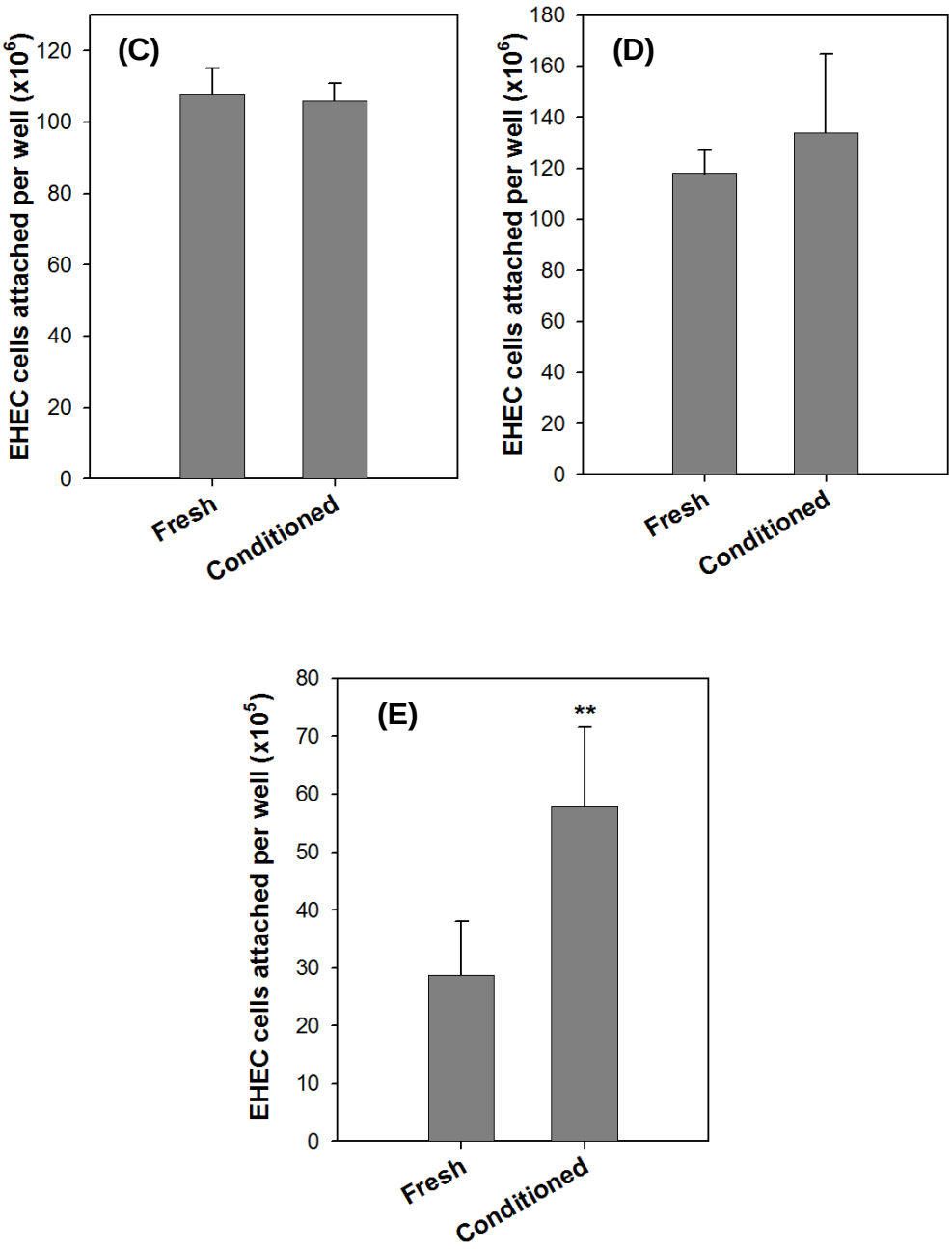
(C)
EHEC cells attached per well (x10^6)
0
20
40
60
80
100
120
Fresh
Conditioned
(D)
EHEC cells attached per well (x10^6)
0
20
40
60
80
100
120
140
160
180
Fresh
Conditioned
(E)
EHEC cells attached per well (x10^5)
**
0
10
20
30
40
50
60
70
80
Fresh
Conditioned

Fig. 6.4. Contd.

demonstrated the inter-kingdom signaling interactions from both perspectives (26, 176). We have shown that EHEC recognize human hormones epi and NE to detect the host cell environment and up-regulate virulence gene expression (26). Additionally, we have establishedthat the commensal bacterial signal indole up-regulates trans-epithelial resistance and reduces pro-inflammatory cytokine expression in human intestinal epithelial cells (176). In the current study, we demonstrate that intestinal epithelial cell secreted protein(s) are detected by EHEC and that those secreted proteins increase EHEC virulence gene expression and colonization.

We studied changes in EHEC gene expression in fresh and conditioned media at different time-points to obtain information about temporal variation in gene expression. The coordinated increase in expression of 32 out of 41 LEE genes strongly suggests a “global” increase in EHEC virulence upon exposure to conditioned medium. In addition, Stx phage genes are also induced, suggesting an increase in EHEC infectivity. Induction of flagellar and fimbrial genes has been associated with virulence (137) and, in current study, we observed that 12 of these important genes were up-regulated (Table 6.2). Iron increases virulence of pathogenic *E. coli, Vibrio, Neisseria* etc. through induction of cytotoxins and neurotoxins (138), and conditioned medium also increased expression of 15 such genes (Table 6.2). Thus, our data suggest that the EHEC virulence machinery is significantly induced upon exposure to epithelial cell-secreted factors that are accumulated in the conditioned medium over a 24 h time-period in our study.

In addition to changes in gene expression, differential regulation of EHEC virulence phenotypes was observed, as colonization of host cells by the pathogen is significantly induced in presence of conditioned medium. Shiga toxins are important markers of EHEC virulence, and we observed that conditioned medium increases intracellular Stx2 titers. Increased expression of

Stx2 along with up-regulation of LEE genes makes EHEC more virulent. It has been proposed that EHEC only expresses its virulence genes after specific recognition of the intestinal environment, as these sets of genes are not expressed in rich media like LB (177). Based on our data, it is intriguing to speculate that such “sensing” of its outside environment is achieved, in part, through these epithelial cell secreted molecules.

Although we attempted to identify the secreted molecule(s), complete characterization was difficult due to several reasons. The HCT-8 cell growth medium contained 10% heat-inactivated horse serum, and this increased the complexity of the sample significantly. Fractionation by size exclusion (gel filtration) chromatography or differential centrifugation was not successful due to an abundance of serum proteins (e.g., albumin, transferrin) that either block the centrifugal filter membranes and/or prevent migration of smaller molecules. The abundance of serum proteins also made protein-based methods (e.g. 2-dimensional gel electrophoresis) difficult. Precipitation of protein fractions was successful; however, none of the fractions showed any activity after resuspension. It is possible that the structure of the molecule(s) were affected during the precipitation and resuspension process; thereby, affecting activity. Additionally, conditioned medium that contained either 1% serum or was serum-free failed to activate EHEC virulence, suggesting the presence of a pre-cursor protein component in the serum.

In summary, we show that intestinal epithelial cell secreted factors are important determinants of EHEC virulence and infection. Phenotypic assays for host cell colonization and shiga toxin production suggest activation of the EHEC infection process. Gene expression data, where we observe the up-regulation of LEE and other virulence related genes, further support this conclusion. It is important to identify the host cell-secreted proteins so that therapies can be developed to target these communication pathways to hinder EHEC infection without adversely affecting the commensal microbiota.

CHAPTER VII

CONCLUSIONS AND RECOMMENDATIONS

7.1 CONCLUSIONS

In the work above, we have successfully shown that prokaryotic (AI-2 and indole) and eukaryotic (epi and NE) GI tract signals are important in EHEC colonization and virulence. We found that eukaryotic hormones epi and NE increase expression of EHEC virulence-related phenotypes, namely chemotaxis, motility, biofilm formation and colonization (Chapter III). Additionally, gene expression studies, where we observed an increase in expression of genes that are associated with virulence and infection, agreed with the phenotypic data. In the case of prokaryotic signals, we observed that while AI-2 also increased these phenotypes (Chapter IV), the stationary phase signal indole attenuated them (Chapter III), indicating the complexity of signaling pathways in bacteria. Once again, genotypic data were in complete agreement with the phenotypic data and demonstrate the robustness of this study. Based on our data, we conclude that the signaling environment in the GI tract impacts the extent of EHEC colonization.

We investigated the effects of the bacterial signal indole on the epithelial cell transcriptome and phenotypes (Chapter V). Since indole is secreted by the commensal bacteria, we hypothesized that indole could be one signal involved in inter-kingdom signaling interactions between commensal bacteria and the host epithelia. Our data show that indole reduces inflammation in host cells, through down-regulation of pro-inflammatory cytokines and factors, like IL-8 and NF-κB, and by up-regulation of anti-inflammatory cytokines, like IL-10. Additionally, indole increases the trans-epithelial resistance of host cells, suggesting an increase in barrier properties and resistance to pathogen colonization that was confirmed by reduced EHEC colonization of indole-pre-treated host cells. We established that these changes in host

cells are indole-specific, as several indole derivatives fail to induce coordinated changes in trans-epithelial resistance and NF-κB production.

The changes in EHEC virulence on exposure to human intestinal epithelial cell-secreted factors were studied (Chapter VI). Transcriptome studies revealed an increase in the expression of LEE Pathogenicity Island genes as well as an increase in production of shiga toxins. EHEC colonization is also induced by 5-fold with conditioned medium. We were able to establish that the molecule causing an increase in EHEC virulence is a protein-based molecule with size greater than 3 kDa.

7.2 RECOMMENDATIONS

There are several opportunities to build on the results obtained. First, one can study the mechanisms of EHEC virulence by changing environmental conditions (e.g. inducing stress) and by constructing EHEC mutants. Second, one can develop experimental strategies to identify the human intestinal epithelial cell-secreted molecule(s) that increases EHEC virulence and colonization (first described in Chapter VI). Third, one can increase the complexity of the experimental setup such that human GI tract environment is mimicked more closely, through the observation of dual species (non-pathogenic and EHEC) colonization of epithelial cells. Fourth, the changes in gene expression of human epithelial cells when exposed to different kinds of bacteria (pathogen vs. non-pathogen) can be investigated. Together, these experiments along with our previous results shall provide a fundamental understanding of the host-pathogen interactions in GI tract infections.

7.2.1 Study the mechanism of EHEC virulence

As discussed earlier, EHEC elicits an SOS response under stress that sends the cells into lytic phase (15), releasing shiga toxins into the environment. Environmental stress can be induced through several factors, including the presence of antibodies and extreme pH and temperatures. One can expose EHEC to such stressful conditions (e.g. highly acidic pH to mimic the conditions in the stomach) and study the changes in intra- and extracellular Stx phage titers. Additionally, colonization of human intestinal epithelial cells with these stressed EHEC cells can help one understand the role of stress in the infection process.

In chapters III, IV and VI, we identified several genes and pathways that are important for EHEC virulence. Hence, the next step could be to create EHEC mutants and study the changes in virulence phenotype, in presence of eukaryotic and prokaryotic signaling molecules. We have recently deleted *hha* gene from the EHEC wildtype strain. It has been established that *hha* is a negative regulator of the LEE operon (178) and deleting it should derepress the LEE operon and make EHEC more virulent. Similarly, one can over-express *hha* to repress the LEE operon and develop strategies to counter EHEC infections.

7.2.2 Identification of human intestinal epithelial cell-secreted factor(s) that increase EHEC virulence and colonization

In Chapter VI, we determined that human epithelial cell-secreted factor(s) increase EHEC virulence. We established that the active molecule is protein-based and larger than 3 kDa in size. However, we were unable to identify the molecule due to the complexity of conditioned medium. The future experiments can include extraction of lipids to confirm that the active molecule is indeed protein-based and not lipid-based. Extraction of lipids can be achieved through liquid-liquid extraction using a chloroform-methanol mixture as described in a previous

study (179). The organic layer shall contain lipids, and subsequently the organic solvents can be evaporated in the presence of N_2. The extracted lipids can then be resuspended in serum-free RPMI and tested for activity.

Cycloheximide is an inhibitor of protein biosynthesis in eukaryotic animals that blocks translational elongation. We can add cycloheximide to HCT-8 cells during preparation of the conditioned medium such that no additional eukaryotic proteins will be collected in the medium. Such conditioned medium should not exhibit any activity, confirming that a cell-secreted protein is indeed responsible for increased virulence of EHEC.

Fractionation of proteins can be achieved through density gradient ultra-centrifugation (DGU) as described by Bhaskar and Reid (180). Here, cesium chloride (CsCl) provides separation of glycoproteins/proteoglycans from pure proteins. The media can be diluted in phosphate buffer and the amount of CsCl should be 0.38 w/v of the total mixture. Using ultra-centrifugation at 100,000 g, several fractions of proteins ranging in density 1.3-1.6 g/ml can be obtained. Albumin has a density of 1.378, in solution (181), and can be separated from other proteins. One can then test all these fractions for activity, and since the complexity of sample has been greatly reduced in this case, mass spectrometry can be employed to identify the active protein.

Since the HCT-8 growth medium contains 10% horse serum, most of the proteins in the medium are of equine origin. Another method, which can potentially be employed, is to calibrate the mass spectrometer such that it only detects human proteins. This experimental design will inherently eliminate all the equine proteins, rendering the sample simpler to analyze. Since fresh medium contains no human proteins, the detection of any proteins in conditioned medium will lead us to the potential active molecule candidates. Identification of the active molecule will help researchers design strategies to counter the EHEC infection process, possibly through the design

of inactive homologs.

7.2.3 Dual species (EHEC and non-pathogenic *E. coli*) colonization of human epithelial cells

An important aspect of EHEC infection is its colonization of the colonic mucosa in the GI tract to initiate infection. The presence of commensal bacteria in the mucosa is extremely important, since signals produced by these bacteria manipulate EHEC virulence phenotypes (25-26). Similarly, the presence of commensal *E. coli* has been shown to inhibit *Salmonella* infection in mice (182) and several studies have pointed out the importance of probiotics in treating infections (140). However, the mechanisms, aside from the role of indole outlined in Chapter V, through which commensals inhibit pathogen infection and the signaling molecules involved in this process are not well understood (141).

In these experiments, the GI tract can be mimicked by developing a HCT-8 monolayer in standard tissue culture and growing non-pathogenic *E. coli* on top. Adding various hormones like NE and dopamine to the experiment will result in simulation of the *in vivo* milieu that EHEC encounters during colonization. Several variables that can be studied are – different strains of commensal bacteria, various mutant strains of *E. coli* (e.g. *tnaA* mutant that lacks indole production) and different relative concentrations of commensal bacteria and EHEC.

Although the above experimental design is robust, it still is not able to capture the *in vivo* environment in totality due to the lack of flow. Flow inside the GI tract leads to spatial bias where host cells in different regions in a flow profile could be differentially colonized. This aspect of colonization can be investigated through the use of microfluidic devices (183-184). A microfluidic system allows cells to be exposed to an environment that more closely resembles the natural surroundings that they encounter (185). Its biggest advantage over traditional tissue-culturing methods is that flow can be generated, as is the case inside the GI tract, and enables the

generation of gradients of signals, of different strengths and profiles, thereby simulating an *in vivo* environment (185). The results will help interpret the role of commensal bacteria in infection prevention as some studies have reported (182).

7.2.4 Changes in intestinal epithelial cell gene expression during colonization with diverse strains of bacteria (pathogen vs. non-pathogen)

One can study changes in epithelial cell gene expression when exposed to different kinds of bacteria, which will help elucidate the mechanisms that are unique to EHEC pathogenesis. To study changes in HCT-8 gene expression during colonization, HCT-8 cells can be exposed to EHEC for different periods of time (3 to 12 hours). The infective dose of EHEC is 100 cfu but this low number of EHEC cells will not be enough to cover all the HCT-8 cells in the flask. Hence, we will need to infect HCT-8 cells with 10^6-10^8 cfu of EHEC to ensure that entire HCT-8 surface is colonized by EHEC ensuring reliable gene expression studies. These studies should be repeated with non-virulent EHEC (Δ*stx*) and commensal *E. coli* to determine pathways and processes that are unique to EHEC colonization that leads to infections. The data generated on HCT-8 gene expression after these microarrays will consist of approximately 38,000 genes and the analysis can be conducted using PathwayAssist software (Stratagene, CA). To our knowledge, a genome-wide study of epithelial cell transcription during colonization with EHEC and non-pathogens; and in presence of various signals has not been previously reported.

Since commensal *E. coli* is present in the vicinity of epithelial cells in the GI tract, we expect divergent HCT-8 gene expression during commensal colonization as compared to EHEC, due to its foreign nature and its release of toxins. These studies will help us elucidate the mechanism of pathogen recognition employed by epithelial cells to counter their deleterious effects.

REFERENCES

1. Costerton WJ, et al. (1994) Biofilms, the customized microniche. *J Bacteriol* 176(8):2137-2142.
2. Hall-Stoodley L, Costerton JW, & Stoodley P (2004) Bacterial biofilms: From the natural environment to infectious diseases. *Nat Rev Microbiol* 2:95-108.
3. Clarke MB & Sperandio V (2005) Events at the host-microbial interface of the gastrointestinal tract. III. Cell-to-cell signaling among microbial flora, host, and pathogens: There is a whole lot of talking going on. *Am J Physiol Gastrointest Liver Physiol* 288:G1105-1109.
4. Green BT, et al. (2004) Adrenergic modulation of *Escherichia coli* O157:H7 adherence to the colonic mucosa. *Am J Physiol Gastrointest Liver Physiol* 287:G1238-1246.
5. Collier-Hyams LS & Neish AS (2005) Innate immune relationship between commensal flora and the mammalian intestine. *Cell Mol Life Sci* 62:1339-1348.
6. Torres AG, Zhou X, & Kaper JB (2005) Adherence of diarrheagenic *Escherichia coli* strains to epithelial cells. *Infect Immun* 73:18-29.
7. Karch H, Tarr PI, & Bielaszewska M (2005) Enterohaemorrhagic *Escherichia coli* in human medicine. *Int J Med Microbiol* 295:405-418.
8. Kaper JB, Nataro JP, & Mobley HLT (2004) Pathogenic *Escherichia coli*. *Nat Rev Microbiol* 2:123-139.
9. Torres AG & Kaper JB (2003) Multiple elements controlling adherence of enterohemorrhagic *Escherichia coli* O157:H7 to HeLa cells. *Infect Immun* 71:4985-4995.
10. Boyce TG, Swerdlow DL, & Griffin PM (1995) *Escherichia coli* O157:H7 and the hemolytic-uremic syndrome. *N Engl J Med* 333(6):364-368.

11. Frenzen PD, Drake A, & Angulo FJ (2005) Economic cost of illness due to *Escherichia coli* O157 infections in the United States. *J Food Prot* 68:2623-2630.

12. Nataro JP & Kaper JB (1998) Diarrheagenic *Escherichia coli*. *Clin Microbiol Rev* 11(1):142-201.

13. Kaper JB & Sperandio V (2005) Bacterial cell-to-cell signaling in the gastrointestinal tract. *Infect Immun* 73:3197-3209.

14. Wong CS, Jelacic S, Habeeb RL, Watkins SL, & Tarr PI (2000) The risk of the hemolytic-uremic syndrome after antibiotic treatment of *Escherichia coli* O157:H7 infections. *N Engl J Med* 342:1930-1936.

15. Alexander M, Martina B, & Helge K (2009) Intrahost genome alterations in enterohemorrhagic *Escherichia coli*. *Gastroenterology* 136(6):1925-1938.

16. Sperandio V, Torres AG, Jarvis B, Nataro JP, & Kaper JB (2003) Bacteria-host communication: The language of hormones. *Proc Natl Acad Sci U S A* 100:8951-8956.

17. Walters M & Sperandio V (2006) Autoinducer 3 and epinephrine signaling in the kinetics of Locus of Enterocyte Effacement gene expression in enterohemorrhagic *Escherichia coli*. *Infect Immun* 74(10):5445-5455.

18. Sperandio V, Torres AG, Girón JA, & Kaper JB (2001) Quorum sensing is a global regulatory mechanism in enterohemorrhagic *Escherichia coli* O157:H7. *J Bacteriol* 183:5187-5197.

19. Giron JA, Torres AG, Freer E, & Kaper JB (2002) The flagella of enteropathogenic *Escherichia coli* mediate adherence to epithelial cells. *Mol Microbiol* 44:361-379.

20. González Barrios AF, et al. (2006) Autoinducer 2 controls biofilm formation in *Escherichia coli* through a novel motility quorum sensing regulator (MqsR, B3022). *J Bacteriol* 188:305-316.

21. Wang D, Ding X, & Rather PN (2001) Indole can act as an extracellular signal in *Escherichia coli*. *J Bacteriol* 183:4210-4216.

22. Domka J, Lee J, & Wood TK (2006) YliH (BssR) and YceP (BssS) regulate *Escherichia coli* K-12 biofilm formation by influencing cell signaling. *Appl Environ Microbiol* 72:2449-2459.

23. Anyanful A, et al. (2005) Paralysis and killing of *Caenorhabditis elegans* by enteropathogenic *Escherichia coli* requires the bacterial tryptophanase gene. *Mol Microbiol* 57:988-1007.

24. Lyte M, Arulanandam BP, & Frank CD (1996) Production of Shiga-like toxins by *Escherichia coli* O157:H7 can be influenced by the neuroendocrine hormone norepinephrine. *J Lab Clin Med* 128:392-398.

25. Lee J, Bansal T, Jayaraman A, Bentley W, & Wood TK (2007) Enterohemorrhagic *Escherichia coli* biofilms are inhibited by 7-hydroxyindole and stimulated by isatin. *Appl Environ Microbiol* 73:4100-4109.

26. Bansal T, et al. (2007) Differential effects of epinephrine, norepinephrine, and indole on *Escherichia coli* O157:H7 chemotaxis, colonization, and gene expression. *Infect Immun* 75:4597-4607.

27. Lutgendorff F, Akkermans LMA, & Söderholm JD (2008) The role of microbiota and probiotics in stress-induced gastrointestinal damage. *Curr Mol Med* 8:282-298.

28. Berg RD (1996) The indigenous gastrointestinal microflora. *Trends Microbiol* 4(11):430-435.

29. Falk PG, Hooper LV, Midtvedt T, & Gordon JI (1998) Creating and maintaining the gastrointestinal ecosystem: What we know and need to know from gnotobiology. *Microbiol Mol Biol Rev* 62(4):1157-1170.

30. Abraham C & Cho JH (2009) Inflammatory bowel disease. *N Engl J Med* 361(21):2066-2078.

31. Turner JR (2009) Intestinal mucosal barrier function in health and disease. *Nat Rev Immunol* 9(11):799-809.

32. Wells JG, et al. (1983) Laboratory investigation of hemorrhagic colitis outbreaks associated with a rare *Escherichia coli* serotype. *J Clin Microbiol* 18(3):512-520.

33. Lim JY, Yoon JW, & Hovde CJ (2010) A brief overview of *Escherichia coli* O157:H7 and its plasmid O157. *J Microbiol Biotechnol* 20(1):1-10.

34. Mead PS, et al. (1999) Food-related illness and death in the United States. *Emerg Infect Dis* 5:607-625.

35. Hurley BP, et al. (1999) Shiga toxins 1 and 2 translocate differently across polarized intestinal epithelial cells. *Infect Immun* 67(12):6670-6677.

36. Elliott SJ, et al. (1998) The complete sequence of the Locus of Enterocyte Effacement (LEE) from enteropathogenic *Escherichia coli* E2348/69. *Mol Microbiol* 28(1):1-4.

37. Hemrajani C, et al. (2010) NleH effectors interact with Bax inhibitor-1 to block apoptosis during enteropathogenic *Escherichia coli* infection. *Proc Natl Acad Sci U S A* 107(7):3129-3134.

38. Schmidt H, Karch H, & Beutin L (1994) The large-sized plasmids of enterohemorrhagic *Escherichia coli* O157 strains encode hemolysins which are presumably members of the *E. coli* α-hemolysin family. *FEMS Microbiol Lett* 117(2):189-196.

39. Schmidt H, Henkel B, & Karch H (1997) A gene cluster closely related to type II secretion pathway operons of Gram-negative bacteria is located on the large plasmid of enterohemorrhagic *Escherichia coli* O157 strains. *FEMS Microbiol Lett* 148(2):265-272.

40. Tatsuno I, et al. (2001) *toxB* gene on PO157 of enterohemorrhagic *Escherichia coli* O157:H7 is required for full epithelial cell adherence phenotype. *Infect Immun* 69(11):6660-6669.

41. Lee J, Jayaraman A, & Wood TK (2007) Indole is an inter-species biofilm signal mediated by SdiA. *BMC Microbiol* 7:42.

42. Lee J-H & Lee J (2010) Indole as an intercellular signal in microbial communities. *FEMS MIcrobiol Rev* 34:426-444.

43. Smith T (1897) A modification of the method for determining the production of indol by bacteria. *J Exp Med* 2:543-547.

44. Karlin DA, Mastromarino AJ, Jones RD, Stroehlein JR, & Lorentz O (1985) Fecal skatole and indole and breath methane and hydrogen in patients with large bowel polyps or cancer. *J Cancer Res Clin Oncol* 109(2):135-141.

45. Zuccato E, et al. (1993) Role of bile acids and metabolic activity of colonic bacteria in increased risk of colon cancer after cholecystectomy. *Dig Dis Sci* 38(3):514-519.

46. Winzer K, Hardie KR, & Williams P (2002) Bacterial cell-to-cell communication: Sorry, can't talk now -- gone to lunch! *Curr Opin Microbiol* 5(2):216-222.

47. Lee J, et al. (2008) Indole cell signaling occurs primarily at low temperatures in *Escherichia coli*. *ISME J* 2(10):1007-1023.

48. Hirakawa H, Inazumi Y, Masaki T, Hirata T, & Yamaguchi A (2005) Indole induces the expression of multidrug exporter genes in *Escherichia coli*. *Mol Microbiol* 55:1113-1126.

49. Chant EL & Summers DK (2007) Indole signalling contributes to the stable maintenance of *Escherichia coli* multicopy plasmids. *Mol Microbiol* 63(1):35-43.

50. Lee J, Attila C, Cirillo SLG, Cirillo JD, & Wood TK (2009) Indole and 7-hydroxyindole diminish *Pseudomonas aeruginosa* virulence. *Microb Biotechnol* 2(1):75-90.

51. Kamath AV & Vaidyanathan CS (1990) New pathway for the biodegradation of indole in *Aspergillus niger*. *Appl Environ Microbiol* 56(1):275-280.

52. Reading NC & Sperandio V (2006) Quorum sensing: The many languages of bacteria. *FEMS Microbiol Lett* 254(1):1-11.

53. Fuqua C, Parsek MR, & Greenberg EP (2001) Regulation of gene expression by cell-to-cell communication: Acyl-homoserine lactone quorum sensing. *Annu Rev Genet* 35:439-468.

54. Bassler BL, Wright M, Showalter RE, & Silverman MR (1993) Intercellular signalling in *Vibrio harveyi*: Sequence and function of genes regulating expression of luminescence. *Mol Microbiol* 9(4):773-786.

55. Chen X, et al. (2002) Structural identification of a bacterial quorum-sensing signal containing boron. *Nature* 415(6871):545-549.

56. Xavier KB & Bassler BL (2005) Interference with AI-2-mediated bacterial cell-cell communication. *Nature* 437:750-753.

57. Fong KP, Chung WO, Lamont RJ, & Demuth DR (2001) Intra- and interspecies regulation of gene expression by *Actinobacillus actinomycetemcomitans* LuxS. *Infect Immun* 69:7625-7634.

58. Sperandio V, Mellies JL, Nguyen W, Shin S, & Kaper JB (1999) Quorum sensing controls expression of the type III secretion gene transcription and protein secretion in enterohemorrhagic and enteropathogenic *Escherichia coli*. *Proc Natl Acad Sci U S A* 96:15196-15201.

59. Chung WO, et al. (2001) Signaling system in *Porphyromonas gingivalis* based on a LuxS protein. *J Bacteriol* 183(13):3903-3909.

60. Lenz DH, et al. (2004) The small RNA chaperone Hfq and multiple small RNAs control quorum sensing in *Vibrio harveyi* and *Vibrio cholerae*. *Cell* 118(1):69-82.

61. Sperandio V, Torres AG, & Kaper JB (2002) Quorum sensing *Eschericia coli* regulators B and C (QseBC): A novel two-component regulatory system invovled in the regulation of flagella and motility by quorum sensing in *E. coli*. *Mol Microbiol* 43:809-821.

62. McNab R, et al. (2003) LuxS-based signaling in *Streptococcus gordonii*: Autoinducer 2 controls carbohydrate metabolism and biofilm formation with *Porphyromonas gingivalis*. *J Bacteriol* 185:274-284.

63. Rasmussen TB, et al. (2000) How *Delisea pulchra* furanones affect quorum sensing and swarming motility in *Serratia liquefaciens* MG1. *Microbiology* 146(12):3237-3244.

64. Mathesius U, et al. (2003) Extensive and specific responses of a eukaryote to bacterial quorum-sensing signals. *Proc Natl Acad Sci U S A* 100(3):1444-1449.

65. Kravchenko VV, et al. (2008) Modulation of gene expression via disruption of NF-κB signaling by a bacterial small molecule. *Science* 321:259-263.

66. Goyal RK & Hirano I (1996) The enteric nervous system. *N Engl J Med* 334(17):1106-1115.

67. Straub RH, Wiest R, Strauch UG, Härle P, & Schölmerich J (2006) The role of the sympathetic nervous system in intestinal inflammation. *Gut* 55(11):1640-1649.

68. Josefsson E, Bergquist J, Ekman R, & Tarkowski A (1996) Catecholamines are synthesized by mouse lymphocytes and regulate function of these cells by induction of apoptosis. *Immunology* 88(1):140-146.

69. Magro F, et al. (2002) Impaired synthesis or cellular storage of norepinephrine, dopamine, and 5-hydroxytryptamine in human inflammatory bowel disease *Dig Dis Sci* 47:216-224.

70. Lyte M & Ernst S (1992) Catecholamine induced growth of Gram-negative bacteria. *Life Sci* 50:203-212.

71. Freestone PP, Haigh RD, & Lyte M (2007) Specificity of catecholamine-induced growth in *Escherichia coli* O157:H7, *Salmonella enterica*, and *Yersinia enterocolitica*. *FEMS Microbiol Lett* 269:221-228.

72. Lyte M, et al. (1997) Norepinephrine-induced expression of the K99 pilus adhesin of enterotoxigenic *Escherichia coli*. *Biochem Biophys Res Commun* 232:682-686.

73. Yoshimura T, et al. (1987) Purification of a human monocyte-derived neutrophil chemotactic factor that has peptide sequence similarity to other host defense cytokines. *Proc Natl Acad Sci U S A* 84(24):9233-9237.

74. Mukaida N (2003) Pathophysiological roles of interleukin-8/CXCL8 in pulmonary diseases. *Am J Physiol Lung Cell Mol Physiol* 284:L566-577.

75. Djeu J, Matsushima K, Oppenheim J, Shiotsuki K, & Blanchard D (1990) Functional activation of human neutrophils by recombinant monocyte- derived neutrophil chemotactic factor/IL-8. *J Immunol* 144(6):2205-2210.

76. Carré PC, et al. (1991) Increased expression of the interleukin-8 gene by alveolar macrophages in idiopathic pulmonary fibrosis. A potential mechanism for the recruitment and activation of neutrophils in lung fibrosis. *J Clin Invest* 88(6):1802-1810.

77. Tager AM, Wu J, & Vermeulen MW (1998) The effect of chloride concentration on human neutrophil functions: Potential relevance to cystic fibrosis. *Am J Respir Cell Mol Biol* 19(4):643-652.

78. Bellocq A, et al. (1998) Neutrophil alveolitis in bronchioloalveolar carcinoma: induction by tumor-derived interleukin-8 and relation to clinical outcome. *Am J Pathol* 152(1):83-92.

79. Fiorentino D, Bond M, & Mosmann T (1989) Two types of mouse T helper cell. IV. Th2 clones secrete a factor that inhibits cytokine production by Th1 clones. *J Exp Med* 170(6):2081-2095.

80. Fiorentino D, et al. (1991) IL-10 acts on the antigen-presenting cell to inhibit cytokine production by Th1 cells. *J Immunol* 146(10):3444-3451.

81. Jinquan T, Larsen C, Gesser B, Matsushima K, & Thestrup-Pedersen K (1993) Human IL-10 is a chemoattractant for CD8+ T lymphocytes and an inhibitor of IL-8-induced CD4+ T lymphocyte migration. *J Immunol* 151(9):4545-4551.

82. Kühn R, Löhler J, Rennick D, Rajewsky K, & Müller W (1993) Interleukin-10-deficient mice develop chronic enterocolitis. *Cell* 75(2):263-274.

83. Davies JM, Sheil B, & Shanahan F (2009) Bacterial signalling overrides cytokine signalling and modifies dendritic cell differentiation. *Immunology* 128(1pt2):e805-e815.

84. Zhang S & Wang Q (2008) Factors determining the formation and release of bioactive IL-12: Regulatory mechanisms for IL-12p70 synthesis and inhibition. *Biochem Biophys Res Commun* 372(4):509-512.

85. Werling D, Hope JC, Howard CJ, & Jungi TW (2004) Differential production of cytokines, reactive oxygen and nitrogen by bovine macrophages and dendritic cells stimulated with Toll-like receptor agonists. *Immunology* 111(1):41-52.

86. Hochrein H, et al. (2000) Interleukin (IL)-4 is a major regulatory cytokine governing bioactive IL-12 production by mouse and human dendritic cells. *J Exp Med* 192(6):823-834.

87. Pasparakis M (2009) Regulation of tissue homeostasis by NF-κB signalling: Implications for inflammatory diseases. *Nat Rev Immunol* 9(11):778-788.

88. Ghosh S, May MJ, & Kopp EB (1998) NF-κB and Rel proteins: Evolutionarily conserved mediators of immune responses. *Annu Rev Immunol* 16(1):225-260.

89. Van Antwerp DJ, Martin SJ, Kafri T, Green DR, & Verma IM (1996) Suppression of TNF-α-induced apoptosis by NF-κB. *Science* 274(5288):787-789.

90. Sakon S, et al. (2003) NF-κB inhibits TNF-induced accumulation of ROS that mediate prolonged MAPK activation and necrotic cell death. *EMBO J* 22(15):3898-3909.

91. Gribar SC, Anand RJ, Sodhi CP, & Hackam DJ (2008) The role of epithelial Toll-like receptor signaling in the pathogenesis of intestinal inflammation. *J Leukoc Biol* 83:493-498.

92. Jenner RG & Young RA (2005) Insights into host responses against pathogens from transcriptional profiling. *Nat Rev Micro* 3(4):281-294.

93. Palliser D, et al. (2004) A role for Toll-like receptor 4 in Dendritic cell activation and cytolytic CD8+ T cell differentiation in response to a recombinant heat shock fusion protein. *J Immunol* 172(5):2885-2893.

94. Freestone PP, Haigh RD, Williams PH, & Lyte M (1999) Stimulation of bacterial growth by heat-stable, norepinephrine-induced autoinducers. *FEMS Microbiol Lett* 172:53-60.

95. Freestone PP, et al. (2002) Growth stimulation of intestinal commensal *Escherichia coli* by catecholamines: A possible contributory factor in trauma-induced sepsis. *Shock* 18:465-470.

96. Lyte M, et al. (1997) Norepinephrine induced growth and expression of virulence associated factors in enterotoxigenic and enterohemorrhagic strains of *Escherichia coli*. *Adv Exp Med Biol* 412:331-339.

97. Chen C, R BD, Xie Y, Green BT, & Lyte M (2003) Catecholamines modulate *Escherichia coli* O157:H7 adherence to murine cecal mucosa. *Shock* 20:183-188.

98. Vlisidou I, et al. (2004) The neuroendocrine stress hormone norepinephrine augments *Escherichia coli* O157:H7-induced enteritis and adherence in a bovine ligated ileal loop model of infection. *Infect Immun* 72:5446-5451.

99. Clarke MB, Hughes DT, Zhu C, Boedeker EC, & Sperandio V (2006) The QseC sensor kinase: A bacterial adrenergic receptor. *Proc Natl Acad Sci U S A* 103:10420-10425.

100. Hansen MC, Palmer RJ, Jr, Udsen C, White DC, & Molin S (2001) Assessment of GFP fluorescence in cells of *Streptococcus gordonii* under conditions of low pH and low oxygen concentration. *Microbiology* 147:1383-1391.

101. Yu HS & Alam M (1997) An agarose-in-plug bridge method to study chemotaxis in the Archaeon *Halobacterium salinarum*. *FEMS Microbiol Lett* 156:265-269.

102. Sperandio V, Li CC, & Kaper JB (2002) Quorum-sensing *Escherichia coli* regulator A: A regulator of the LysR family involved in the regulation of the locus of enterocyte effacement pathogenicity island in enterohemorrhagic *E. coli*. *Infect Immun* 70:3085-3093.

103. Pratt LA & Kolter R (1998) Genetic analysis of *Escherichia coli* biofilm formation: Roles of flagella, motility, chemotaxis and type I pili. *Mol Microbiol* 30:285-293.

104. Herzberg M, Kaye IK, Peti W, & Wood TK (2006) YdgG (TqsA) controls biofilm formation in *Escherichia coli* K-12 through autoinducer 2 transport. *J Bacteriol* 188:587-598.

105. Isaacs H, Chao D, Yanofsky C, & Saier MH (1994) Mechanism of catabolite repression of tryptophanase synthesis in *Escherichia coli*. *Microbiology* 140:2125-2134.

106. Ren D, Bedzyk LA, Ye RW, Thomas SM, & Wood TK (2004) Stationary-phase quorum-sensing signals affect autoinducer-2 and gene expression in *Escherichia coli*. *Appl Environ Microbiol* 70:2038-2043.

107. Ren D, Bedzyk LA, Ye RW, Thomas SM, & Wood TK (2004) Differential gene expression shows natural brominated furanones interfere with the autoinducer-2 bacterial signaling system of *Escherichia coli*. *Biotechnol Bioeng* 88:630-642.

108. Sircili MP, Walters M, Trabulsi LR, & Sperandio V (2004) Modulation of enteropathogenic *Escherichia coli* virulence by quorum sensing. *Infect Immun* 72:2329-2337.

109. Wang L, Hashimoto Y, Tsao CY, Valdes JJ, & Bentley WE (2005) Cyclic AMP (cAMP) and cAMP receptor protein influence both synthesis and uptake of extracellular autoinducer 2 in *Escherichia coli*. *J Bacteriol* 187:2066-2076.

110. Xavier KB & Bassler BL (2005) Regulation of uptake and processing of the quorum-sensing autoinducer AI-2 in *Escherichia coli*. *J Bacteriol* 187:238-248.

111. Daigle F, Fairbrother JM, & Harel J (1995) Identification of a mutation in the *pst-phoU* operon that reduces pathogenicity of an *Escherichia coli* strain causing septicemia in pigs. *Infect Immun* 63:4924-4927.

112. Buckles EL, Wang X, Lockatell CV, Johnson DE, & Donnenberg MS (2006) PhoU enhances the ability of extraintestinal pathogenic *Escherichia coli* strain CFT073 to colonize the murine urinary tract. *Microbiology* 152:153-160.

113. Nohno T, Saito T, & Hong JS (1986) Cloning and complete nucleotide sequence of the *Escherichia coli* glutamine permease operon (glnHPQ). *Mol Gen Genet* 205:260-269.

114. Linton KJ & Higgins CF (1998) The *Escherichia coli* ATP-binding cassette (ABC) proteins. *Mol Microbiol* 28:5-13.

115. Kloosterman TG, et al. (2006) Regulation of glutamine and glutamate metabolism by GlnR and GlnA in *Streptococcus pneumoniae*. *J Biol Chem* 281:25097-25109.

116. Costa M, Brookes SJ, & Hennig GW (2000) Anatomy and physiology of the enteric nervous system. *Gut* 47(Suppl 4):15-19.

117. Eisenhofer G, Aneman A, Hooper D, Rundqvist B, & Friberg P (1996) Mesenteric organ production, hepatic metabolism, and renal elimination of norepinephrine and its metabolites in humans. *J Neurochem* 66:1565-1573.

118. Lyte M & Bailey MT (1997) Neuroendocrine-bacterial interactions in a neurotoxin-induced model of trauma. *J Surg Res* 70:195-201.

119. Chen C, Lyte M, Stevens MP, Vulchanova L, & Brown DR (2006) Mucosally-directed adrenergic nerves and sympathomimetic drugs enhance non-intimate adherence of *Escherichia coli* O157:H7 to porcine cecum and colon. *Eur J Pharmacol* 539:116-124.

120. Ahlman H, et al. (1981) On the presence of serotonin in the gut lumen and possible release mechanisms. *Acta Physiol Scand* 112:263-269.

121. Ahlman H, DeMagistris L, Zinner M, & Jaffe BM (1981) Release of immunoreactive serotonin into the lumen of the feline gut in response to vagal nerve stimulation. *Science* 213:1254-1255.

122. Moreira CG, et al. (2006) Bundle-forming pili and EspA are involved in biofilm formation by enteropathogenic *Escherichia coli*. *J Bacteriol* 188:3952-3961.

123. Gophna U, et al. (2001) Curli fibers mediate internalization of *Escherichia coli* by eukaryotic cells. *Infect Immun* 69:2659-2665.

124. Taga ME, Miller ST, & Bassler BL (2003) Lsr-mediated transport and processing of AI-2 in *Salmonella typhimurium*. *Mol Microbiol* 50:1411-1427.

125. Ren D, et al. (2005) Differential gene expression for investigation of *Escherichia coli* biofilm inhibition by plant extract ursolic acid. *Appl Environ Microbiol* 71:4022-4034.

126. Macfarlane S & Dillon JF (2007) Microbial biofilms in the human gastrointestinal tract. *J Appl Microbiol* 102:1187-1196.

127. Kendall MM, Rasko DA, & Sperandio V (2007) Global effects of the cell-to-cell signaling molecules autoinducer-2, autoinducer-3, and epinephrine in a *luxS* mutant of enterohemorrhagic *Escherichia coli*. *Infect Immun* 75:4875-4884.

128. DeLisa MP, Wu C-f, Wang L, Valdes JJ, & Bentley WE (2001) DNA microarray-based identification of genes controlled by Autoinducer 2 - stimulated quorum sensing in *Escherichia coli*. *J Bacteriol* 183:5239-5247.

129. Surette MG & Bassler BL (1998) Quorum sensing in *Escherichia coli* and *Salmonella typhimurium*. *Proc Natl Acad Sci U S A* 95(12):7046-7050.

130. Wang L, Li J, March JC, Valdes JJ, & Bentley WE (2005) *luxS*-dependent gene regulation in *Escherichia coli* K-12 revealed by genomic expression profiling. *J Bacteriol* 187(24):8350-8360.

131. Leclerc H, Mossel DAA, Edberg SC, & Struijk CB (2001) Advances in the bacteriology of the coliform group: Their suitability as markers of microbial water safety. *Annu Rev Microbiol* 55(1):201-234.

132. Wang X, et al. (2006) Impact of biofilm matrix components on interaction of commensal *Escherichia coli* with the gastrointestinal cell line HT-29. *Cell Mol Life Sci* 63:2352-2363.

133. Hartl DL & Dykhuizen DE (1984) The population genetics of *Escherichia coli*. *Annu Rev Genet* 18(1):31-68.

134. Prigent-Combaret C, Vidal O, Dorel C, & Lejeune P (1999) Abiotic surface sensing and biofilm-dependent regulation of gene expression in *Escherichia coli*. *J Bacteriol* 181(19):5993-6002.

135. Domka J, Lee J, Bansal T, & Wood TK (2007) Temporal gene-expression in *Escherichia coli* K-12 biofilms. *Environ Microbiol* 9:332-346.

136. Widmer KW, Jesudhasan PR, Dowd SE, & Pillai SD (2007) Differential expression of virulence-related genes in a *Salmonella enterica* serotype Typhimurium *luxS* mutant in response to autoinducer AI-2 and poultry meat–derived AI-2 inhibitor. *Foodborne Pathog Dis* 4:5-15.

137. Lane MC, et al. (2005) Role of motility in the colonization of uropathogenic *Escherichia coli* in the urinary tract. *Infect Immun* 73(11):7644-7656.

138. Telang S, et al. (2001) Strain-specific iron-dependent virulence in *Escherichia coli*. *J Infect Dis* 184:159-165.

139. Lyte M, Arulanandam BP, & Frank CD (1996) Production of Shiga-like toxins by *Escherichia coli* O157:H7 can be influenced by the neuroendocrine hormone norepinephrine. *J Lab Clin Med* 128(4):392-398.

140. Medellin-Pena MJ, Wang H, Johnson R, Anand S, & Griffiths MW (2007) Probiotics affect virulence-related gene expression in *Escherichia coli* O157:H7. *Appl Environ Microbiol* 73:4259-4267.

141. Reid G, Howard J, & Gan BS (2001) Can bacterial interference prevent infection? *Trends Microbiol* 9:424-428.

142. Hoarau C, et al. (2008) Supernatant from *Bifidobacterium* differentially modulates transduction signaling pathways for biological functions of human dendritic cells. *PLoS ONE* 3:e2753.

143. Kelly D, et al. (2004) Commensal anaerobic gut bacteria attenuate inflammation by regulating nuclear-cytoplasmic shuttling of PPAR-γ and RelA. *Nat Immunol* 5:104-112.

144. Ewaschuk JB, et al. (2008) Secreted bioactive factors from *Bifidobacterium infantis* enhance epithelial cell barrier function. *Am J Physiol Gastrointest Liver Physiol* 295:G1025-1034.

145. Vikström E, Tafazoli F, & Magnusson K-E (2006) *Pseudomonas aeruginosa* quorum sensing molecule N-(3 oxododecanoyl)-l-homoserine lactone disrupts epithelial barrier integrity of Caco-2 cells. *FEBS Lett* 580:6921-6928.

146. Jahoor A, et al. (2008) Peroxisome proliferator-activated receptors mediate host cell proinflammatory responses to *Pseudomonas aeruginosa* autoinducer. *J Bacteriol* 190:4408-4415.

147. Ferreira CS (2005) Refractive index matching applied to fecal smear clearing. *Rev Inst Med Trop Sao Paulo* 47(6):347-350.

148. Tian J & Andreadis ST (2009) Independent and high-level dual-gene expression in adult stem-progenitor cells from a single lentiviral vector. *Gene Ther* 16:874-884.

149. Huang Z, Senocak F, Jayaraman A, & Hahn J (2008) Integrated modeling and experimental approach for determining transcription factor profiles from fluorescent reporter data. *BMC Syst Biol* 2(1):64.

150. Elsinghorst EA & Kopecko DJ (1992) Molecular cloning of epithelial cell invasion determinants from enterotoxigenic *Escherichia coli*. *Infect Immun* 60(6):2409-2417.

151. Alaniz RC, Deatherage BL, Lara JC, & Cookson BT (2007) Membrane vesicles are immunogenic facsimiles of *Salmonella typhimurium* that potently activate dendritic cells, prime B and T cell responses, and stimulate protective immunity *in vivo*. *J Immunol* 179(11):7692-7701.

152. Draghici S, et al. (2007) A systems biology approach for pathway level analysis. *Genome Res* 17(10):1537-1545.

153. Krause G, et al. (2008) Structure and function of claudins. *Biochim Biophys Acta - Biomem* 1778(3):631-645.

154. Kim Y, Kim S-H, Whang K-Y, Kim Y-J, & Oh S (2008) Inhibition of *Escherichia coli* O157:H7 attachment by interactions between lactic acid bacteria and intestinal epithelial cells. *J Microbiol Biotechnol* 18(7):1278-1285.

155. Walz A, Schmutz P, Mueller C, & Schnyder-Candrian S (1997) Regulation and function of the CXC chemokine ENA-78 in monocytes and its role in disease. *J Leukoc Biol* 62(5):604-611.

156. Hasegawa Y, et al. (2007) Gingival epithelial cell transcriptional responses to commensal and opportunistic oral microbial species. *Infect Immun* 75:2540-2547.

157. Hu X, Chen J, Wang L, & Ivashkiv LB (2007) Crosstalk among Jak-STAT, Toll-like receptor, and ITAM-dependent pathways in macrophage activation. *J Leukoc Biol* 82(2):237-243.

158. O'Mahony C, et al. (2008) Commensal-induced regulatory T cells mediate protection against pathogen-stimulated NF-κB activation. *PLoS Pathog* 4(8):e1000112.

159. Chaouche-Drider N, et al. (2009) A commensal *Helicobacter* sp. of the rodent intestinal flora activates TLR2 and NOD1 responses in epithelial cells. *PLoS ONE* 4(4):e5396.

160. Smith EA & Macfarlane GT (1996) Enumeration of human colonic bacteria producing phenolic and indolic compounds: Effects of pH, carbohydrate availability and retention time on dissimilatory aromatic amino acid metabolism. *J Appl Bacteriol* 81:288-302.

161. Yang SK, Eckmann L, Panja A, & Kagnoff MF (1997) Differential and regulated expression of C-X-C, C-C, and C-chemokines by human colon epithelial cells. *Gastroenterology* 113(4):1214-1223.

162. Henderson B, Poole S, & Wilson M (1996) Microbial/host interactions in health and disease: Who controls the cytokine network? *Immunopharmacology* 35(1):1-21.

163. Cowell BA, Evans DJ, & Fleiszig SMJ (2005) Actin cytoskeleton disruption by ExoY and its effects on *Pseudomonas aeruginosa* invasion. *FEMS Microbiol Lett* 250(1):71-76.

164. Athman R, et al. (2005) *Shigella flexneri* infection is dependent on villin in the mouse intestine and in primary cultures of intestinal epithelial cells. *Cell Microbiol* 7(8):1109-1116.

165. Veiga E, et al. (2007) Invasive and adherent bacterial pathogens co-opt host clathrin for infection. *Cell Host Microbe* 2(5):340-351.

166. Frankel G, et al. (1998) Enteropathogenic and enterohaemorrhagic *Escherichia coli*: More subversive elements. *Mol Microbiol* 30(5):911-921.

167. Cho H, Lasco TM, Allen SS, Yoshimura T, & McMurray DN (2005) Recombinant guinea pig Tumor Necrosis Factor Alpha stimulates the expression of Interleukin-12 and the inhibition of *Mycobacterium tuberculosis* growth in macrophages. *Infect Immun* 73(3):1367-1376.

168. Scheidegger A, et al. (2005) Differential effects of Interferon-γ and Tumor Necrosis Factor-α on *Toxoplasma gondii* proliferation in organotypic rat brain slice cultures. *J Parasitol* 91(2):307-315.

169. Jandu N, et al. (2009) Enterohemorrhagic *Escherichia coli* O157:H7 gene expression profiling in response to growth in the presence of host epithelia. *PLoS ONE* 4(3):e4889.

170. Mrsny RJ, et al. (2004) Identification of hepoxilin A_3 in inflammatory events: A required role in neutrophil migration across intestinal epithelia. *Proc Natl Acad Sci U S A* 101(19):7421-7426.

171. McCormick BA (2007) Bacterial-induced hepoxilin A_3 secretion as a pro-inflammatory mediator. *FEBS J* 274(14):3513-3518.

172. Ju JS, et al. (2006) A novel 40-kDa protein containing six repeats of an Epidermal Growth Factor-like domain functions as a pattern recognition protein for lipopolysaccharide. *J Immunol* 177(3):1838-1845.

173. Ren D, Bedzyk L, Thomas S, Ye R, & Wood T (2004) Gene expression in *Escherichia coli* biofilms. *Appl Microbiol Biotechnol* 64:515-524.

174. Köhler B, Karch H, & Schmidt H (2000) Antibacterials that are used as growth promoters in animal husbandry can affect the release of Shiga-toxin-2-converting bacteriophages and Shiga toxin 2 from *Escherichia coli* strains. *Microbiology* 146(5):1085-1090.

175. Anderson NL & Anderson NG (2002) The human plasma proteome. *Mol Cell Proteomics* 1(11):845-867.

176. Bansal T, Alaniz RC, Wood TK, & Jayaraman A (2010) The bacterial signal indole increases epithelial cell tight junction resistance and attenuates indicators of inflammation. *Proc Natl Acad Sci U S A* 107(1):228-233.

177. Russell RM, Sharp FC, Rasko DA, & Sperandio V (2007) QseA and GrlR/GrlA regulation of the Locus of Enterocyte Effacement genes in enterohemorrhagic *Escherichia coli*. *J Bacteriol* 189(14):5387-5392.

178. Sharma VK & Zuerner RL (2004) Role of *hha* and *ler* in transcriptional regulation of the *esp* operon of enterohemorrhagic *Escherichia coli* O157:H7. *J Bacteriol* 186(21):7290-7301.

179. Sougioultzis S, et al. (2006) *Saccharomyces boulardii* produces a soluble anti-inflammatory factor that inhibits NF-κB-mediated IL-8 gene expression. *Biochem Biophys Res Commun* 343(1):69-76.

180. Bhaskar KR & Reid L (1981) Application of density gradient methods for the study of mucus glycoprotein and other macromolecular components of the sol and gel phases of asthmatic sputa. *J Biol Chem* 256(14):7583-7589.

181. Chick H & Martin CJ (1913) The density and solution volume of some proteins. *Biochem J* 7:92-96.

182. Hudault S, Guignot J, & Servin AL (2001) *Escherichia coli* strains colonising the gastrointestinal tract protect germfree mice against *Salmonella typhimurium* infection. *Gut* 49:47-55.

183. Wieder KJ, et al. (2005) Optimization of reporter cells for expression profiling in a microfluidic device. *Biomed Microdevices* 7:213-222.

184. Mitchell P (2001) Microfluidics--downsizing large-scale biology. *Nat Biotechnol* 19:717-721.

185. Weibel DB, DiLuzio WR, & Whitesides GM (2007) Microfabrication meets microbiology. *Nat Rev Micro* 5(3):209-218.

VITA

Name: Tarun Bansal

Address: 200 Jack E. Brown Building
Department of Chemical Engineering
3122 TAMU
College Station, TX 77843-3122

Email Address: tarrun1@gmail.com

Education: B. Tech., Technology of Pharmaceuticals and Fine Chemicals,
U.D.C.T., University of Mumbai, 2005
Ph.D., Chemical Engineering, Texas A&M University, 2010